THE FUNCTIONAL INTEGRATION OF ADULT NEURAL PROGENITOR CELLS INTO INTACT AND COMPROMISED PRIMARY NEURAL NETWORKS IN A MICROELECTRODE ARRAY CO-CULTURE SYSTEM

By

CRYSTAL LYNN STEPHENS

A DISSERTATION PRESENTED TO THE GRADUATE SCHOOL
OF THE UNIVERSITY OF FLORIDA IN PARTIAL FULFILLMENT
OF THE REQUIREMENTS FOR THE DEGREE OF
DOCTOR OF PHILOSOPHY

UNIVERSITY OF FLORIDA

2012

To my family, William, Patricia, Cheryl, Chanel and Benjamin Stephens

ACKNOWLEDGMENTS

I acknowledge the J. Crayton Pruitt Family Department of Biomedical Engineering for giving me the opportunity, and providing an enriching, didactic environment that encouraged me to work and learn in an exciting field of study.

I thank the members of the Stem Cell Research Laboratory, Rachel, Lan, Aditya and Vik for being wonderful lab mates. I am grateful for their help and support with my research, and for the fun times we had in and out of the lab. I know I have made many lasting friendships, and have many fond memories throughout the years. I also thank my undergraduate researchers, Ellen and Crystal, for their excellent work and assistance.

I thank my committee members, Dr. Mingzhou Ding and Dr. Charles Jason Frazier for their essential recommendations for my projects, and for driving me to aim higher with my goals and to be confident in my work.

I thank Dr. Brandi Ormerod, my advisor and committee chair, for her investment of time and thought into my research. Her guidance and encouragement was invaluable to my research and my growth as a scientist, and as a person.

I thank Dr. Tom DeMarse, my co-chair, for his guidance and support. I truly appreciate the time and work he devoted to my education and research projects.

Lastly, I thank my family for their love and encouragement throughout my years in school. I thank my parents for lending me the confidence to pursue a doctorate in a field that I am passionate about even though I may find it challenging at times. I also thank my brother and sisters for supporting me even as they pursue their own careers. I hope that I can be as supportive and inspiring for them, as they were for me.

TABLE OF CONTENTS

page

LIST OF FIGURES

LIST OF ABBREVIATIONS

BDNF	Bone-derived neurotrophic factor
BrdU	Bromodeoxyuridine
CNS	Central nervous system
DAPI	4’,6-diamidino-2-phenylindole
DMEM	Dulbecco’s modified eagle medium
EGF	Epidermal growth factor
ES	Equine serum
ESC	Embryonic stem cell
FBS	Fetal bovine serum
FEP	Fluorinated ethylene-propylene
FGF	Fibroblast growth factor
GABA	gamma-Aminobutyric acid
GFAP	Glial fibrillary acidic protein
GFP	Green fluorescent protein
LTP	Long-term potentiation
MEA	Microelectrode array
NMDA	N-Methyl-D-aspartic acid
NPC	Neural progenitor cell
NT-3	Neurotrophin-3
OGD	Oxygen-glucose deprivation
PBS	Phosphate buffered saline
PEI	Polyethyleneimine
vGAT	Vesicular GABA transporter
vGlut	Vesicular glutamate transporter

Abstract of Dissertation Presented to the Graduate School
of the University of Florida in Partial Fulfillment of the
Requirements for the Degree of Doctor of Philosophy

THE FUNCTIONAL INTEGRATION OF ADULT NEURAL PROGENITOR CELLS INTO INTACT AND COMPROMISED PRIMARY NEURAL NETWORKS IN A MICROELECTRODE ARRAY CO-CULTURE SYSTEM

By

Crystal Lynn Stephens

May 2012

Chair: Brandi Ormerod
Cochair: Thomas DeMarse
Major: Biomedical Engineering

Neural stem/progenitor cell research is on the cusp of achieving real strategies for central nervous system repair. Recent studies provide evidence that grafts can survive, functionally integrate, and ultimately augment damaged neural networks. However, understanding the impact of functional integration on existing brain circuitry is an understudied area of research. This dissertation employs microelectrode arrays (MEAs), which facilitate real-time optical and electrophysiological data collection across entire neural networks, to first determine the faculty for adult hippocampal neural progenitor cell (NPC) derivatives to produce spontaneous action potentials and network bursts when cultured alone, and then to investigate the effects of adult NPC addition to intact or damaged primary neural networks. MEA-plated primary cultures transition through high frequency “superbursting” that is ultimately refined into mature, regular burst patterns. When plated alone, adult NPC-progeny fail to establish synchronized bursting that primary and embryonic stem cell-derived cultures readily form. However, NPCs evoke re-emergent superbursting in primary neural cultures. Developmental superbursting is thought to accompany heightened plasticity both in culture

preparations, and across brain regions. This work also uses online MEA recordings to show activity degradation during hypoxia-ischemia via oxygen-glucose deprivation (OGD), and investigate the ability of subsequent NPC addition to protect or restore network activity. Spike rates initially rise during the first 5min of OGD due to increased asynchronous activity between bursts. Action potentials decrease in amplitude, and all activity ultimately ceases by ~16min. Spontaneous activity recovers following reperfusion after 20min-OGD, but little recovery is observed after longer durations. Shorter duration OGD may effectively model the silenced circuits found in the penumbra of a stroke while longer OGD might effectively model the dying circuits found in the core. NPC addition 24hrs following 3hr-OGD increases low-level proliferation, and decreases cell death, preferentially protecting mature neurons from oxidative stress and death for at least a week after OGD exposure. Although co-culture in OGD-compromised primary cultures did not affect NPC behavior, NPCs partially rescued network activity. The MEA co-culture model established in this dissertation is an effective bioassay for examining the effects of potential neuroregenerative therapies on existing network activity, before these strategies are translated *in vivo*.

CHAPTER 1
GENERAL INTRODUCTION

The Concept of Neuroregeneration

Before the discovery of adult neurogenesis by Altman and Das in the 1960s (Altman and Das, 1965), the scientific community generally believed that the central nervous system (CNS) had little or no ability to regenerate. The complexity of the structure and function of the brain was thought to be too delicate to be disrupted by the introduction of new cells. This dogma, established by Ramón y Cajal persisted across decades of neuroscience research (for review, Colucci-D'Amato et al., 2006). Decades later, the *in vitro* isolation and expansion of dividing neural cells in the 1990s (Reynolds and Weiss, 1992; Lois and Alvarez-Buylla, 1993; Luskin, 1993) erupted a new renaissance in neuroscience research with the notion that these “neural stem cells” could be utilized for neural repair (Gage, 2000). If new neurons were added to the intact adult brain on a daily basis, perhaps they could be introduced into an injured or diseased brain to replace or augment damaged tissue.

Although animal models and even clinical trials have supported the notion that neural stem cell transplantation, or their derivatives, is a feasible treatment strategy, studies have provided mixed results in their demonstrations of functional and behavioral recovery (for example, Freed et al., 2001; Olanow et al., 2003). This is partly due to confounding factors, such as inconsistent number and/or type of cells grafted, and varying methods of transplantation. Means to increase harvest yield, quickly proliferate, and differentiate stem cells into specific target cell types are currently under investigation. However, functionally integrating cell grafts into mature neural tissue, promoting cell survival and controlling interactions with existing neural tissue to replace

damaged or dead cells remains elusive. Perhaps a highly sensitive, noninvasive, *in vitro* system for testing the effects of new treatments could be used to answer some of these questions in an inexpensive, yet remarkably informative, manner.

Neural Progenitor Cell Origins and Other Stem Cell Sources

Stem cells are unique populations of cells that exhibit clonality, the ability to self-renew, and potentiality, the ability to generate multiple cell types. Recent convention refers to less clonal and less potential cells as progenitor cells (Fabel et al., 2003). Therefore, neural stem cells harvested from adult neural tissue that divide, but generate only cell types of the CNS will be described in this dissertation as neural progenitor cells (NPCs). NPCs are committed to differentiating into the neuron, astrocyte and oligodendrocyte cell subtypes found in the brain and spinal cord (Gage, 2000). Neurons are the functional cells of the nervous system that communicate with one another typically through chemical messages transmitted across synapses that generate propagated spikes of cell membrane voltages, called action potentials. Astrocytes and oligodendrocytes generally serve as supporting cells for the neural network (Kandel et al., 2000).

There are several different sources of NPCs, each with unique advantages for neural repair (Ormerod et al., 2008). NPCs can be produced from embryonic stem cells (ESCs) or harvested from fetal or adult brain tissue (Palmer et al., 1997; Svendsen et al., 1999; Palmer et al., 2001). ESCs were first generated from mouse blastocysts by culturing the inner cell mass from pre-implantation embryos on fibroblast feeder layers. The resulting cultures contain populations of ESCs that grow in colonies (for review, Smith, 2001). Thomson *et al.* later isolated human ESCs that do not require feeder layers (Thomson et al., 1998). ESC-derived neurons develop spontaneous action

potentials after 21 days and limited synchronous bursting after 5-6 weeks (Ban et al., 2007; Illes et al., 2007). However, they can develop into any cell type, including teratomas, and of course have obvious ethical issues. Although the production of teratomas, or a tumor containing all three germ layers, in immunodeficient mice is actually a test of clonality and multipotency used to show the successful generation of ESCs (Smith, 2001), their proficiency in forming teratomas is a serious health risk and barrier to their clinical use. The risk of tumorogenesis, however, can be overcome by pre-differentiating *all* cells before engraftment (Brederlau et al., 2006).

Shinya Yamanaka and James Thomson's labs attempted to overcome some of the ethical and medical issues of ESCs by introducing ESC-specific genes into somatic cells using retroviral vectors to generate induced pluripotent stem cells (iPSCs) (Takahashi and Yamanaka, 2006; Yu et al., 2006; Takahashi et al., 2007). Given the correct conditions, iPSCs can generate cell types from any germ layer, including mature neurons, but these cells also require pre-differentiation before engraftment (Takahashi et al., 2007).

NPCs can also be derived from immortalized lineages of transgenic mice that can be readily propagated, and can differentiate and integrate in an engraftment site-specific manner, but these cells lack the ability to survive long term when implanted into adult mouse brains (Snyder et al., 1992). Furthermore, immortalized neural stem cell lines differ significantly from nonimmortalized lines, and even subclones of the same line, because they secrete additional growth factors and cytokines, express different genetic markers, and do not maintain karyotypic stability (Mi et al., 2005). These cell lines

cannot be generalized and are used with caution depending on the goal of the experiment.

Adult NPCs exist throughout the fetal and adult mammalian brain but only actively divide to produce neuroblasts in the subventricular zone (SVZ) of the lateral ventricles, and the subgranular zone (SGZ) of the dentate gyrus, supporting neurogenesis in the olfactory bulbs and hippocampal granule cell layer, respectively, throughout life. In the rodent brain, and presumably the human brain, the rostral migratory stream contains progenitor cells that migrate from the SVZ, differentiating and dividing as the cells travel the long distance towards the olfactory bulb where they continually replenish the mature neuronal population (Doetsch et al., 1997). Evidence of a rostral migratory stream in the adult human brain is still under debate (Sanai et al., 2004; Curtis et al., 2007). New cells of the SGZ of the dentate gyrus migrate to the granular cell layer (GCL) of the hippocampus, where they mature into granule cell neurons and exhibit electrophysiology that may contribute to long-term memory formation and influence behavior (Aimone et al., 2006). Adult NPCs can be harvested from adult brains and grown continuously *in vitro* as floating neurospheres or monolayers (Gage et al., 1998). In addition, media conditions have now been formulated that promote differentiation of neural or glial populations, however the shift in fate is not that robust (Takahashi et al., 1999). Nonetheless, the addition of neurons to existing hippocampal and olfactory bulb neural circuits suggests that the brain holds potential to integrate new neurons following injury or disease.

The origin of NPCs, or whether more than one type of NPC exists, remains under debate. Mature quiescent astrocytes start to proliferate after injury and have the

potential to form neurospheres *in vitro*. However, these cells do not stray from astrocyte lineage *in vivo* (Buffo et al., 2008). Due to the different neurogenic niches in the adult brain, the types of cells that are produced may be influenced by the interactions between NPCs and their local environment that predict their mature fate, as well as their lineage (Goldman, 2003). For example, NPCs harvested from the SVZ differentiate into hippocampal neurons when transplanted into the SGZ (Suhonen et al., 1996).

Recent experiments suggest that there may be two distinct populations of neural progenitors in the adult CNS (Zhao et al., 2008). In the adult SVZ, a GFAP-positive stem cell gives rise to proliferative NPCs that produce migrating neuroblasts, as well as oligodendrocytes (Merkle et al., 2004). The work of Steiner *et al* supported Goldman by demonstrating that proliferating cells in the SGZ could either be glial fibrillary acidic protein (GFAP, known to be an astrocyte marker) -positive or double-cortin (DCX, an immature neuronal marker) –positive but never both, indicating two independent populations of dividing cells in the glial and neuronal lineages, respectively. Because proliferating cells had the propensity to express GFAP but no other astrocyte markers or astrocytic characteristics, GFAP expression alone may not be enough to characterize a cell as an astrocyte (Steiner et al., 2004). Current techniques used to harvest adult NPCs are not specific to any one cell-type. If more than one progenitor cell exists, adult NPC-lines would have a heterogeneous population. The cells used in for the experiments in this dissertation do not express GFAP when fixed immediately after a 12-hour exposure to BrdU, a cell division marker, suggesting that they are not a GFAP+ve population of cells. Regardless of the true origin of endogenous progenitor

cells, they may be great sources of regenerative potential if researchers can engineer them to produce the desired phenotypes for any particular treatment.

Adult NPCs were chosen for the experiments in this dissertation because they can be harvested from multiple adult, living and cadaveric CNS regions, they exhibit restricted neural lineage potential, and are relatively safe and karyotypically stable at moderate passages (Reynolds and Weiss, 1992; Palmer et al., 1995; Arsenijevic et al., 2001; Palmer et al., 2001; Seaberg et al., 2005). These properties are advantageous in that adult NPCs could potentially be harvested and transplanted autologously, which reduces the need for donors, and diminishes the risk of immune response to the transplant. Recipients would also be safe from the risk of tumor development, and the outcome of cell lines, given the right conditions, could be generalized. However, unlike ESC-derived neurons, the ability of adult NPC-derivatives to form neural networks is unknown. Therefore, experiments included in Chapter 2 of this dissertation will plate NPCs alone, and look for development of synchronous bursting, evidence of network formation.

The Neurogenic Niche Provides Clues for Therapeutic Strategies

Neurogenesis is a dynamic process that is affected by both exogenous factors and cell-intrinsic factors. The anatomy and physiology of regions promoting neurogenesis has been examined extensively (Doetsch et al., 1997; Palmer et al., 1997), however, the key to maintaining neurogenesis in these unique niches of the brain remains elusive. The observation that some areas of the brain encourage neurogenesis while others appear to inhibit it despite widespread presence of NPCs is interesting, because if the mechanisms that cause this phenomenon were discovered, neurogenesis could be directed where needed for neural repair. Modifying the environment through external

behavior (i.e. exercise) modifies behavior via NPC-mediated neurogenesis, which is an exciting revelation indicative of an extremely plastic and dynamic process that could be manipulated with clinical therapies. Defining these neurogenic niches is the first step in ultimately engineering therapeutic strategies that either recruit endogenous NPCs, or direct transplanted NPCs. New lineage information is expected in the future, as more is being delineated about CNS cell biology with new technologies. Researchers are gathering lots of information about NPC biology that should provide a toolbox for transplant or recruitment of endogenous NPCs for neural repair.

There is some evidence that links neurogenesis to the anatomical organization of vasculature (Mercier et al., 2002; Mirzadeh et al., 2008; Tavazoie et al., 2008). Key factors known to be necessary to grow NPCs alone in culture in order to maintain proliferation and prevent differentiation have been identified, whereas other conditions encourage neuronal cell fate and survival. Fibroblast growth factor-2 (FGF) and epidermal growth factor (EGF), for example, activate downstream pathways responsible for proliferation. Laminin, a CNS extracellular matrix molecule, will encourage neural growth when used as a substrate in culture. Extracellular signaling molecules will also lead to progenitor differentiation. Retinoic acid, for example, will cause a small shift neuronal cell fate, and neurotrophins will aid in neural survival (Takahashi et al., 1999). Full understanding of the mechanisms driving NPC division and differentiation of their progeny must be obtained before NPCs can have clinical applications. The recipient brain region may need to be prepared, by perhaps adding these factors during transplant, if the target region is not a reliable source for generating them alone.

Adult Neurogenesis: A Benchmark for Functional Integration

In order to engineer tailored strategies for a particular disease or injury with a predictable and favorable outcome, researchers need to decode how to control functional integration or the formation of new networks, of transplanted or endogenous NPC-derived neurons. Adult neurogenesis is an excellent example to turn to for clues about how to introduce transplanted cells, because new endogenous neurons integrate into the hippocampus and olfactory bulb in the adult mammalian brain on a daily basis.

The hippocampus is involved in the encoding and storage of episodic memory in humans (Scoville and Milner, 2000; Leuner et al., 2006). Researchers have assumed for years that the new GCL neurons in the adult brain are involved with this type of learning, but due to the indirect nature of the experiments, relationships between new neuron number and measures of hippocampal function remain correlational. Rodent models focus on using navigational memory related tasks such as the Morris water maze, in which rats learn to swim to a hidden platform in a pool of water to ask how new neurons contribute to the integrity of the hippocampus. Changes in neurogenesis are measured by quantifying both the number of new cells (birthdated by a synthesis-phase marker, such as the thymidine analogue bromodeoxyuridine; BrdU) produced in the dentate gyrus, and their phenotype, as well as by the number of new neurons that survive over time (Ormerod and Galea, 2001).

The contribution of new granule neurons to hippocampal function has not yet been revealed, but studies have shown that strains of mice with high-level neurogenesis outperform strains with low-level neurogenesis on hippocampus-dependent tasks (Kempermann and Gage, 2002), and neurogenesis has been linked to learning and memory by several groups (Gould et al., 1999; Kempermann and Gage, 2002; Ormerod

et al., 2004; Jaako-Movits and Zharkovsky, 2005; Winocur et al., 2006). Manipulations that chronically deplete hippocampal neurogenesis also produce concomitant impairments in cognition, particularly hippocampus-dependent memory (Raber et al., 2004; Rola et al., 2004; Snyder et al., 2005). These data further support the notion that established neuronal circuits in the adult brain are amenable to the functional integration of new neurons.

In addition, introducing animals to a running wheels or exposing them to enriched environments increases the rate at which new neurons are produced and the proportion of neurons that survive over time, respectively (Ehninger and Kempermann, 2003; Tashiro et al., 2007). Although evidence is mounting that neurons produced in the adult hippocampus do integrate into existing circuitry to improve function, variability in the results of many studies, likely due to variability in experiment (BrdU injection) and task (trials per day, room setup, etc), have made the establishment of a direct connection difficult (Piatti et al., 2011; Marrone et al., 2012; Song et al., 2012).

The maturation of endogenous new adult hippocampal neurons closely follows the development of the embryonic brain, taking about 4 weeks to exhibit both GABAergic and glutamatergic synapses, although the exact function of these new cells remains unknown (Esposito et al., 2005). When injected into the dentate gyrus, whole cell recordings of these cells do show some evidence for spontaneous activity (van Praag et al., 2002; Piatti et al., 2011). An approach in which the integration of new cells can be monitored over time may facilitate our understanding of whether transplanted cells or mobilized endogenous cells could be enticed to integrate functionally into a diseased or injured circuit.

Transplantation Studies Provide Evidence of Functional Integration

NPCs hold the potential for the clinical treatment of neurodegenerative disease, such as Parkinson's disease, Alzheimer's disease, or stroke, to name a few (Levy et al., 2004; Roybon et al., 2004). Parkinson's disease essentially impairs motor skills and speech as a result of decreased stimulation of the motor cortex from the basal ganglia due to insufficient dopamine production (Hoglinger et al., 2004). NPC transplantation would provide a treatment or possible cure to Parkinson's disease if they could successful replace the dopaminergic cells.

In 1989, Lindvall and colleagues reported the results of the first human clinical trial, which transplanted ventral mesencephalon tissue from 8-10 week old aborted human fetuses into the putamen of Parkinson's disease patients. The grafts produced modest motor improvement in 2 late-stage patients. Of the approximately 300 Parkinson's patients who have since undergone fetal tissue transplants, only a few have enjoyed long-term positive clinical benefits (Clarkson, 2001; Le Belle and Svendsen, 2002; Winkler et al., 2005). Because of the efficacy of this approach in some patients, the National Institutes of Health initiated two double-blind placebo controlled studies in 1993. In the Denver-Columbia trial (Freed et al., 2001), no persistent improvement in the motor part of the UPDRS was observed among transplant patients (n = 19; at 12 months). However, in a subgroup of younger patients (< 60 years old) a statistically significant 30-35% reduction was observed across the post graft evaluation period. In the Tampa–Mount Sinai trial (Olanow et al., 2003), a progressive 6-month post-surgical improvement in UPDRS scores was observed but gradually declined to no significant difference at 24 months. There are likely compounding factors that led to the failure of the placebo-controlled trials that include lack of immunosuppression, quality and

consistency of transplanted tissue, patient selection, transplant parameters and unexpected side effects such as dyskinesia. Although the impact of systems' regulators on transplanted cells is not fully understood, the effects of hormones, stress, neuroinflammation and life experience on endogenous NPCs has been well documented (Gould et al., 1992; Cameron et al., 1993; Nilsson et al., 1999; van Praag et al., 1999; Mizumatsu et al., 2003; Monje et al., 2003; Ormerod et al., 2003). Clearly these crucial issues remain to be resolved and are discussed in a recent review by Winkler et al., 2005. The clinical improvement shown in the subgroup of younger patients provides hope that stem cell strategies would produce functional improvement if more parameters for success were understood.

Monitoring the extent, to which implanted NPCs become functional *in vivo,* is very limited using current engraftment techniques. There have been more experiments examining neural networks generated from ESCs than from adult NPC-derived cells perhaps because adult NPC-derived cells are more difficult to grow in culture than ESCs. ESCs can give rise to inhibitory and excitatory neurons (Bain et al., 1995; Strubing et al., 1995). hESC-derived neurons receive postsynaptic currents both *in vitro* and *in vivo,* and begin to burst via synaptic integration (Weick et al., 2011). When injected into fetal mouse brains, mouse ESC-derived NPCs demonstrate widespread migration and differentiation into multiple neuronal subtypes (Wernig et al., 2004). Looking at single cell development *in vitro*, they appear to extend outgrowths contacting other ESCs and have been shown to become electrically excitable with patch clamp after 11 to 14 days (Copi et al., 2005). When plated onto adult hippocampal slices, they

migrate into the slice and receive input from primary cells, expressing excitatory (AMPA and NMDA) and inhibitory (GABA) receptors (Benninger et al., 2003).

When pre-differentiated human ESCs were transplanted into a 6-OHDA (6-hydroxydopamine)-lesion rat model of Parkinson's disease, the grafted cells had excellent survival rates and expressed neuronal markers. However, few displayed a dopaminergic neuronal phenotype. Reversal of lesion-induced motor deficits was not observed. In addition, ESCs pre-differentiated for less than 20 days developed into severe teratoma, indicating that prolonged pre-differentiation is essential when using ESC-derived NPCs (Brederlau et al., 2006). In a similar experiment, adult-derived NPCs pre-differentiated into dopaminergic neurons were transplanted into the striatum of the same 6-OHDA-lesion rat model with the addition of glial cell-line derived neurotrophic factor (GDNF), known to enhance the survival of dopaminergic neurons. However, long-term survival of the implanted NPCs was not established and behavior after transplantation did not improve (Ostenfeld et al., 2002).

Plating NPCs on an established long-term biologically relevant neural circuit will have many advantages. *In vitro* analysis will allow for an easily accessible model to examine the interactions between NPCs, and between NPCs and primary neural cells. The cellular activity can be tightly controlled and monitored for long periods of time, which allows for an in-depth analysis of how the surrounding environment influences cell fate, and in turn, how transplanted cells influence existing brain circuitry. Grafted cells could potentially cause serious problems, and it is important that we understand these possibilities. Generating NPCs for transplant into the adult brain for the purpose of neural repair is a growing focus of research but it remains unknown how and if these

cells will functionally integrate into the existing neuronal circuits. The idea of using cell transplants to treat neurodegenerative disease is not new, and early work has shown some promise and some pitfalls. Although transplant studies can detect effects of functional integration through changes in behavior, and then posthumously look for histological markers as evidence of differentiation, synaptogenesis and synaptic activity, MEAs can serve as a missing link, an assay of electrophysiological changes in real-time. A system stripped of systems regulators, known to influence neurogenesis, where progenitor cell progeny could be directly observed over time, may contribute to a clearer picture about added cell fate and functionality.

Microelectrode Array (MEA) Technology

For this dissertation, co-culture methods and MEA technology were combined to develop a novel *in vitro* cell transplantation model in order to provide simultaneous access to optical and electrophysiological data across an entire neural network from 59 electrodes, while easily manipulated by adding cells, factors and/or simulated injury. Primary, embryonic day 18 dissociated cortical cells have been well characterized on MEAs, and consistently develop a mature, stable network of monolayer-cultured primary cells that can be grown for long-term experiments lasting months or even years (Kamioka et al., 1996; Potter and DeMarse, 2001). MEAs are an effective platform for investigating the internal dynamics of neuronal networks, pattern generation and evolution of network organization as the dissociated fetal cells organize themselves into spontaneously active dynamic systems. After these cultured networks have matured, they become functionally stable in terms of axon density, inter-circuit connectivity, and plasticity (Gross and Kowalski, 1999), permitting chronic recording and manipulation. Therefore, primary cultures grown on MEAs appear to establish a biological neural

circuit that could be used to examine how NPC transplantation would influence a diseased or damaged circuit and in turn, how an established circuit would influence the behavior of transplanted NPCs.

Van Pelt, *et al* characterized the development of cultured neural networks on MEAs. Spontaneous action potentials are observed within one week with periods of elevated firing rates. In the second and third weeks, network bursts, short episodes of sustained synchronous firing at many sites followed by a variable quiescent phase with few action potentials, are present. The bursts evolve gradually, broadening to about two seconds in the third week followed by drastic shortening after one month. In earlier weeks (before 30 days *in-vitro*), network bursts are preceded by a ramp-like phase of low firing, followed by almost or complete silences. At later stages, such bursts have a sudden onset and are often followed by an after discharge of lower intensity firing that is later described as superbursts. At the end of three weeks *in-vitro*, bursts reach their maximum duration. This is attributed to maximum dendritic spine and shaft synapse density numbers. GABAergic inhibitory feedback and dendritic spine pruning cause these long, less intense bursts, which shift the balance of synaptic excitation and inhibition towards the latter (van Pelt et al., 2004).

In immature neurons, gamma-aminobutyric acid (GABA), the inhibitory neurotransmitter, exerts dual properties (both excitatory and inhibitory actions). This phenomenon is caused by the reversed potential of the $GABA_A$ receptor-activated chloride conductance (E-GABA) that reverses at -35mV. On the one hand, $GABA_A$ receptor-mediated depolarization excites immature neurons. Also, it activates voltage-gated Ca^{2+} channels and potentiates the activity of the NMDA receptors (excitatory) via

attenuation of their voltage-dependent Mg^{2+} block. GABAergic synapses in the fetal rat hippocampus are established before glutamatergic ones. Glutamate synapses will not be established as long as the target neuron has not reached a certain degree of maturity, which occurs in 3-4 weeks (Ben-Ari, 2001). ESCs cultured on MEAs give a good indication of how adult NPCs would behave. ESC-derived neural cultures developed spontaneous action potentials after 21 days (Mistry et al., 2002) and synchronous burst patterns after 5-6 weeks (Illes et al., 2007). Activity development of ESC derivatives is slightly delayed compared to primary cortical cultures, which exhibit spontaneous action potentials as early as three days *in vitro* and synchronous network bursting by two weeks *in vitro* (Maeda et al., 1995). Thus, adult NPCs should be expected to also show delayed maturation. Electronic stimulation or delivery of differentiation factors may also be needed to control progenitor cell fate, synapse formation and electrical response patterns. For therapeutic applications, NPC-derived neurons must integrate into the brain by forming the correct synapses as to be beneficial to brain function. Adding new neurons that develop undesired *de novo* networks could cause more deleterious effects than the disease that is being treated, by causing problems such as epilepsy from over excitation of the surrounding tissue, or loss of brain function due to inhibition (Buzsáki et al., 1991). The MEA co-culture model described in this dissertation could help to understand the effects of added NPCs to existing CNS circuitry, a vital part of engineering transplantation strategies.

Investigating NPC Addition to Damaged Neural Networks Using a Hypoxic-Ischemic Stroke Model

Applying the MEA co-culture assay system to test the effect of transplanted cells on *damaged* neural circuitry could uncover valuable information about the mechanisms

of functional recovery in the absence of confounding systems regulators. Previous experiments used MEAs to monitor the effects of hypoxia/ischemia on cardiomyocytes (Yeung et al., 2009); however, stroke models in cortical networks have only previously been recorded using 1-7 electrodes *in vivo* (Kass and Lipton, 1982; Rosner et al., 1986). Ischemic stroke is an excellent prototype of acquired brain injury, because *in vitro* and *in vivo* models have been established, are well characterized, and affect many areas of the brain.

Cell death and loss of function in the central nervous system (CNS) due to ischemia is a complicated cascade of cellular mechanisms that in recent years has gradually been deciphered. Briefly, lack of blood flow leads to a rapid depletion of ATP that halts active Na^+/K^+ pumps (Madl and Burgesser, 1993), and in turn causes cells to swell, and reverse glutamate transporters. Located mainly on astrocytes, glutamate transporters use the sodium gradient to clean glutamate from the extracellular space to prevent neuronal excitotoxicity (Zerangue and Kavanaugh, 1996). However, ischemic conditions reverse the gradient, and glutamate is released out into the extracellular space (Szatkowski et al., 1990). During severe ischemia, neurons develop a large membrane depolarization due to the influx of Na^+ (Calabresi et al., 1999), ultimately leading to mitochondrial dysfunction, generation of reactive oxygen species (including the over expression of Cu/Zn superoxide dismutase (SOD; Fukui et al., 2002), and cell death (Rossi et al., 2000). White matter is not excluded from injury as immature oligodendrocytes and oligodendrocyte progenitors are particularly susceptible to ischemia-related death (Fern and Moller, 2000; Tekkok and Goldberg, 2001; Back et al., 2002). Previous studies have shown that NPC grafts increase neuron survival and

promote limited recovery following ischemia *in vivo*, however, how they preserve function and whether they increase survival of other cell types remains unclear (Hodges et al., 1996; Sinden et al., 1997; Modo et al., 2002; Harms et al.).

Hypotheses regarding the mechanisms of functional improvement following the transplantation of stem cells or their progeny suggest that they may provide trophic support that thwarts further cell death, stimulate an endogenous repair process or the production/secretion of neurotransmitter, or perhaps integrate into existing circuitry to amplify compromised signaling (Ben-Hur et al., 2004; Ormerod et al., 2008). Neural stem cell grafts into ischemic CA1 lesions in the rat hippocampus exhibit pre- and post-synaptic markers and develop properties of mature, normal hippocampal neurons within the infarct (Aoki et al., 1993). NPCs also induce plasticity through secretion of trophic factors (Andres et al., 2011; Modo et al., 2003; Lee et al., 2007). Additionally, systems regulators might have an influence or interaction with any protective effects or functional integration of added cells. A post-hypoxic/ischemic environment may affect the behavior of NPCs because, for one, NPCs have metabolic glutamate receptors that are implicated in the regulation of proliferation, differentiation, and survival (Melchiorri et al., 2007). Proliferation of endogenous NPCs does in fact increase within minutes of ischemia in the dentate gyrus (Liu et al., 1998; Takagi et al., 1999; Kee et al., 2001; Yagita et al., 2001). Neurogenesis is also induced in nonneurogenic regions, specifically the striatum, where neuroblasts migrate from the SVZ after stroke and differentiate into functional neurons resembling those that died in the lesion (Arvidsson et al., 2002; Thored et al., 2006). Activated neural stem cells also contribute to stroke-induced neurogenesis and neuroblast migration toward the infarct boundary (Zhang et al., 2004).

How and if stem cells or their derivatives are influenced by these mechanisms remains unclear. Applying MEA technology to stroke models can facilitate online monitoring of network activity during a hypoxic-ischemic event, and may shed light upon how to improve the longevity of new neurons.

Specific Aims

The goal of this dissertation is to investigate the ability of adult NPC-generated neurons to form neuronal networks, and influence existing neural activity in mature neuronal networks that are intact, or compromised by OGD. Concurrently, exhaustive phenotyping of the composition of NPC progeny, and the primary cultures, is performed to better understand the electrophysiological data, and in turn determine how the surrounding primary cells influence NPC maturation.

The experiments described in Chapter 2 aim to study the effects of adding adult NPCs on electrophysiological activity in an *in vitro* cell culture model of a mature neural network. The hypothesis for this study is that given the correct environment, NPC-derived neurons could functionally integrate into an existing neural network, to significantly impact its activity as the new cell population differentiates and matures. NPCs will first be plated alone to determine whether they are capable of forming neural networks and spontaneous bursting. Then, primary neural cells will be plated and allowed to reach a mature, stable state of bursting before GFP-expressing NPCs are added to the cultures. The addition of NPCs is expected to initially lower network activity as they generate the appropriate proteins for transmission, but as the cells mature, they will function similarly to neurons surrounding them, thus strengthening the network. Changes in spike rate per channel, and overall spike rate, burst rate, and superburst

rate per array are measured. Concurrently, changes to NPC fate will be examined immunocytochemically.

The studies described in Chapter 3 aim to establish an ischemic stroke model by applying OGD to primary cultures on MEAs. Recovery of network activity along with cell death rates will be measured after different lengths of OGD exposure times in order to determine a benchmark for modeling the effects of NPC addition on a compromised network. For the first time, MEA-plated cultures are recorded *during* OGD to delineate how network activity breaks down during ischemic conditions. Particularly vulnerable cell phenotypes will be detected immunocytochemically, in addition to cell death markers and Cu/Zn SOD.

Finally, Chapter 4 uses the established *in vitro* brain injury model for stroke to observe changes in NPC-derived neurons due to neural activity in injured neural networks. Twenty four hours following OGD exposure, NPCs, NPC-conditioned media or fibroblasts are added to the post-ischemic primary neural cultures in order to determine if any neuroprotective effects are due to NPC addition, trophic factors secreted by NPC-derived cells, or by the physical addition of cells (Boehler et al., 2007). Changes in cell death, oxidative stress, and the fate and survival in GFP-positive NPC progeny will be examined immunocytochemically. The hypothesis for this study is that NPC-derived cells will functionally integrate into a mature network in an attempt to repair damaged primary neural cultures. Neural activity after the cell addition will be monitored to 1) look for any rescued activity due to the addition of NPCs as evidence that the NPCs can repair the damaged network and 2) observe NPC-derived cell survival and differentiation on any remaining active sites versus inactive sites. The work

in this dissertation will demonstrate the convenience and applicability of the MEA co-culture system to test the effects of NPC addition and/or other potential therapies on a biologically relevant neural network.

CHAPTER 2
ADULT NEURAL PROGENITOR CELLS REACTIVATE SUPERBURSTING IN MATURE NEURAL NETWORKS

Introduction

Reports of potentiated behavioral recovery in some animal models of human CNS syndromes suggest that transplanted stem cell derivatives may replace or augment damaged neural networks (Nikkhah et al., 1994b). However, the mechanism(s) behind potentiated recovery in animal studies remain elusive (Winkler et al., 2005; Ormerod et al., 2008). Monitoring the effects of stem cell derivatives on neural activity as they differentiate and mature could provide insight about the optimal parameters (i.e. cell numbers and endpoints) to employ in preclinical studies (Winkler et al., 2005). Here we use microelectrode array (MEA) technology, which allows the longitudinal collection of both optical and electrophysiological data across neural cultures (Potter and DeMarse, 2001; Maccione et al., 2010), to test whether long-term adult rat neural progenitor cell (NPC)-generated cultures generate *de novo* networks and/or integrate functionally into pre-established rat primary neural networks.

Employing stem cell sources that generate neurons with spontaneous networking capability may facilitate stem cell strategies seeking to replace dead neural circuits. MEA technology has revealed that human and mouse embryonic stem cell (ESC)-derived neurons generate intensity-dependent evoked potentials and spontaneous synchronized network bursts within ~5-6 weeks of plating that are remarkably similar to those generated by networked primary neurons (Ban et al., 2007; Illes et al., 2007; Heikkila et al., 2009). Because NPCs can be harvested from multiple adult living and cadaveric CNS regions, exhibit restricted neural lineage potential, and are relatively safe and karyotypically stable at moderate passages (Reynolds and Weiss, 1992;

Palmer et al., 1995; Arsenijevic et al., 2001; Palmer et al., 2001; Seaberg et al., 2005), they are attractive candidates for CNS replacement strategies. However, their ability to generate neurons with *de novo* networking capability is unknown. Here we examine whether adult rat hippocampal NPC-derived neurons spontaneously generate novel networks, like their human and mouse ESC counterparts.

Decades of MEA research have revealed that primary neurons reliably generate activity patterns that stabilize with time (Gross and Kowalski, 1999; van Pelt et al., 2004; Wagenaar et al., 2006). For example, fetal primary hippocampal and cortical neurons initially generate isolated action potentials (within 3-5 days) but eventually generate synchronized action potentials (within ~ 2 weeks) that evolve into short high-frequency bursts of activity (within ~ 4 weeks) that persist for the lifetime of the culture. Often before stabilizing, these *ex vivo* neural networks transiently generate clusters of bursts called superbursts (Wagenaar et al., 2006), reminiscent of GABA receptor-mediated recurrent bursts generated by neural networks in diverse regions of the developing mammalian brain (de Lima and Voigt, 1997; Voigt et al., 2001; Opitz et al., 2002). Here we also test whether the activity of pre-existing electrophysiogically mature rat neuronal networks are affected by the addition of adult rat hippocampal NPCs.

Material and Methods

Preparation of Microelectrode Arrays Dishes and 8-well LabTek Chamber Slides

Electrophysiological data was collected from cells plated on microelectrode array (MEA) dishes with a square grid of 60 planar Ti/TiN microelectrodes 30μm in diameter, spaced 200μm apart (Multichannel Systems, Reutlingen, Germany) and immunocytochemical data was collected from cells plated on 8-well LabTek chambers

that were paraformaldehyde-fixed at 14-day intervals throughout the experiment. MEA- and LabTek-plated cultures were generated from the same pool of dissociated cells for each experiment. Just before use, a 100μl drop of 0.1% (w/v) polyethyleneimine (PEI) in borate buffer (Sigma-Aldrich) solution was placed on the center of each autoclaved MEA dish or sterile LabTek well. After one hour, the dishes and chambers were rinsed and dried before a 20μl droplet of mouse laminin (Sigma; 1mg/ml in PBS) was placed on the center of each MEA (covering the electrode region) or center of each LabTek well, which was then incubated at 37°C for one hour. Cell suspension was then placed directly onto the laminin droplet, which ensured identical plating densities in the dishes and wells. Once the cells adhered to the laminin-covered substrate (~20min), media was topped off to 1ml in MEAs and 400μl per well in the LabTek chambers.

Neural Progenitor Cell Harvest and Expansion

The rat hippocampal NPCs used in this study were descended from a line generated by Dr. Hiroki Toda (Toda et al., 2003). Briefly, the minced hippocampi of adult female Fisher 344 rats (Harlan, Sprague Dawley) were digested in papain (2.5 units/ml; Worthington Biochemical, Freehold, NJ), dispase II (1 unit/ml; Roche Applied Science) and DNase I (250 units/ml; Worthington Biochemical) solution at 37°C for 45 min and then triturated gently. The dissociated tissue was fractionated in a 50% and then 20% Percoll solution by centrifugation for 10min at 20,000 x g to capture NPCs. Fractionated cells were plated onto poly-L-ornithine/laminin-coated dishes in DMEM/F-12 (1:1) medium containing 10% fetal bovine serum (FBS) for 24 hours and then the medium was replaced with DMEM/F12 (1:1) supplemented with N2 (Invitrogen) and 20ng/ml recombinant human fibroblast growth factor-2 (FGF-2; Genzyme, Cambridge,

MA). At approximately passage 20, the NPCs were infected with the replication-deficient GFP-expressing recombinant retrovirus, LZRS-CAMut4GFP to express green fluorescent protein (GFP) and passaged weekly until abundant GFP expression was observed. All GFP^+ NPCs used in the current study had been passaged ~32-35 times. Previous work has shown that adult NPCs remain genetically stable after this moderate number of passages (Palmer et al., 2001).

Preparation of NPC Cultures

To test whether long-term NPC cultures establish dynamic neural networks and to determine their cellular composition after long-term culture, NPCs were plated on MEA dishes and in 8-well LabTek chambers, respectively. To test whether they modulate the activity of mature neural networks, they were also co-cultured with mature bursting neural cultures. In both cases, NPCs were thawed and grown for 1 week on polyornithine/laminin-coated 100mm tissue culture-treated plates in 'NPC growth media' composed of 20ng/ml fibroblast growth factor (FGF; Peprotech, Inc, Rocky Hill, NJ), 20 ng/ml epidermal growth factor (EGF; Sigma), and N2 (Gibco/Invitrogen) in DMEM/F12 with L-glutamine (Mediatech, Inc) before being passaged in 0.1% trypsin at 37°C. The passaged cells were resuspended in 'NPC differentiation media' composed of 2ng/ml FGF, 100nM all-trans retinoic acid (Acros/Thermo Fisher), 10ng/ml brain derived neurotrophic factor (BDNF; Peprotech, Inc), 10ng/ml neurotrophin-3 (NT-3; Peprotech, Inc.), and 1% (v/v) fetal bovine serum in D-MEM/F12 with L-glutamine to drive progeny more toward a neuronal versus glial fate (Takahashi et al., 1999). A 100µl droplet of media containing 10,000 NPCs was placed in the center of empty PEI/laminin-coated MEAs (n=5) or PEI/laminin-coated 8-well LabTek chambers (n=3). Electrophysiological

activity was recorded weekly for 8wks from MEA-plated cultures and phenotypes were quantified using immunocytochemistry and confocal microscopy in LabTek-plated NPC cultures that were paraformaldehyde-fixed at 2, 4 and 6 weeks after plating. In both growth and differentiation conditions ~70% of cells in the NPC-generated cultures expressed green fluorescent protein (data not shown).

Preparation of Primary Cultures

The neocortices (without hippocampi) dissected from embryonic Day 18 (E18) Sprague Dawley rats (n = 2 per experiment) were shipped to the University of Florida from Brain Bits (Springfield, Illinois) in Hibernate B solution and were stored at 4°C until use. Within 48h of arrival, the tissue was dissociated enzymatically in a solution of papain (20 units/ml; Worthington Biochemical; Lakewood, NJ) and deoxyribonuclease 1 (2000 units/ml, Worthington Biochemical) in GlutaMax-supplemented DMEM (1x; Invitrogen) at 37 °C for 30min before being triturated 10x gently and pelleted for 3min at 1500rpm. The pelleted cells were re-suspended in 'primary culture growth media' consisting of 10% equine serum (Hyclone) + 1% Cellgro Antibiotic-Antimycotic solution (Mediatech, Inc.; Herndon, VA) in DMEM/GlutaMax (Invitrogen) and plated by placing a 100µl droplet of primary culture growth media containing 25,000 cells in the center of PEI-laminin-coated MEA dishes for electrophysiological characterization (n = 12) or PEI/laminin-coated LabTeks for immunocytochemical characterization (n = 17; $\geq$ 2 wells per staining set). Thus, 25K cells were plated per array or LabTek well (~ 4,000/mm^2), which is within plating densities known to generate robust and stable network-wide electrophysiological activity (for example Wagenaar et al., 2006). Every 3 days, 50% of the media was replaced with fresh growth media. Media changes were conducted at

least 24 hours prior to a recording session to avoid disrupting electrophysiological activity.

Preparation of NPCs for Co-Culture

At 40 days after plating, dishes were randomly assigned to either the 10,000 NPC, 50,000 NPC, NPC-conditioned media or fresh media control group and the co-culture experiment was initiated. Media was removed from the primary culture and a 100µl droplet of 'primary culture growth media' containing 10,000 NPCs was added to the center of each LabTek chamber well-plated primary culture and a 100µl droplet containing either 10,000 or 50,000 NPCs was added to each MEA-plated primary culture (Appendix A). Once the NPCs adhered to the primary cultures (5-10 minutes), primary culture growth media was added to fill the well or dish (~ 400µl per LabTeK chamber well and 1ml per MEA dish) and a teflon lid with a FEP membrane was added (Potter and DeMarse, 2001). Control cultures were fed with 25% NPC-conditioned media or fresh media containing no cells. Every 24 hours (to compensate for increased cell densities), 50% of the media was replaced with fresh media.

Immunocytochemistry

LabTek-plated cells were fixed with 4% paraformaldehyde for 10 minutes and rinsed repeatedly between immunostaining steps with TBS (pH 7.4). The cells were blocked in 3% normal donkey serum (NDS) and then incubated overnight in a cocktail of three primary antibodies that included rabbit or mouse anti-β-Tubulin (1:500; Covance; to visualize immature neurons), mouse anti-neuronal nuclei (NeuN; 1:500; Chemicon International; to visualize mature neurons), guinea pig anti-glial fibrillary acidic protein (GFAP; 1:750; Advanced Immunochemical; to visualize astrocytes) or mouse anti-S100β (1:500; Sigma Aldrich; to visualize astrocytes), rabbit anti-NG2 (1:1000;

Chemicon International; to visualize oligodendrocyte precursors), rabbit anti-rat vesicular GABA transporter (vGAT; 1:500; Chemicon International; to visualize inhibitory neurons), guinea pig anti-vesicular glutamate transporter 1 (vGlut1; 1:5000; Chemicon International; to visualize excitatory neurons) and/or rabbit anti-ki67 (1:500; Novocastro distributed by Leica Microsystems; to visualize dividing cells) at 4°C. The following day, the sections were incubated in the appropriate FITC-, Cy3-, or Cy5-conjugated secondary antibody (anti-goat IGg, anti-mouse IGg, anti-guinea pig IGg, and anti-rabbit IGg, respectively 1:500; Jackson ImmunoResearch) for 4 hours. Then cells were DAPI-stained (1:20,000 in TBS for 20min; Calbiochem) and then cover slipped under PVA-DABCO. A subset of MEA-plated cells was stained identically to confirm concordance among their phenotypes with LabTek-plated cells. In addition, because mean (±S.E.M.) percent of cells co-expressing S100β and GFAP was high (96.83±3.16% at 2 weeks, 84.46±8.41% at 4 weeks and 93.53±4.13% at 6 weeks), we employed anti-GFAP to phenotype astroglia.

Confocal and Epifluorescent Microscopy

Confocal Images (512x512 pixels) of LabTek-plated cultures were taken using a Zeiss LSM 710 fully spectral Laser Scanning Confocal Microscope (with 405, 440, 488, 532, 635 laser lines) with a 20x objective (3x optical zoom) through the z-plane (5 stacks) of DAPI positive cells and GFP/DAPI$^+$ cells in primary cultures and in co-cultures. Visible laser line intensities were maintained below 15%. DAPI-positive cells with appropriate neuron, astrocyte and oligodendrocyte morphologies and intense staining with the appropriate antibodies in primary cultures served as positive controls to which exposure levels and gain were set to exclude nonspecific staining among GFP$^+$

cells (NPCs). Cell densities and phenotypes were determined from images taken in 8-10 non-overlapping fields of view taken diagonally from each of the 4 corners of > 2 wells (> 500 cells per well). In primary cultures and NPC cultures, the density of $DAPI^+$ or $DAPI/GFP^+$ cells (number primary cells or NPC-generated cells per mm^2, respectively), the proportion of $DAPI^+$ or $DAPI/GFP^+$ cells expressing neuronal (β-tubulin and/or NeuN) or glial (GFAP or NG2) markers and the fraction of neurons (β-$tubulin^+$ or $NeuN^+$) co-labeled with vGlut or vGAT was calculated. In co-cultures, the fraction of $DAPI/GFP^+$ cells relative to $DAPI^+$ cells, the proportion of $DAPI/GFP^+$ cells co-labeled with neuronal or glial markers and the fraction of new neurons (GFP/β-$tubulin^+$) co-labeled with vGlut or vGAT was calculated. Fluorescent images of immunostained MEAs were taken using a Zeiss reflected light fluorescent microscope using a 20x or 40x objective and cell densities and phenotypes determined as described above.

Electrophysiological Data Collection

Changes in extracellular potential were recorded at each of the 59 recording electrodes over 10 minute sessions. In the NPC culture experiment, activity was recorded every 2-3 days for 56 days after plating to monitor isolated and synchronous activity. In the co-culture experiment, activity was recorded every 3 days from 3-39 days after plating to establish the development of mature electrophysiological activity among primary cultures and then every 2 days for 90 days after NPC addition to monitor changes in activity among the mature neural networks. The MEA signals, sampled at 25 kHz, were amplified and digitized using Multichannel Systems (Reutlingen, Germany) MEA1060 amplifier and A/D hardware. The cultures were allowed to equilibrate for ~2min after being placed into the $C0_2$ and temperature controlled recording chamber

before recording was initiated. Spike events were extracted and stored online for later offline processing using a software package custom written by Dr. Thomas B. DeMarse.

Action potentials (or spikes) were detected online as upward or downward excursions beyond 5x the estimated median threshold of quiescent noise estimated during a series of brief 1s periods over 15s before each recording session. Electrodes exhibiting spike frequencies less than 0.1Hz were deemed “inactive” based on previous reports of minimum steady firing rates (Latham et al., 2000; Boehler et al., 2007). Spike waveforms occurring 1ms before and 2ms after peak spike height were saved and used to remove duplicate detections of multiphasic spikes and visually inspect for artifacts. All data and relevant contextual information aforementioned were recorded to a file from which spike, burst and superburst frequencies were quantified offline. We calculated and report the mean (±S.E.M.) time after plating that action potentials emerged (in weeks after plating), mean spike rate per session adjusted for active electrodes (Hz) and mean percent active electrodes per session in NPC-generated cultures, primary cultures and NPC/primary cell co-cultures.

Network bursts are sudden increases followed by sudden decreases in firing frequencies among neurons in brain regions, organotypic cultures or cell cultures (Gross and Kowalski, 1999). We defined network bursts based upon inter-spike intervals similarly to previous reports that defined network bursts as activity with 0.1 to 2s inter-spike intervals recorded at > 3 or > 14 electrodes (Gross and Kowalski, 1999; Tabak and Latham, 2003). Activity that was reliably categorized as a network burst by visual inspection typically showed action potentials across > 10 electrodes with < 0.2s inter-spike intervals. Because these parameters fell within the conservative end of

previously reported definitions, we chose to employ them to define network bursts in our culture and co-culture experiments. We calculated and report the mean (±S.E.M.) time after plating that network bursts emerged (in days and weeks) and burst rates (per minute and per session) in NPC-generated cultures, primary cultures and NPC/primary cell co-cultures. No evidence of contamination was noted in any of the MEA dishes during the extended culture period.

Superbursts were defined as a cluster of >10 consecutive network bursts (> 30 bursts/min) separated from other clusters by a quiescent period >10x longer than the mean inter-burst interval within the cluster. These parameters were chosen in reference to previous work that defined a superburst as at least 50% of all large and medium bursts occurring inside tight clusters with inter-superburst intervals > than 10x longer than inter-burst intervals (Wagenaar et al., 2006). We confirmed these parameters by visual inspection of raster plots in which the smallest distinguishable superburst met these criteria. We calculated and report the mean (±S.E.M.) number of superbursts detected per recording session, the percent network bursts occurring *within* a superburst as well as burst rates detected between and within superbursts in NPC-generated cultures, primary cultures and co-cultures.

Statistical Analyses

All group statistical tests were conducted using Statplus Software (Analysoft Incorporated; Vancouver, BC, Canada). To determine whether adult NPC-generated cultures develop network-wide activity, we compared the dependent variables (percent active electrodes, spike rates (Hz), burst rates, superburst rates, percent activity in superbursts, number of superbursts and spike rates) across weeks 1-

7 after plating using one-way ANOVAs. Changes in viability (cell densities) and cell phenotypes (percent immature neuron, mature neuron, astrocyte, or oligodendrocyte precursor and percent neurons expressing glutamatergic and GABAergic phenotypes) among NPC progeny were examined across time after plating (2, 4, and 6 weeks) using one-way ANOVAs. To confirm that primary cultures exhibited mature bursting activity before NPC addition (and random group assignment) and to characterize changes in their bursting activity after co-culture, we examined the dependent variables (spike rate, burst rate, percent change in spike rate from baseline, percent change in burst rate from baseline, percent active electrodes, percent activity in superbursts, and number of superbursts) between groups (fresh media control, NPC-conditioned media control, 10K NPCs-added and 50K NPCs-added) across days after plating (3-39) or weeks after NPC addition (weeks 1-3) using two-way ANOVAs. To phenotype primary cultured cells and co-cultured NPC progeny, we examined cell density and cell phenotype (percent dividing cells and percent immature neurons, transitioning neurons, mature neurons, astrocytes, and oligodendrocyte precursors or percent neurons expressing glutamatergic or GABAergic phenotypes) across time after the initiation of co-culture (2, 4, and 6 weeks) using one-way ANOVAs. Newman-Keuls post-hoc tests were employed to explore main and interaction effects and all α levels were set at 0.05.

Results

Adult NPC-Generated Neurons that Retain Immature Phenotypes are Incapable of Ensemble Activity

Adult NPCs were plated on MEAs and observed for several weeks. Because activity across NPC-generated cultures did not evolve robustly across recording sessions within each week we analyzed the mean ($\pm$S.E.M.) percent of plate-wide

active electrodes, electrode-wide spike rates and plate-wide synchronized bursts collected during the last session of each week (Figure 2-1). Action potentials emerged in the 2nd week after plating (Figures 2-1A-B), presumably coincident with the emergence of active neurons. Activity at some electrodes persisted, disappeared or emerged latently (Figures 2-1C-K) suggesting asynchronous neuronal differentiation and turnover among adult NPC-generated neurons.

The percent active electrodes (> 0.1 Hz) across MEA plates did increase with time ($F_{(6,28)} = 5.42$, $p < 0.001$; Figure 2-1A). Relative to the 1st (zero activity) and 2nd week after plating the percent active electrodes significantly increased in the 5th week (p's< 0.05) and peaked in the 6th week (p's < 0.05). However, the peak percent of active electrodes (~9%) was much lower than the peak percentage we had expected from primary neurons or pluripotent stem cell derived neurons (Figure 2-1A vs. 2-3C, for example), suggesting that few functional NPC-generated neurons were present. Spike rates on active electrodes remained consistently low across weeks (~1Hz; $F_{(6,28)} = 1.03$; *n.s.*; Figure 2-1B) suggesting that NPC-generated neurons failed to integrate into a functional network. In fact, raster plots of action potentials recorded at each electrode over time confirmed that although adult NPC-derived neurons fired action potentials, their activity never synchronized into bursts characteristic of networked neurons (Figures 2-1C, F and I).

MEA-plated NPC-derived cultures were imaged after each weekly recording session using phase contrast microscopy to monitor their location and density relative to each electrode. Figure 2-1 E, H and K shows adult NPC-generated cells at the same electrode locations 2, 4 and 6wks after plating. Dissociated NPCs were small, round

and phase bright upon plating. Many of these cells proliferated over the first 2 weeks producing dense colonies of cells that had extended a process (Figure 2-1E). Shriveled phase-dark cells floating above the adherent cell layer, indicative of cell death, were observed at this time point. During the 3rd and 4th week, proliferation and death stabilized at a low-level and cells migrating out of the colonies established during the proliferative phase appeared to increase the culture confluency (Figure 2-1H). At this point, most cells possessed extensive branches and either round or oval cell bodies typical of neurons or flattened irregular shaped cell bodies typical of astrocytes. Although low-level proliferation may have persisted through later weeks, the increased culture confluency appeared to be mediated by more elaborate branching and further migration (Figure 2-1K vs. H).

Cultures were fixed and stained at 2, 4 and 6 wks after plating and the proportion NPC-derived cells that expressed immature neuroblast (β-tubulin$^+$), differentiated neuron (NeuN$^+$), astrocyte (GFAP$^+$), and oligodendrocyte (NG2$^+$) phenotypes was scored (Figure 2-2). Oligodendrocytes were not detected at any time point. An ANOVA on phenotypes revealed that preferred phenotypes changed significantly across weeks ($F_{(4,18)} = 6.00$; $p < 0.001$; Figure 2-2). While the percent of NPC-derived immature neurons increased across weeks (week 6 > weeks 2 and 4; *p's* < 0.001), the proportion of astrocytes and mature neurons remained consistently low (week 2 = week 4 = week 6; *n.s.*). By the 6th week after plating, a significantly higher percent of adult NPC-generated cells expressed immature neuronal phenotypes versus either astrocyte ($p <$ 0.001) or mature neuronal ($p < 0.001$) phenotypes.

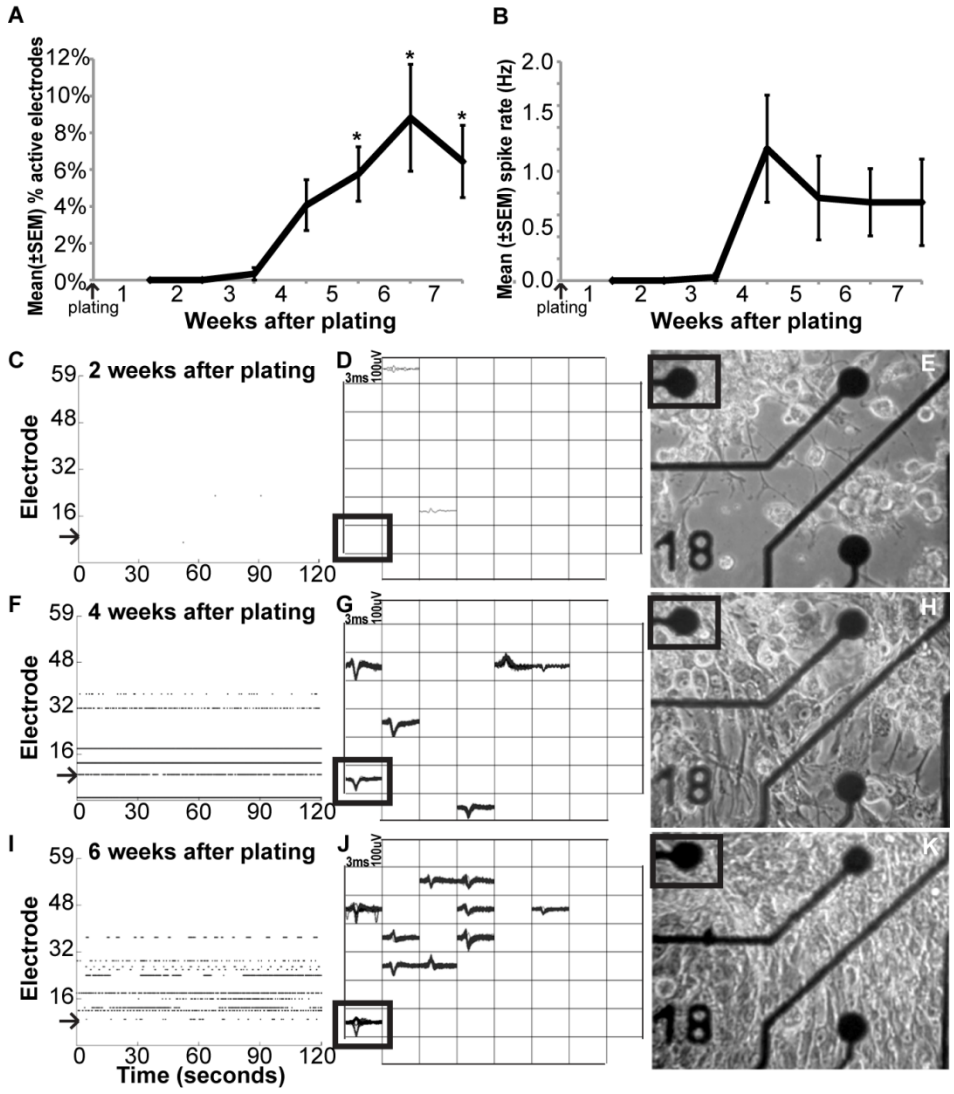

Figure 2-1. Neurons in adult hippocampal NPC-derived cultures fail to develop network activity. The electrophysiological activity of adult hippocampal NPC-generated cultures was monitored for 7wks (n = 5). (A) The mean (±S.E.M.) % active electrodes significantly increased after 5wks (*p's* < 0.05), but only ~8% of electrodes detected action potentials (compare Figures 2-3A-C). (B) Mean (±S.E.M.) spike rates (Hz) on active electrodes did not increase across weeks. Raster plots from recordings at 2 (C), 4 (F), and 6 (I) weeks confirm action potentials do not synchronize. Waveform maps captured at 2 (D), 4 (G), and 6 (J) weeks after plating show persistent, transient and latent activity at electrodes. Phase contrast micrographs (20x objective) show extensive migration and branching among cells in the same MEA location following 2 (E), 4 (H) and 6 (K) weeks after plating. Arrows (C, F, I) and boxes (D-K) show activity and cells at the same electrode 2, 4, and 6wks after plating. $^{*}p<0.05$ relative to plating.

A

Antibody	Phenotype	Time after plating		
		2 weeks	4 weeks	6 weeks
Neuronal				
β-tubulin	Immature Neurons	4.8 ± 2.4	6.8 ± 3.2	25.5 ± 4.9**†
NeuN	Mature Neurons	0.7 ± 0.4	2.1 ± 1.5	2.2 ± 0.6
Glial				
GFAP	Astrocytes	0.4 ± 0.4	0.8 ± 0.5	7.9 ± 2.2
NG2	Oligodendrocyte precursors	0.0 ± 0.0	0.0 ± 0.0	0.0 ± 0.0

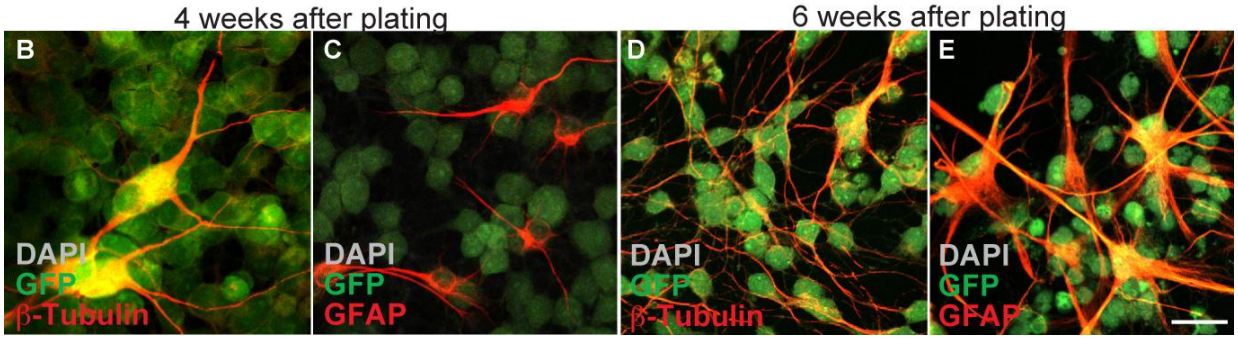

Figure 2-2. Adult hippocampal NPCs produced neurons that retain immature phenotypes and few astrocytes. The proportion of GFP-expressing adult hippocampal NPC-derived cells expressing immature (β-tubulin) and mature (NeuN) neuronal markers or astrocyte (GFAP) and oligodendrocyte precursor (NG2) markers at 2, 4 and 6wks after plating was quantified on confocal laser scanning microscope digital images (20x objective with 3x digital zoom; n = > 500 cells in 4 wells per staining condition). No $NG2^+$ cells were detected. (A) While the % of adult NPC-generated immature neurons increased across weeks (weeks 2 and 4 < week 6; *p's* < 0.001), the % of astrocytes and mature neurons did not increase from week 2 (weeks 4 and 6 *n.s.*). By the 6^{th} week after plating, more immature neurons were detected than astrocytes (p < 0.001) or mature neurons (p < 0.001), suggesting that adult NPCs generate primarily neurons that retain immature phenotypes. (B-E) show confocal images of GFP-expressing NPC progeny (in green) that co-express the immature neuronal marker β-tubulin (in red) at 2wks (B) and 6wks after plating (D) or the astroglial marker GFAP (in red) at 2wks (C) and 6wks (E) after plating. Scale bar - 25 μm. $^{***}p$<0.001 between phenotypes; $^{\dagger}p$<0.001 within wks.

Primary Neural Cultures Develop Neural Ensemble Behavior Coincident with Neuronal Maturation

Cells were isolated from E18 rat cortices and plated on MEAs. Activity within each primary culture was recorded for 10min every 3d after plating to confirm that neurons generated stable and mature synchronized network-wide bursting prior to co-culture with NPCs. As expected, the mean (±S.E.M.) spike rates and burst rates generated by neurons in primary cultures increased across days after plating (spike rate: $F_{(12,104)}$ = 16.02; $p < 0.001$ and burst rate: $F_{(12,104)} = 41.04$; $p < 0.001$; below). In addition, the mean (± S.E.M.) percent of active electrodes within MEA dishes increased across days after plating until stabilizing on day 14 ($F_{(12,104)} = 40.91$; $p < 0.001$; Figure 2-3C), consistent with the timelines reported by other groups (Gross and Kowalski, 1999; van Pelt et al., 2004; Wagenaar et al., 2006).

Action potentials emerged within 3-5 days (mean ± S.E.M: 0.14 ± 0.03Hz; Figure 2-3A) and network bursts emerged by the 2nd week (Days 8-14) after plating (0.98 ± 0.07bursts/min; Figure 2-3B) when increases in percent active electrodes within each MEA dish had already plateaued (Figure 2-3C). During the 3rd week (Days 15-21) after plating, spike frequency increased to 1.03 ± 0.18Hz; (Day 20 vs. Days 3 and 5; *p values* < 0.05). Burst rates also increased to 3.13 ± 0.63/min (Day 20 vs. Days 3-17, *p values* < 0.04).

At the beginning of the 4th week after plating (~Day 26), the cultures began generating prolonged clusters of bursts separated by several minutes of quiescence (a.k.a. ‘superbursts’; Figure 2-4B). During this transient superburst period (~ Days 26-33) we observed peak spike rates (2.65 ± 0.15Hz; days 26-36 > days 20 and 23; *p values* < 0.05), network burst rates (13.79 ± 0.80/min; days 26-33 > day 23 > day 20; *p*

values < 0.004) across the majority of active electrodes (mean ± S.E.M: 80.1 ± 5.94%; Figure 2-3 and 2-4). Network bursting plateaued during the 5th week after plating (days 29-35) with mean spike rates of 2.80 ± 0.19 Hz and burst rates of 14.14 ± 0.73/min (Figure 2-3). We added NPCs, NPC-conditioned media or fresh media to MEAs on day 39 and resumed recordings.

To better understand how cell composition promotes the evolution of bursting, we fixed and stained primary cells in parallel with the development of ensemble activity (2 weeks), superburst patterns (4 weeks) and network stabilization (6 weeks) in their MEA-plated counterparts (Figure 2-5). The percent of differentiated cells detected across weeks was consistently high (~81-85%; Figure 2-5A; $F_{(2,30)} = 0.19$; *n.s*.). While the percent of glial phenotypes detected remained consistently high across weeks, decreased percentages of immature (week 2 > weeks 4 and 6; *p values* < 0.05) and transitioning (weeks 2 and 4 > week 6; *p values* < 0.001) neurons but increased percentages of mature neurons were detected (weeks 2 and 4 < week 6; $p = 0.08$ and 0.02, respectively; effect of phenotype: $F_{(4,30)} = 138.64$; $p < 0.001$; phenotype by week interaction effect: $F_{(8,30)} = 4.44$; $p < 0.001$; Figure 2-5A-D). The majority of 4wk-old neurons expressed vesicular glutamate and a small proportion expressed vesicular GABA (Figure 2-5E-F), suggesting the presence of abundant functional synapses among these networked primary neurons.

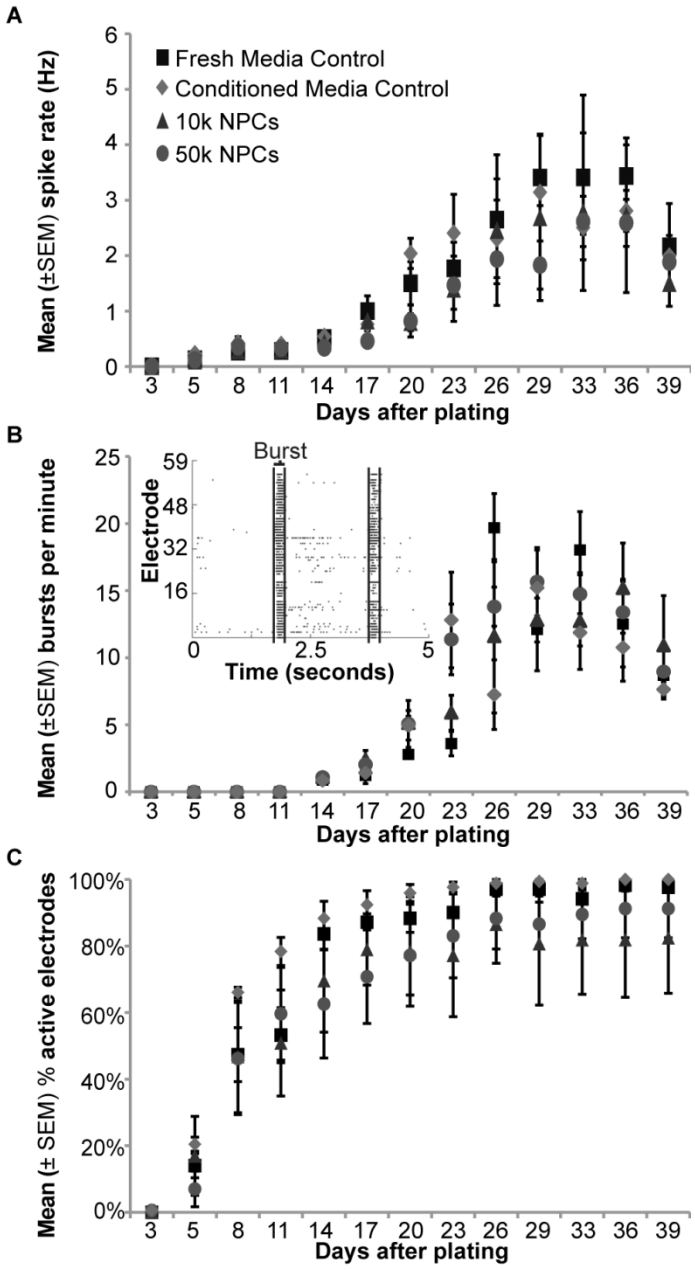

Figure 2-3. Primary cultures develop stable network bursting within weeks of plating. (A) Action potentials appeared within 3d of plating. Mean (±S.E.M) spike rates (Hz) increased in the 3rd wk (20d vs. 3-5d; *p's* < 0.05) and then peaked in the 4th wk when superbursts were observed (26-36d > 20-23d; *p's* < 0.05) before plateauing (26-39d; *n.s.*). (B) Network bursts were first detected in the 2nd wk after plating and increased in the 3rd wk (20d vs. 3-17d; *p's* < 0.05), peaking in the 4th wk when superbursts were detected (26-33d > 23d > 20d; *p's* < 0.005) before plateauing (26-39d, *n.s.*). Inset - raster plot showing action potentials detected simultaneously on most electrodes (a burst), twice within 5s. (C) Mean (±S.E.M) % active electrodes increased rapidly across days (14-39d > 11, 8d > 5d > 3d; *p's* < 0.05) before plateauing on Day 14.

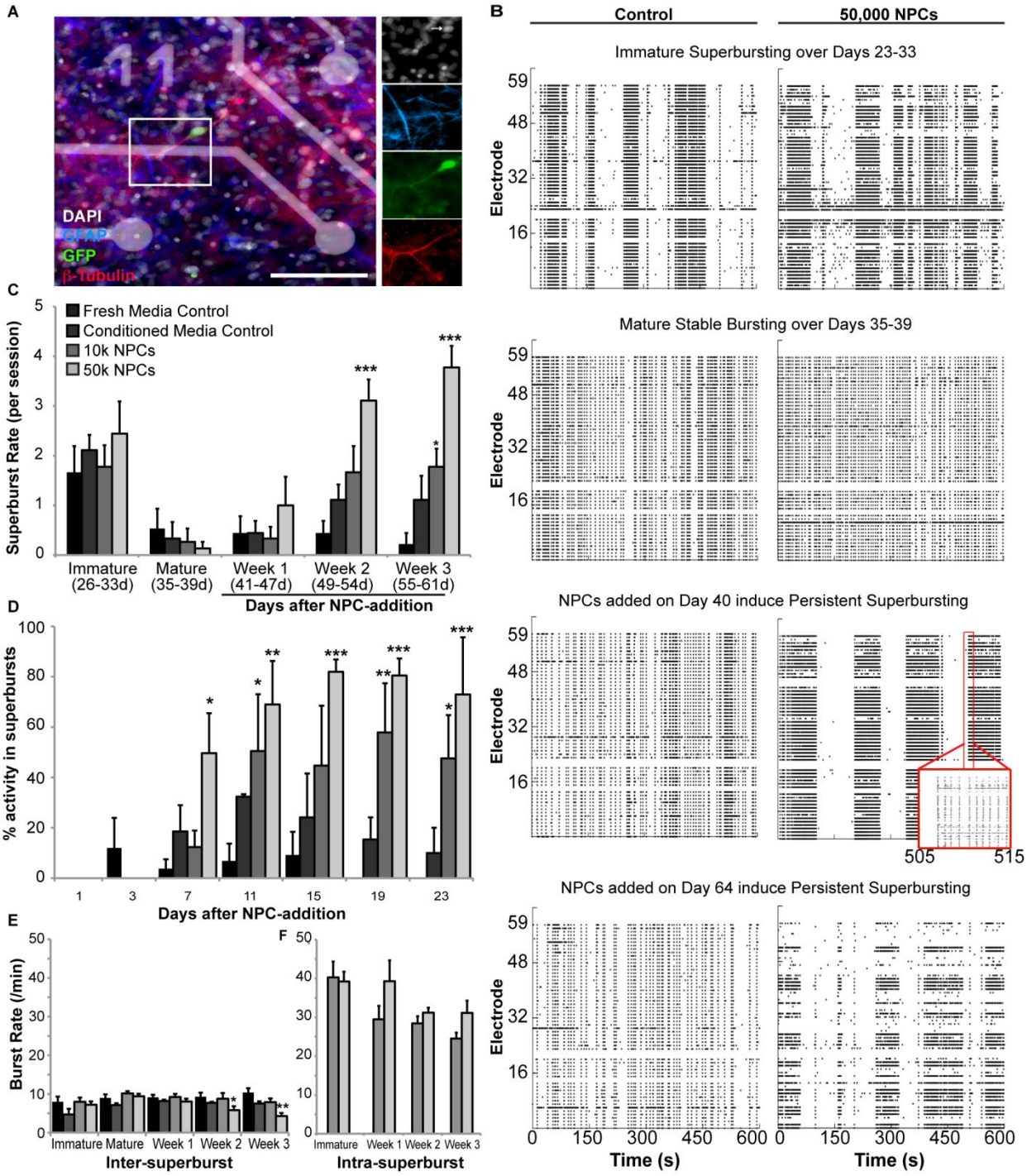

Figure 2-4. NPCs and/or their progeny revert neuronal ensemble activity to an immature status. (A) A fluorescent image showing a GFP$^+$ NPC-derived (in green) β-Tubulin$^+$ (in red) neuron among MEA-plated primary cells. The co-culture was fixed and immunostained to show primary (DAPI$^+$) and NPC-derived (DAPI/GFP$^+$) astrocytes (GFAP$^+$; in blue) and neurons (β-Tubulin$^+$; in red) 50 days after NPC addition. Scale bar - 100 μm. (B) Representative raster plots

showing action potentials detected in primary cultures by electrodes 1-59 (y-axis) during a 600s session (x-axis). Superbursts were detected in all primary cultures during the 4th week after plating (Days 23-33; First Row) before permanent stable bursting activity emerged in the 6th week (Days 35-39; Second Row). Superbursting re-emerges in primary cultures 1wk after 50K NPCs (and 2wks after 10K NPCs) are added and persists for at least 3wks (Days 41-61), whereas fresh media control cultures continue exhibiting stable burst patterns (Third Row and C). *Inset* –a 10s zoom showing that superbursts are composed of high frequency bursts. The addition of 50K NPCs also induced persistent superbursting activity in 64d-old fresh media controls (Bottom Row). (C) The mean (+S.E.M.) number of superbursts detected in primary cultures increases the 4th week and then subsides in the 5th week after plating as stable bursting activity emerges in the 6th week. Superburst frequency in mature primary cultures increased significantly in the 2nd and 3rd week after 50K NPCs were added (p's < 0.0001) and in the 3rd week after 10K NPCs were added ($p < 0.05$), but not at any time point after NPC-conditioned media was added, relative to fresh media controls (n = 3 cultures per group). Superburst frequencies were similar in immature (4wk-old) cultures and following NPC addition. (D) Shows the mean (±S.E.M.) % of activity in superbursts recorded after NPC or media addition. Across sessions, most activity consisted of superbursts beginning in the 2nd week after the addition of 50K NPCs (p's < 0.05) and the 3rd week after the addition of 10K NPCs (p's < 0.05), relative to fresh media. After emergence, superbursting activity persisted for the duration of the experiment in the 50K NPC added group (p's < 0.01) and tended to persist in the 10K NPC added group (p's = 0.07). We found that inter-superburst and intra-superburst burst rates (B *inset)* were similar to those detected in primary cultures as they transitioned to a mature state (~4wks after plating), suggesting that NPCs induce the re-emergence of superbursting activity, normally produced by neurons as they mature. We examined inter-superburst (E) and intra-superburst burst rates (B *inset* and F) to determine whether the strength of bursting and superbursting was NPC-density dependent. Inter-superburst rates significantly decreased in the 2nd and 3rd weeks after 50K NPCs (*p values* < 0.05), but not in the 10K NPC supplemented or NPC-conditioned media groups, relative to fresh media controls. This effect is likely because superburst frequency was also significantly elevated in the 50K NPC group (C). (F) Within superbursts, mean (±S.E.M.) burst rate frequencies were similar in primary cultures as they transitioned to a mature state (~4wks after plating) and following NPC addition. These data suggest that NPCs induce the re-emergence of superbursting activity, typically produced by neurons as they mature. *$p < 0.05$, **$p < 0.01$, ***$p < 0.001$, relative to fresh media controls.

A

Antibody	Phenotype	Time after plating 2 weeks	4 weeks	6 weeks
Neuronal				
β-tubulin	Immature Neurons	10.1 ± 1.6	1.9 ± 1.1*	2.2 ± 1.0*
NeuN/β-tubulin	Transition Neurons	15.5 ± 2.3	14.7 ± 2.4	1.9 ± 1.6**
NeuN	Mature Neurons	0.5 ± 0.4	4.9 ± 2.7†	12.0 ± 2.7*
Neural subtype				
vGlut	Glutamate	14.9 ± 4.2	81.1 ± 3.2	
vGAT	GABA	6.9 ± 6.3	30.6 ± 8.5	
Glial				
GFAP	Astrocytes	46.2 ± 2.3	51.5 ± 3.8	53.4 ± 3.1
NG2	Oligodendrocyte precursors	8.4 ± 2.4	12.5 ± 1.3	15.9 ± 3.0

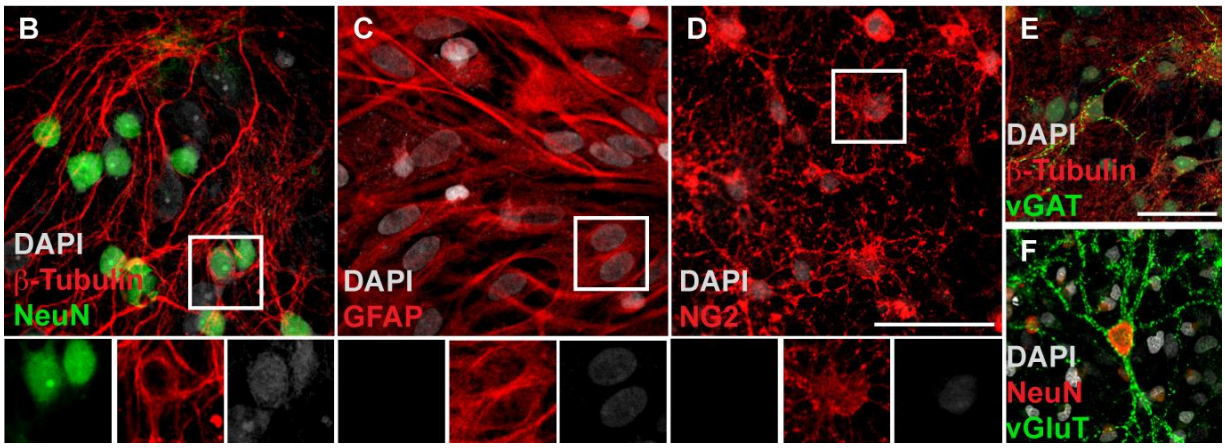

Figure 2-5. Dissociated primary cultures produce robust numbers of neurons, astrocytes and oligodendrocytes. (A) The % DAPI$^+$ primary cells expressing markers of immature neurons (β-Tubulin), transitioning neurons (β-Tubulin and NeuN), mature neurons (NeuN), astrocytes (GFAP) and oligodendrocytes (NG2) were calculated at 2, 4 and 6wks after plating. While the % of astrocytes and oligodendrocyte precursors remained consistent across wks (*p*'s, *n.s.*), the percentage of immature (wk 2 > wks 4 and 6; *p*'s < 0.05) and transitioning (wks 2 and 4 > wk 6; *p*'s < 0.001) neurons decreased while the % of mature neurons increased (wks 2 and 4 < wk 6; *p*'s = 0.08 and 0.02, respectively). (B-F) Representative confocal images of DAPI$^+$ (in gray) neurons, astrocytes and oligodendrocyte precursors detected in 6 week-old primary cultures (B-D). B shows immature (β-Tubulin; red) and mature (NeuN; green) neurons. Note that NeuN and β-Tubulin is co-expressed in some cells. Many neurons in 4 wk-old cultures expressed (E) vesicular GABA- (vGAT) or (F) vesicular glutamate- (vGlut), suggesting the presence of functional excitatory and inhibitory neurons at the same time point that superbursting activity emerges. Scale bar - 50μm. * $p < 0.05$, ** $p < 0.01$ and † $p = 0.08$ relative to week 2.

NPCs Evoke Re-Emergent Superbursting In Pre-Established Mature Neural Networks

We recorded electrophysiological activity for 10 minutes every 48 hours for an additional 50 days to determine the effects of adding undifferentiated adult NPCs to these mature neural networks. There was no statistically significant effect of NPC addition on spike rate (percent change from Day 39 baseline; effect of group: $F_{(3,96)}$ = 0.54, *n.s.*) at any point across days after the initiation of co-culture (effect of day: $F_{(11,96)}$ = 1.41, *n.s.* and interaction effect: $F_{(33,143)}$ = 0.64, *n.s.*). There was, however, an effect of NPC addition on burst rate (percent change from Day 39 baseline; effect of group: $F_{(3,96)}$ = 9.67, $p < 0.001$) that persisted across days after the initiation of co-culture (effect of day: $F_{(11,96)}$ = 0.65, *n.s.*; interaction effect: $F_{(33,143)}$ = 0.24, *n.s.*). Relative to control MEAs maintained in fresh media (+1.9 ± 5.0%), burst rate was unaffected by the addition of NPC-conditioned media (-7.8 ± 2.3%; *n.s.*), but significantly increased following the addition of 10K NPCs (70.2 ± 1.79%; $p < 0.001$) and tended to increase following the addition of 50K NPCs (37.8 ± 8.1%; $p = 0.07$). Raster plots showing recorded action potentials across electrodes revealed that neurons in adult NPC-supplemented primary cultures, but not media-supplemented primary cultures, were generating superbursts reminiscent of those generated transiently by developing primary cultures (Figure 2-4B).

An ANOVA revealed that superburst frequency was elevated by NPC addition ($F_{(3,96)}$ = 18.91; $p < 0.001$), but differentially across weeks after addition (effect of week: $F_{(2,96)}$ = 10.97; $p < 0.001$; week by group interaction effect: $F_{(6,107)}$ = 2.90; $p < 0.05$). Specifically, the frequency of network-wide superbursts increased in cultures supplemented with 10K NPCs ($p < 0.05$) or 50K NPCs ($p < 0.001$), but did not change among cultures supplemented with NPC-conditioned media (*n.s.*), relative to fresh

media. The onset of re-emergent superbursts among electrophysiologically mature primary cultures was NPC number-dependent. Relative to neurons in the fresh media control group, neurons in the 50K NPC-supplemented group generated significantly more superbursts in week 2 ($p < 0.001$) and week 3 ($p < 0.001$), whereas neurons in the 10K-NPC supplemented group only generated increased numbers of superbursts in week 3 ($p < 0.05$; Figure 2-4C). Once superbursting activity was induced by NPC addition (effect of day: $F_{(6,56)} = 8.80$; $p < 0.001$), the majority of electrophysiological events recorded during a session consisted of superbursts (effect of group: $F_{(3,56)} = 20.80$; $p < 0.001$; Figure 2-4D). While the majority of electophysiological events recorded among media control cultures consisted of bursts (with few if any superbursts detected), about 50% of the events were superbursts ~ 1 week after 50K NPCs were added (*p values* < 0.05) and ~2 weeks after 10K NPCs were added *(p's* < 0.05). The majority of events were superbursts by the 2nd week after 50K NPCs were added (> 75%) and by the 3rd week after 10K NPCs were added (>50%). Superburst rates, as well as inter- and intra-superburst burst rates among NPC-supplemented cultures did not differ from those measured in developing primary cultures.

Co-Culture with Electrophysiologically Active Primary Neural Cultures Promotes Differentiation and Maturation of NPC-derived Neurons

The changes in neuronal ensemble behavior paralleled changes in the composition of GFP-expressing NPC-derived cells in parallel co-cultures that were stained immunocytochemically every 2 weeks after co-culture (Figure 2-6). As with the cultures generated by adult NPCs plated alone, we did not detect NPC-derived oligodendrocyte precursors in co-cultures and therefore excluded NG2^{+} phenotypes from our analysis. Relative to NPCs cultured in isolation, co-culture with primary

neurons promoted an increase in NPC-generated cells that expressed the immature neuronal marker β-tubulin versus either the astrocyte marker GFAP ($p < 0.05$) or the mature neuronal marker NeuN ($p < 0.01$, with overall significance of co-culture on phenotype by ANOVA, $F_{(2,63)} = 6.60$; $p < 0.01$).

The phenotypes among co-cultured NPC progeny changed significantly across weeks after co-culture (interaction between week and phenotype: $F_{(4,71)} = 9.02$; $p < 0.001$). At 2 weeks, immature neuronal phenotypes were observed more frequently than either astrocyte phenotypes ($p < 0.001$) or mature neuronal phenotypes ($p < 0.001$) and at 4 weeks, similar proportions of immature neurons and astrocytes were detected (*n.s.*) but more astrocytes were observed than mature neurons ($p < 0.05$). The percent of NPC-generated cells expressing astrocyte phenotypes peaked at 4 weeks (week 2 < week 4 and week 6; *p's* < 0.05). By 6 weeks, all phenotypes were observed among NPC-generated cells with the same frequency.

Unlike the NPCs plated alone, many co-cultured NPCs generated neurons that transitioned from an immature (week 2 > weeks 4 and 6; *p values* < 0.001) to a mature state (week 2 < week 6, $p < 0.05$ and week 2 < week 4, $p = 0.09$). We also note that some NPC-derived neurons died or lost their phenotype between 2 and 4 weeks after co-culture because the percent of total neurons declined significantly (~79% at week 2 versus ~40% at weeks 4 and 6). The majority of immature neurons expressed vesicular glutamate and this decreased with time coincident with an increase in the expression of vesicular GABA (Figure 2-6).

A

Antibody	Phenotype	Time after plating 2 weeks	4 weeks	6 weeks
Neuronal				
β-tubulin	Immature Neurons	75.2 ± 8.8	30.3 ± 9.6***	12.5 ± 12.5***
NeuN	Mature Neurons	4.2 ± 2.7	5.6 ± 3.7	30.2 ± 12.1*
Neuronal subtype (% of β-tubulin⁺ Cells)				
vGlut	Glutamine	91.9 ± 13.5	23.8 ± 13.1	
vGAT	GABA	5.6 ± 5.6	18.8 ± 13.2	
Glial				
GFAP	Astrocytes	9.6 ± 4.9	35.2 ± 8.5*	27.7 ± 10.4
NG2	Oligodendrocyte precursors	0.0 ± 0.0	0.0 ± 0.0	0.0 ± 0.0

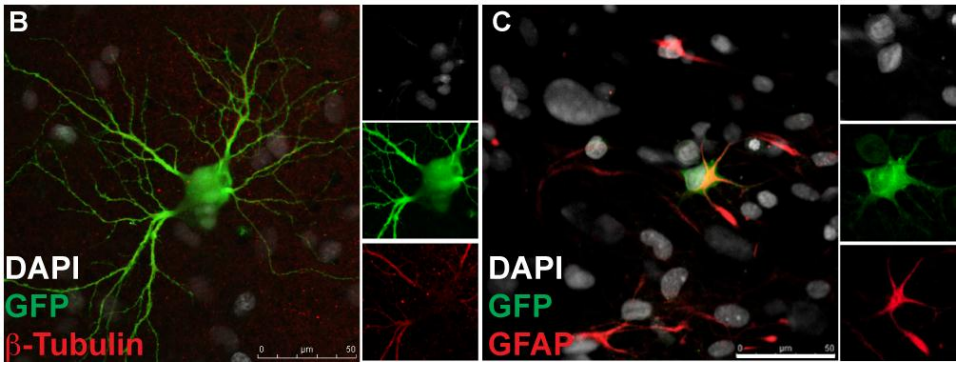

Figure 2-6. Adult NPC progeny mature more quickly and robustly when co-cultured with electrophysiologically mature oligodendrocyte- and astrocyte- rich primary cultures. The proportion of adult hippocampal NPC-derived (GFP^+) cells expressing β-tubulin, NeuN, GFAP or NG2 at 2, 4 and 6wks in co-culture with mature primary neural networks was quantified (A) Most NPC-derived cells were immature neurons after 2wks in co-culture (*p*'s < 0.001 versus astrocytes and mature neurons), astrocytes after 4 weeks in co-culture (*p* < 0.05 versus mature neurons) and all phenotypes were observed with the same frequency by 6wks in co-culture (*n.s.*). Co-cultured adult NPCs generated astrocytes latently (week 2 < week 4 and week 6; *p*'s < 0.05) and produced neurons capable of transitioning from an immature (β-tubulin; week 2 > weeks 4 and 6; *p*'s < 0.001) to a mature state (NeuN; weeks 6 and 4 > week 2; *p*'s < 0.09). The % of total neurons declines significantly from weeks 2 (~79%) to 4 and 6(~40%), suggesting an early vulnerability to cell death. The majority of immature neurons that expressed vesicular glutamate decreased with time coincident with an increase in the expression of vesicular GABA. Confocal laser scanning digital images show adult NPC-derived ($DAPI/GFP^+$) cells co-labeled with the immature neuronal marker β-tubulin (B) and the astrocyte marker GFAP (C). Scale bar - 50 μm. *$p < 0.05$, ***$p < 0.001$ versus 2wks in co-culture.

Discussion

Neurons in primary neocortical cultures synchronize their activity into network-wide bursts (Pine, 1980; Gross and Kowalski, 1999; van Pelt et al., 2004; Wagenaar et al., 2006). This activity transitions through a superbursting phase before stabilizing into a mature state that has been described as analogous to the superbursting activity that is associated with network refinement in the developing mammalian brain (de Lima and Voigt, 1997; Voigt et al., 2001; Opitz et al., 2002). Several prominent differences were observed between primary neural networks and NPC-generated neural networks. Primary neural cultures contained large numbers of astrocytes and oligodendrocytes whereas NPC-generated cultures only contained a few astrocytes and no oligodendrocytes (Figure 2-2 vs. Figure 2-6). In addition, many neurons in primary cultures transitioned from an immature to a mature state, whereas NPC alone-generated cultures contained primarily immature neurons at equivalent times. Our finding that adult NPC-derived neurons, at least grown in standard culture conditions, contain few astrocytes and fail to develop synchronized bursting activity complements the body of work showing that mature glia are required for efficient synaptogenesis and the maturation of network attributes (Banker, 1980; Eroglu and Barres; Kucukdereli et al.).

The addition of NPCs to a pre-established mature network evoked a surprising re-emergence of superbursting activity. Superbursts (~0.2s; Figure 2-5) detected in primary cultures as they mature electrophysiologically are shorter than the continuous ~4s-long bursts (~3-4Hz) recorded in seizure models (Jefferys and Haas, 1982) and more accurately resemble network bursts detected across brain regions developmentally (Galli and Maffei, 1988; Ben-Ari et al., 1989; O'Donovan, 1989;

Peinado, 2000). Superbursting activity is mediated by depolarizing currents at $GABA_A$ receptors on the maturing neurons that activate voltage-gated Ca^{2+} channels, which potentiate the activity of the NMDA receptors (Ben-Ari, 2001). Slow Ca^{2+} wave (0.1-0.5Hz)-mediated neocortical superbursts or 'spindles' are associated with synapse and network formation (Khazipov et al., 2001; Dupont et al., 2006) and long-term potentiation (Lledo et al., 1995; Berridge, 1998). We postulate that because transient superbursts among primary cultures are Ca^{2+} wave-mediated (Opitz et al., 2002; Pasquale et al., 2008) and indistinguishable from re-emergent superbursts in adult NPC-supplemented cultures, that adult NPCs may induce plasticity throughout mature neuronal networks. The ability to establish synchronous bursting suggests that NPCs trigger a remodeling of connectivity and/or synaptic attributes within established networks, potentially by secreting factors that act on networked neurons or by generating *de novo* connections with neurons within the pre-formed network. Of course, dual patch clamp experiments would be required to definitively show that NPC-generated neurons have integrated functionally into pre-established networks but the inability of conditioned medium to evoke bursting activity in the current study is more consistent with the latter hypothesis and we speculate young NPC-derived neurons may mediate these effects. Identifying whether similar mechanisms underlie superbursting activity and NPC-induced re-emergent superbursting activity may clarify the functional and clinical importance of this phenomenon.

Astrocytes present in the primary electrophysiologically mature cultures are likely to promote NPC-derived neuron connectivity in the co-culture context. Our primary cultures (~46% astrocytes/~8% oligodendrocyte precursors; 2 weeks) increased adult

NPC-generated astrocyte and mature neuron yields (Figure 2-2 versus 2-6). These data, and reports that adult NPCs generate functional neurons more efficiently when co-cultured either with astrocytes and brain-derived growth factor (BDNF) (Song et al., 2002a; Song et al., 2002b) or in co-culture with BDNF- and LTP-producing neurons (Babu et al., 2009), suggest that they *could* generate networking neurons in the appropriate niche.

In vivo multicellular recordings have shown that functional processes, such as motor learning and working memory, are mediated by neurons that fire with spatiotemporal coherence (Buzsáki, 2010). These neuronal networks increase in size and interconnectivity with the complexity of the functional process (Pessoa, 2008). Cell replacement strategies may benefit by employing cells that spontaneously generate neurons with network-modifying attributes. ESCs are already attractive candidates because their neuronal progeny quickly network in culture, within grafts and with graft host neurons (Ban et al., 2007; Illes et al., 2007; Heikkila et al., 2009; Tonnesen et al., 2011). In contrast, adult NPCs possess a more restricted application in replacement or augmentation strategies because their neuronal progeny do not establish networks in isolation (Figure 2-1) but may beneficially induce renewed plasticity in pre-existing networks.

Ultimately, the use of cells in therapy will require consideration of both intrinsic properties of the graft and properties of the target niche. We have shown here that cells and niche reciprocally influence each other. Embryonic stem cells are able to generate many neuronal subtypes while tissue-derived NPC progeny appear restricted to more limited subsets of GABAergic or glutamatergic neurons (Peljto and Wichterle; Svendsen

et al., 1998; Dziewczapolski et al., 2003). These differences may be in part, due to a loss of potential as neural progenitors become more specialized over time. For example, ESC-derived NPCs that are propagated in monolayer cultures gradually loose networking capability (Illes et al., 2009), similar to fetal-tissue harvested NPCs that are propagated *in vitro* (Mistry et al., 2002; O'Shaughnessy et al., 2009; Lepski et al., 2011). *In vivo* adult NPCs spontaneously generate neurons that integrate into existing neural circuits (van Praag et al., 1999; Nissant and Pallotto, 2011), but whether they can or should generate *de novo* networks in the absence of a pre-existing network has never been explored. Transplanted ESC- and tissue-derived NPCs only generate neurons in neurogenic regions of the adult brain, but abortive neurogenesis can be stimulated in extra-neurogenic regions by injury or focal cell death (Hoehn et al., 2005). ESC-derived neuronal grafts may bypass niche effects because they contain neurons that are intrinsically capable of establishing networks with one other and host neurons, even in extra-neurogenic regions (Tonnesen et al., 2011).

In the present study, our use of MEAs highlight their utility in defining both intrinsic properties of stem cell derived networks and in assessing how a stem cell-derived population may alter characteristics of an existing network. The persistence of bursting activity produced by mature MEA-plated primary neurons illustrates the stability of network properties established on MEA and the ability to quantitatively measure dynamic effects of maturing stem cell derivatives on neural activity. The MEA system permits control of systems' factors that affect endogenous NPCs and their derivatives, such as hormones and neuroinflammatory molecules (Tanapat et al., 1999; Monje et al., 2003; Ormerod and Galea, 2003; Ekdahl et al., 2009) and parameters hypothesized to

affect transplant efficacy, such as cell number (Winkler et al., 2005). For example, we detected superbursting activity in primary cultures 1 week after 50,000 NPCs and 2 weeks after 10,000 NPCs were added (Figure 2-5). Cellular injury can also be modeled using MEAs. For example, we are currently exploring how adult NPCs modulate the effects of oxygen-glucose deprivation (OGD) on network activity and have early indications that NPC addition restores superbursting activity in mature networks following OGD.

Our present data in combination with earlier work suggests that stem cell strategies could be tailored and even combined to improve the outcome of specific CNS injuries or syndromes. For example, large injuries from stroke may benefit from replacing neuronal networks lost in the injury core and awakening silenced networks in the injury penumbra (Fisher, 1997; Hicks et al., 2009; Shimada and Spees, 2011). One might speculate that ESC-derived neurons are attractive candidates for generating *de novo* core circuitry because they spontaneously generate neurons with networking capability (Ban et al., 2007; Illes et al., 2007; Heikkila et al., 2009) while adult NPCs may be attractive candidates for stimulating persistent plasticity among silenced networks, such as those found in the stroke penumbra.

CHAPTER 3
MICROELECTRODE ARRAY TECHNOLOGY REVEALS THAT VARIABLE DURATION OXYGEN-GLUCOSE DEPRIVATION MAY MODEL DIFFERENT ASPECTS OF STROKE

Introduction

Ischemic stroke is a leading cause of death worldwide, and stroke survivors face compromised quality of life due to loss of function and its associated decrease in occupational utility (for review, Dhamoon et al., 2010). Both *in vitro* and *in vivo* models of hypoxia-ischemia have revealed mechanisms associated with stroke-induced cell death (for example, Szatkowski et al., 1990; Madl and Burgesser, 1993; Calabresi et al., 1999). Fewer studies have identified mechanisms that affect the quiescent neural circuits that survive ischemic stroke but likewise lose their function (Zhu et al., 2011).

Although *in vitro* models cannot fully recapitulate the exquisite cytoarchitecture of the brain, simplified biologically relevant circuits exposed to oxygen-glucose deprivation (OGD) may provide insight into the mechanisms that damage neurons *in vivo* because they arguably produce similar stroke pathology to those observed *in situ* (Harms et al., 2001; Meloni et al., 2001). Multi-electrode array (MEA) technology permits the simultaneous collection of optical and electrophysiological data within a culture for months (Potter and DeMarse, 2001), and the development of activity in cultures established from a number of brain regions has been well characterized. For example, fetal rat dissociated cortical cultures develop spontaneous action potentials and network bursts that evolve predictably over several weeks to reach a mature, functionally stable state by 35-40 days (Kamioka et al., 1996; van Pelt et al., 2004; Stephens et al., 2012). Since the neural activity can be tightly controlled, monitored for long periods, and is highly sensitive to pharmacological manipulations, MEAs offer a stable platform for

performing in-depth analyses of how hypoxia/ischemia and subsequent therapies influence neural networks. These cultures are attractive options for inexpensive high-throughput assays for screening new pharmacological or cellular engraftment strategies because they are highly sensitive, non-invasive, reduce the need for animal experiments, and provide less restricted access for electrophysiological and immunocytochemical data collection. To our knowledge, MEAs have only been employed to monitor the effects of hypoxia/ischemia on cardiomyocytes (Krinke et al., 2009; Yeung et al., 2009). The behavior of neuronal networks during OGD has not been examined using MEAs, but can give an unprecedented view of the network degradation of spontaneous activity from 59 sites simultaneously that has only previously been recorded from a handful of electrodes placed *in vivo* (Kass and Lipton, 1982; Rosner et al., 1986).

Here we combine OGD with MEA technology and immunocytochemisty to measure the breakdown of the activity in an established neural network during hypoxic-ischemic conditions. We employ different durations of OGD to identify exposure levels corresponding with moderate to significant levels of cell death, and observe the immediate and delayed effects of variable durations of OGD on neuronal activity. Experiments are mirrored on multiwell chamber LabTeks to for specific cell phenotypes, in combination with cell death and distress markers, in order to investigate how and by influencing what cell populations could treatment options ameliorate some of the damage in the aftermath stroke.

Material and Methods

Generation of Primary Cultures

Embryonic day 18 (E18) sprague dawley rat neocortices (n=2) were purchased and shipped from Brain Bits (Springfield, Illinois) in Hibernate B™ solution and stored overnight at 4°C upon arrival. The following day, they were dissociated in a solution of papain and DNase I (20 units/ml and 2000 units/ml, respectively; Worthington Biochemical; Lakewood, NJ) l) in GlutaMax-supplemented DMEM (Invitrogen) at 37°C for 30min. The cells were then triturated ~10x gently, pelleted for 3min (1500rpm) and resuspended in DMEM/GlutaMax (Gibco; Grand Island, NY) containing 10% equine serum (Hyclone; Logan, UT) and 1% Cellgro Antibiotic-Antimycotic (Mediatech, Inc.; Herndon, VA). A 100µl droplet of media containing ~ 25K cells directly onto a laminin droplet placed onto the center of each polyethyleneimine (PEI)-laminin-coated MEA (n = 18) and LabTek (n = 16; $\geq$2 wells per staining set), producing a cell density of ~4,000 cells/mm^2 known to generate robust network-wide electrophysiological activity (for example, Wagenaar et al., 1999). Every 3d (> 24h prior to a recording session), 50% of the media was replaced with fresh media.

MEA and Multiwell Chamber LabTek Preparation

Electrophysiological data was recorded from cells plated on MEAs consisting of a square grid of 60 planar Ti/TiN microelectrodes (30µm d spaced 200µm apart; Multichannel Systems, Reutlingen, Germany) and immunocytochemical data was collected from cells plated on 8-well LabTek chambers. The cultures plated on MEAs and in LabTeks wells were generated from the same pool of dissociated cells for each experiment. Before plating, 100µl of 0.1% (w/v) PEI in borate buffer (Sigma-Aldrich; St. Louis, MO) was placed on the center of each autoclaved MEA dish or sterile LabTek

well for 1h. The dishes and chambers were then rinsed and dried before a 20µl droplet of mouse laminin (Sigma-Aldrich; 1mg/ml in PBS) was placed onto the center of their surfaces for 1h at 37°C. Once cells adhered to the laminin substrate (~10min) media was added to 400µl in each LabTek well and 1ml in each MEA.

Oxygen-Glucose Deprivation

We first examined the effects of variable duration OGD on the death of subtypes of cells in a subset of LabTek-plated cultures. Once neurons in MEA-plated primary cultures exhibited the synchronized bursting activity typical of electrophysiologically mature neural networks (day 40) LabTek- and MEA-plated cultures were assigned to either the OGD control group (100% fresh media change) or the 60 min, 120 min,180 min of OGD (n = 3 MEAs and n = 6 LabTeks per group). Activity was recorded from 3 OGD-exposed MEA-plated cultures during the exposure.

First, we simultaneously measured the dissolved oxygen (DO) content in cell media and the oxygen content in the air inside of the incubator for 180min in order to measure the rate at which oxygen leaves the media (Figure 1E; n=3). An ANOVA showed a change in DO overtime ($F_{(19,62)} = 47.0$; $p < 0.001$), and post hoc analyses showed DO began to drop from baseline after 30min ($p = 0.062$), and significantly dropped after 60min (all $p < 0.001$). Therefore, we decided to keep the cell media in the hypoxic incubator overnight before use in the OGD experiments. Pipetting the media into the cultures in preparation for OGD would indeed re-oxygenate the media, but studies have shown that oxygen uptake by cells exceeds the oxygen diffusion coefficient in a cell density-dependent manner, and therefore we believe that the cellular environment rapidly becomes hypoxic (Bambrick et al.).

All media was replaced on MEA- and LabTeK-plated cultures assigned randomly to OGD groups with DMEM devoid of glucose and sodium pyruvate and containing low L-glutamine (GIBCO cat. no. 11966) that had been incubated in hypoxic conditions (37°C, 0.1% O_2, 5.0% CO_2, 94.1% N_2) overnight. These hypoxic DMEM-fed cultures were placed immediately into a hypoxic incubator (37°C, 0.1% O_2, 5.0% CO_2, 94.1% N_2) for 60, 120 or 180min. Immediately after OGD exposure, the hypoxic DMEM was replaced with fresh media and the cultures were returned to a normoxic incubator (37°C, 20.95% O_2, 5.0% CO_2). All media on MEA- and LabTek-plated cultures assigned randomly to the control group was completely replaced with fresh media just before and after the experimental groups were exposed to OGD.

Immunocytochemistry and Microscopy

LabTek-plated cells were stained with PI (250mg/ml TBS; Sigma-Aldrich) for 15 min and then fixed with 4% paraformaldehyde for 10min and rinsed repeatedly between immunostaining steps with tris-buffered saline (TBS; pH 7.4). The cells were blocked in a solution of 3% normal donkey serum (NDS) and 0.1% triton-x in TBS and then incubated overnight in a cocktail of 3 primary antibodies that could include: rabbit or mouse anti-β-Tubulin (1:500; Covance), mouse anti-neuronal nuclei (NeuN; 1:500; Chemicon International), guinea pig anti-glial fibrillary acidic protein (GFAP; 1:750; Advanced Immunochemical), rabbit anti-NG2 (1:1000; Chemicon International), and Cu/Zn SOD (1:500; Millipore) at 4°C. The following day, the sections were incubated in the appropriate FITC-, Cy3-, or Cy5-conjugated maximally adsorbed secondary antibody (1:500; Jackson ImmunoResearch) for 4hrs. Subsets of cells immunostained with mouse anti-NeuN or rabbit anti-β tubulin were also stained with rabbit anti-rat

vesicular $GABA_A$ transporter (vGAT; 1:500; Chemicon International), and/or guinea pig anti-vesicular glutamate transporter 1 (vGlut1; 1:5000; Chemicon International) and then the appropriate secondaries. All immunostained cells were DAPI-stained (1:20,000 in TBS for 20min; Calbiochem) before being coverslipped under PVA-DABCO.

lmages of immunostained LabTek-plated cultures were taken using a Zeiss LSM 710 fully spectral Laser Scanning Confocal Microscope with a 63x oil objective (5 z-stacks). Visible laser line intensities were maintained below 15%. $DAPI^+$ cells with neuron, astrocyte and oligodendrocyte morphologies and intense staining with the appropriate antibodies in primary cultures served as positive controls to which exposure levels and gain were set to exclude nonspecific staining. The percent of PI^+ DAPI-labeled nuclei were quantified as a measure of cell death. Densities of mature and immature neurons, astrocytes, oligodendrocyte precursors, as well as percent PI^+ and percent Cu/Zn SOD^+ cells of each phenotype was quantified to detect any cell type particularly vulnerable to OGD. Immature and mature neurons surround by vesicular glutamate and GABA were measured to detect neuronal responses to OGD. The sum of five non-overlapping images taken diagonally from each corner of >2 wells (>500 cells/well) was averaged to find the mean cell density, or % of each cell type, or total DAPI-labeled cells.

Electrophysiology

As described previously (Stephens et al., 2012), changes in extracellular potential were recorded over 10min sessions every 3d from 3-43d after plating. Cultures were equilibrated for ~2min after being placed into the amplifier before recording was initiated. Their activity was sampled at 25 kHz and signal was amplified and digitized using Multichannel Systems (Reutlingen, Germany) MEA1060 amplifier and A/D

hardware. Spike events were extracted and stored online for further offline processing using a software package custom written by Dr. Thomas B. DeMarse. In the subset of MEA-plated cells that were recorded during OGD exposure, recordings began immediately after the hypoxic incubator door was closed and continued for the 180min exposure to OGD.

At the starting point of each recording, the acquisition software estimated the quiescent noise signal during a brief “learning phase”. Action potentials, or spikes, were detected online as signal deviations beyond five times the median threshold from the quiescent signal. Electrodes exhibiting spike frequencies >0.1Hz were deemed “active” based on previous reports of minimum firing rates (Latham et al., 2000; Boehler et al., 2007). Waveforms between 1ms before and 2ms after detected spikes were saved and used to remove duplicate detections of multiphasic spikes and visually inspect for artifacts. Network bursts were defined as spike detected at >10 electrodes within 0.2sec inter-spike intervals. All data and relevant contextual information aforementioned were recorded to a file from which spike and burst frequency, spike amplitude, percent active electrodes and burst duration were quantified offline. The percent of spikes in interburst intervals during minutes 1-4 of OGD was compared to baseline by taking samples 5 interburst intervals from each of the 3 MEAs and comparing using a paired-sample’s t-test. The mean and standard deviation of the spike rates, burst rates and burst durations for each minute of the baseline recordings were calculated, and used to obtain the normal score of spike rates, burst rates and burst durations of each minute during OGD.

Statistical Analysis

Statistical tests were conducted using Statistica Software (StatSoft, Inc; Tulsa, OK). We examined changes in viability (PI-labeled cells) as percent of total DAPI-labeled nuclei across OGD-exposure times (0, 60, 120, or 180 min) using a one-way ANOVA. Percent dead cells (PI) and oxidative stress (percent SOD-labeled cells) that were co-labeled with cell phenotypes (immature or mature neuron, astrocyte and oligodendrocyte) were examined between control and OGD with two-way ANOVAs. Also, cell density between each phenotype and control or OGD, and % vGlut or vGAT between β-tubulin$^+$ or NeuN$^+$ neurons and control or OGD were examined with two-way ANOVAs. For the MEA analysis, the dependent variables (spike rate, burst rate, spike amplitude, percent active electrodes, and burst duration) across days after plating were compared using repeated measures ANOVAs. Changes in spike rate, spike amplitude, burst rate, percent active electrodes, and burst duration during OGD were determined using repeated measures ANOVAs across minutes of OGD-exposure. The % spikes during interburst intervals during minutes 1-4 of OGD was compared to baseline using a paired student's t-test. The baseline spike rate at each electrode was correlated with spike rate during minutes 1-4 of OGD using a Pearson's correlation coefficient. Lastly, the percent of baseline spike rate, and percent active electrodes, between OGD exposure times (20, 60 or 180 min) and time of recording (1h or 3d after exposure) were compared using two-way ANOVAs. Newman-Keuls post-hoc tests were employed, unless otherwise noted, to reveal group differences and α levels = 0.05.

Results

Mature Neurons are Particularly Vulnerable to the Effects of Long Duration OGD

We first examined total cell death in fresh media control cultures versus cultures exposed to OGD for 60, 120 or 180 min (Figure 1A-B). An ANOVA on the mean (±S.E.M.) percent of $DAPI^+$ nuclei co-labeled with the cell death marker PI revealed significant effects of OGD exposure duration on cell death ($F_{(3,23)} = 31.51$; $p < 0.001$). Significantly more dead cells were found in cultures exposed to OGD for either 120 minutes ($p < 0.001$) or 180 minutes ($p < 0.001$; Figure 3-1A), relative to control cultures. We further characterized the effects of a 180 min OGD exposure on cell death and oxidative stress because this duration of OGD exposure killed ~50% of the culture, which often serves as a benchmark for exploring the mechanisms of stroke-induced cell death (Meloni et al., 2001; Hirt et al., 2004).

We next quantified the percent of $NeuN^+$ mature neurons, β-tubulin$^+$ immature neurons, $GFAP^+$ astrocytes and $NG2^+$ oligodendrocyte precursors co-labeled with the cell death marker PI in OGD-exposed and control cultures (Figure 3-1C). An ANOVA revealed significant effects of OGD exposure ($F_{(1,24)} = 191.12$; $p < 0.001$), dying cell subtype ($F_{(3,24)} = 5.12$; $p < 0.01$) and a significant OGD exposure by dying cell subtype interaction ($F_{(3,31)} = 5.88$; $p < 0.01$) on PI^+ cells. Cell death among all cell subtypes was similarly low in control cultures. OGD exposure increased the death of all cell subtypes ($p < 0.001$), but more OGD-induced death was detected among $NeuN^+$ mature neurons than all other cell types (*all p values* < 0.05), and more dead $NG2^+$ oligodendrocyte precursors were detected than $GFAP^+$ astrocytes ($p < 0.05$).

PI binds to the DNA of cells with compromised nuclear membranes, indicative of necrosis *and* apoptosis. Cells that undergo rapid necrosis may not remain intact, and therefore would not be stained by PI. Because PI does not label all stages of apoptotic and necrotic cell death, we calculated densities of immature neurons, mature neurons, astrocytes and oligodendrocyte precursors as a secondary measure of vulnerability to OGD-induced cell death (Figure 3-1D-L). An ANOVA revealed that although cell subtype densities differed ($F_{(3,40)} = 44.7$; $p < 0.001$), there was neither an effect of OGD on cell subtype densities ($F_{(1,40)} = 1.47$; *n.s.*) nor a statistically significant OGD exposure by cell subtype density interaction ($F_{(3,47)} = 0.600$; *n.s.*). Specifically, astrocytes were detected in greater densities than all other cell types (*all p values* < 0.001). Because our proportion data suggested that neurons were more vulnerable to the effects of OGD than glia, we ran planned comparisons on densities of mature and immature neurons in control versus OGD-exposed cultures. Planned comparisons revealed lower densities of both mature and immature neurons in OGD-exposed cultures versus control cultures ($p < 0.01$ and $p < 0.05$, respectively). PI labels only cells whose nuclei are compromise but still intact. Although PI staining showed cell death across all phenotypes, the loss of cell density of neurons suggests that rapid necrosis may occur in neurons, whereas glia may succumb to apoptosis.

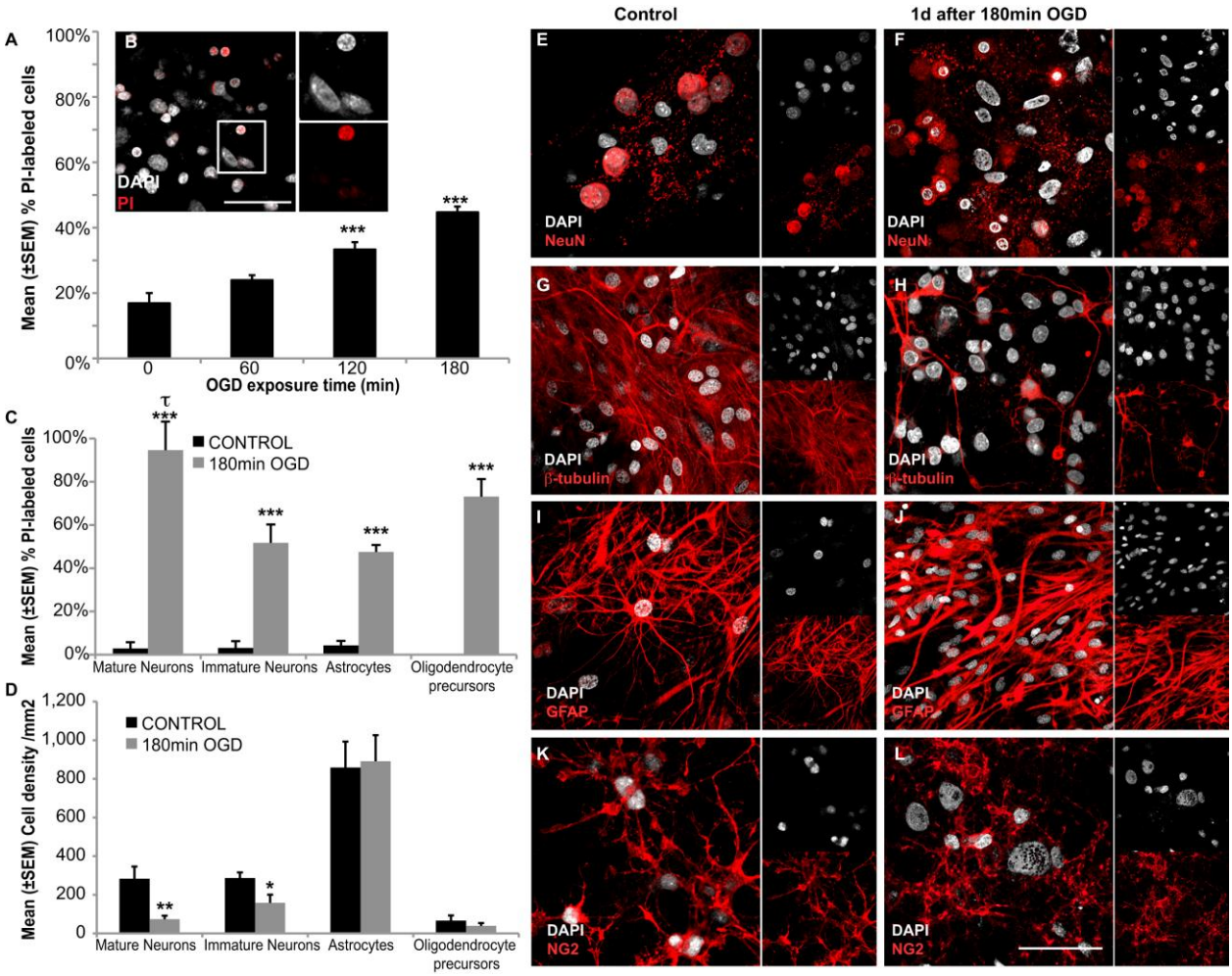

Figure 3-1. Significant cell death occurs after 120 min of OGD exposure, primarily in mature neurons. Primary cultures were exposed to 60, 120 or 180 min of OGD or fresh media change (control) at 40d *in vitro* **(A)**. Immediately following OGD exposure, cultures were exposed to propidium iodide (PI), fixed, and DAPI-stained. The mean (±S.E.M.) percent PI-labeled dead/dying cells of total DAPI-labeled nuclei was calculated. 120-min and 180-min OGD exposures resulted in significant levels of cell death compared to control (*p's* < 0.001). **(B)** A confocal image of cells after 180 min of OGD exposure displays the DAPI-labeled nuclei of all cells (grey) and the PI-labeled nuclei of dead/dying cells (red). **(C)** The percent PI^+ cells expressing different phenotype markers was quantified. **(D)** Cell densities of different phenotypes were compared between control (no OGD) cultures and cultures fixed immediately following 180 min OGD (no reperfusion). The expression of $NeuN^+$ mature neurons had decreased, but the densities of other phenotypes including β-$tubulin^+$ immature neurons, $GFAP^+$ astrocytes and $NG2^+$ oligodendrocytes remained unchanged. **(E-L)** Confocal images of neurons, astrocytes and oligodendrocyte precursors 1d after OGD-exposure. Note the DAPI-labeled nucleus in all cells (grey). (**E)** Normal $NeuN^+$ mature neurons appear healthy relative to (**F)** $NeuN^+$ mature neurons after OGD that have

shriveled nuclei. (**G)** β-tubulin^{+} immature neurons in normal cultures versus **(H)** OGD exposed cultures that have less extensive branching. GFAP^{+} astrocytes in normal cultures **(I)** versus 1d post OGD cultures **(J)** that show little change in morphology. NG2^{+} oligodendrocyte precursors in normal cultures **(K)** versus 1d post OGD cultures **(L)** that have noticeably condensed and fragmented processes. Scale bar – 50μm; *p<0.05, **p<0.01, ***p<0.001 for OGD relative to controls; $^{\tau}p$<0.05 between phenotypes

To examine whether glutamatergic or GABAergic signaling was altered by OGD exposure, the percent of mature and immature neurons expressing vesicular glutamate (vGlut) or vesicular GABA (vGAT) was quantified in OGD-exposed and control cultures (Figure 3-2A). An ANOVA revealed significant effects of OGD exposure ($F_{(1,24)}$ = 6.70; p < 0.05), and neuron age ($F_{(3,24)}$ = 25.4; p < 0.001) as well as a significant OGD exposure and neuron age interaction effect ($F_{(3,31)}$ = 3.06; p < 0.05) on the expression of vGlut and vGAT. We found a higher percent of NeuN^{+} mature neurons expressing vGlut or vGAT than the percent of immature β-tubulin^{+} neurons expressing either vesicle (***p's*** < 0.001). Among mature neurons, more were consistent with a glutamatergic (vGlut^{+}) versus GABAergic (vGAT^{+}) phenotype (p < 0.05) whereas similar percentages of immature neurons expressed glutamatergic and GABAergic phenotypes (p = 0.22). Relative to a complete media change, OGD-exposure decreased the number of mature neurons expressing either vGAT (p < 0.01) or vGlut (p < 0.05), whereas the number of immature neurons expressing either vesicle was unaffected by exposure to OGD (Figure 3-2 A-E).

Of the surviving cells, we quantified the percent of neurons and glia that expressed the oxidative stress marker Cu/Zn SOD (Figure 3-2 F-G). An ANOVA found significant effects of cell subtype ($F_{(3,18)}$ = 10.4; p < 0.001) and exposure to OGD ($F_{(1,18)}$ = 8.48; p < 0.05) and an OGD exposure by cell subtype interaction ($F_{(3,18)}$ = 3.41; p < 0.05).

Specifically, astrocytes were more likely to express Cu/Zn SOD than oligodendrocytes (*p < 0.05)* and tended to express Cu/Zn SOD more than neurons (*all p values < 0.1)*. However, OGD increased neuronal Cu/Zn SOD (*all p values* < 0.01).

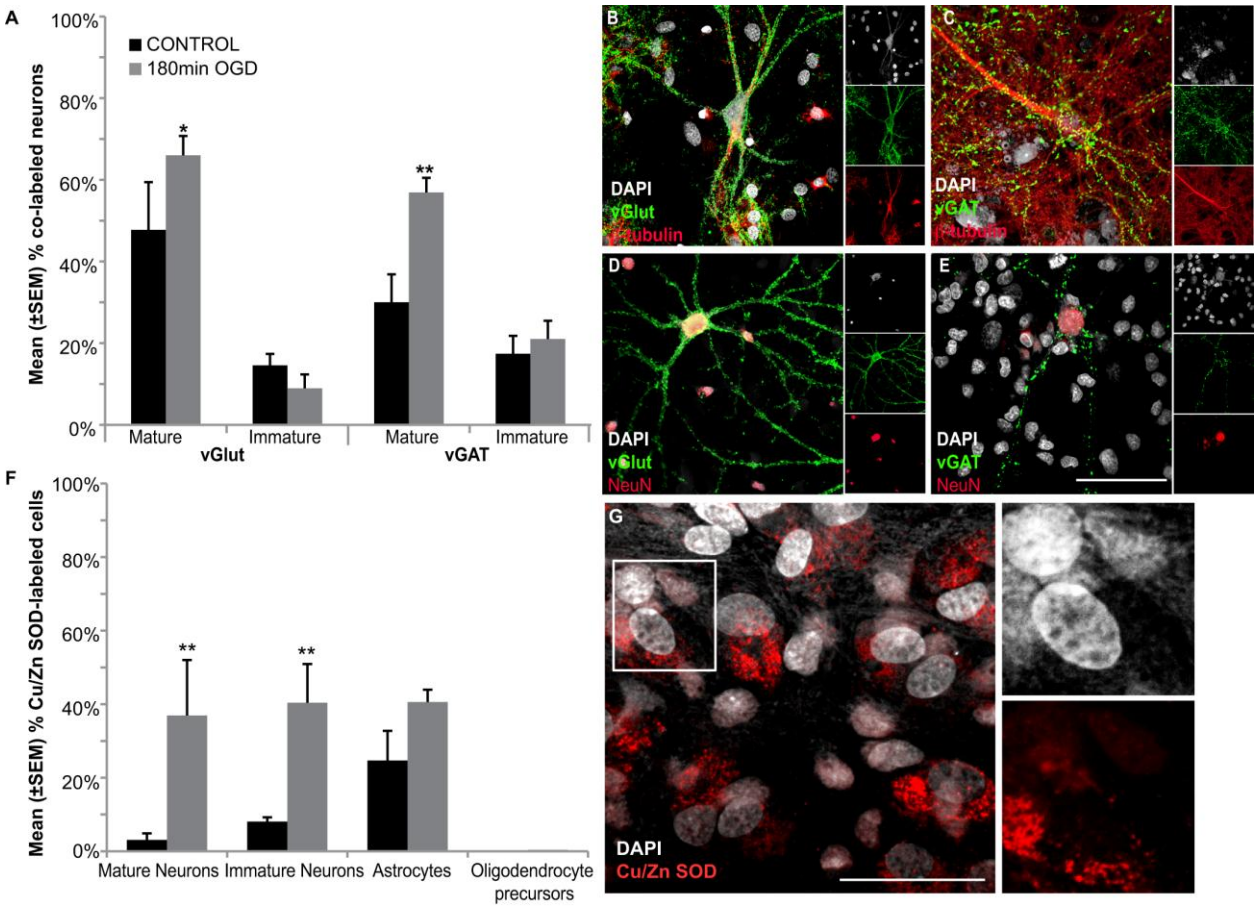

Figure 3-2. OGD increases the presence of vesicular glutamate and GABA transporters, and Cu/Zn SOD. **(A)** The co-expression of mature or immature neuronal markers (NeuN or β-tubulin, respectively) and vesicular glutamate (vGlut) or $GABA_A$ (vGAT) transporter relative to total neurons in culture was quantified, and found to have increased in mature neurons following OGD exposure. **(B-C)** Confocal images show immature neurons (β-tubulin; red) co-expressing **(B)** vGlut, and **(C)** vGAT (green). **(D-E)** Confocal images show mature neurons (NeuN; red) co-expressing **(D)** vGlut, and **(E)** vGAT (green). **(F)** Cells fixed and stained for Cu/Zn SOD, which is expressed in cells as a response to oxidative stress, revealed an increase in SOD^+ neurons following OGD **(G)** Confocal images display a Cu/Zn SOD^+ (red) cell 1d following OGD and DAPI-labeled (grey) cell nuclei. Scale bars – 50μm, $^{\dagger}p<0.1$, $*p<0.05$, $**p<0.01$

Neuronal Network Activity in Primary Cultures Matured Along an Expected Timeline

The activity generated by neurons within each MEA-plated primary culture was recorded for 10 min every 2-3 days to confirm that it had matured into the synchronized bursting expected of mature neuronal networks prior to OGD exposure (Kamioka et al., 1996; van Pelt et al., 2004; Stephens et al., 2012). The mean (±S.E.M.) spike rate, indicative of unit activity increased across days after plating ($F_{(14,210)}$ = 24.1; p < 0.001; Figure 3-3A). Higher spike rates were detected during all recording sessions (Days 6-38) relative to the first recording session (*p's* < 0.001 versus Day 3), and generally increased across weeks (Days 9 and 12 < Days 26-38; Days 15-21 < Days 28-36; *p's* < 0.05) until plateauing in approximately the 4th week after plating. Similarly, the mean (±S.E.M.) percent of active electrodes within MEA dishes also increased across days after plating ($F_{(14,210)}$ = 173; p < 0.001; Figure 3-3B), with increases detected over each recording session (Days 15-38 > 12, 9 > 6 > 3; *p's* < 0.001) until stabilizing on Day 15. Burst rates, indicative of network activity, increased across days after plating ($F_{(14,210)}$ = 30.1; p < 0.001; Figure 3-3C). Burst duration (Figure 3-3D) increased across days after plating ($F_{(14,210)}$ = 18.8; p < 0.001), peaking when superburst patterns were observed (Days 12-18 > Days 21-38; all p < 0.05) and then plateaued by Day 24 (Days 24-38, *n.s.*) with mean (±S.E.M.) burst durations of 0.761 ± 0.097sec at 1.75 ± 0.25 bursts/min. Because network bursting detected on ~75% of active electrodes had plateaued with mean (±S.E.M) spike rates of 2.27 ± 0.25Hz on day 38, we began the OGD experiment on day 40.

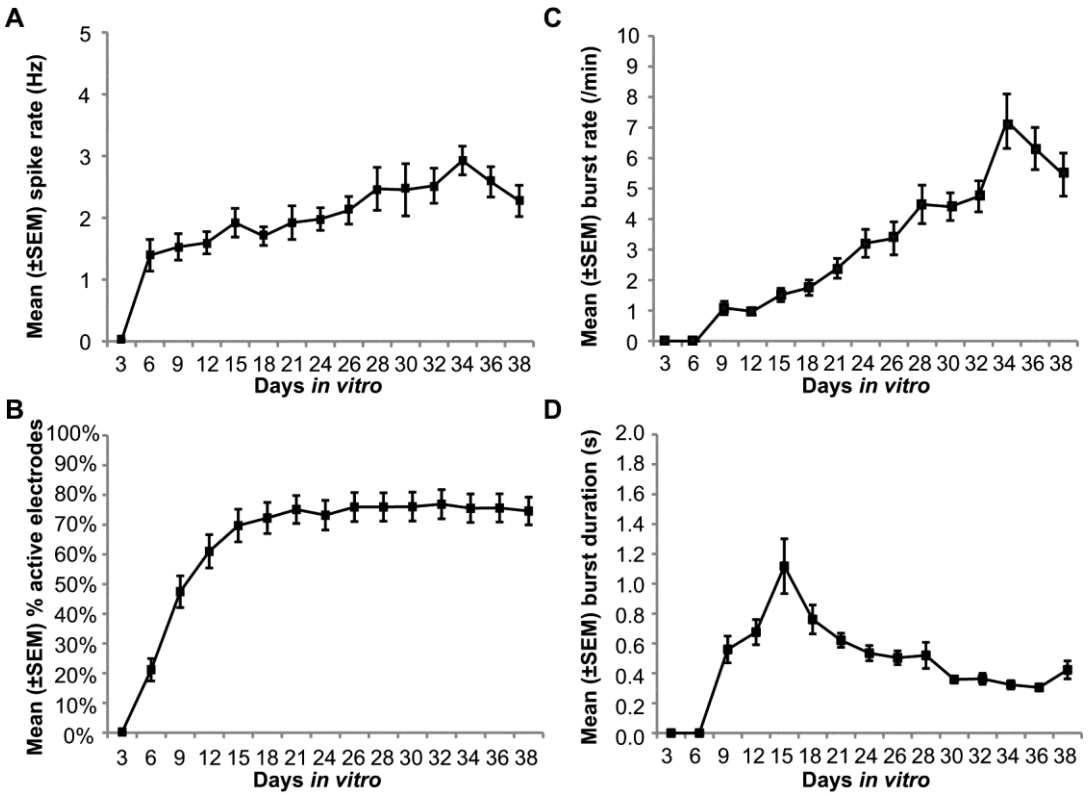

Figure 3-3. Primary cultures provide a stable baseline of activity 35-40d *in vitro*. The electrophysiological activity of primary cultures plated on MEAs was recorded for 10min every 2-3d to confirm the development of 'mature' bursting activity prior to the OGD experiment. **(A)** Action potentials were detected within 3-6d *in vitro*. Mean (±S.E.M.) spike rates (Hz) increased after three weeks *in vitro* (day 24 vs 3 and 6; *p's* < 0.05) and then plateaued by 28d (28-38d; *n.s.*). **(B)** The mean (±S.E.M.) percent active electrodes increased rapidly (days 15-38 > 12, 9 > 6 > 3; *p's* < 0.001) until plateauing by 18d. **(C)** Network bursts were first detected in the second week *in vitro.* Mean (±S.E.M.) burst rates significantly increased after three weeks *in vitro* (day 24 vs. days 9-21; *p's* < 0.05) before stabilizing by 34d (days 34-38; *n.s.*). **(D)** Mean (±S.E.M.) burst duration peaked during immature bursting activity (days 12-18 > days 21-38; *p's* < 0.05) and then plateaued by day 24 (days 24-38, *n.s.*).

OGD Exposure Affects Network Activity in a Time-Dependent Fashion

We next recorded from a subset of MEA-plated cultures (n = 3) during OGD exposure to better understand how variable OGD exposure durations may affect neuronal activity. Figure 3-4A-C shows a representative raster plot of action potentials detected on each electrode (1-59; y-axis) during the first 30 min of OGD (x-axis). Almost immediately after OGD exposure, asynchronous action potentials emerged during the normally relatively quiescent inter-burst-intervals (between network bursts). Burst durations decreased across time and burst activity appeared to degrade by ~12 min after the onset of OGD exposure. A moderate amount of asynchronous activity persisted until ~16 min after the onset of OGD exposure, when the cultures became relatively silent, with the exception of a few occasional isolated action potentials. In support of the hypothesis that OGD exposure initially desynchronizes activity in neuronal networks, we found that the mean (±S.E.M.) percent of spikes generated between bursts increased during the first 4 min of OGD exposure, relative to baseline ($t(14) = 4.39$; $p < 0.001$; Figure 3-4D).

Consistent with the qualitative data we observed on raster plots of neuronal activity, an ANOVA confirmed that the mean (±S.E.M.) percent of active electrodes decreased across time after onset of exposure to OGD ($F_{(30,62)} = 13.2$; $p < 0.001$; Figure 3-4E). Relative to baseline (~77% active electrodes), the percent active electrodes decreased significantly by ~12 min after the onset of OGD exposure when only ~37% of the electrodes were active ($p < 0.05$), continually declining to the point that on average, activity was only detected on ~2 electrodes per min at ~ 27 min.

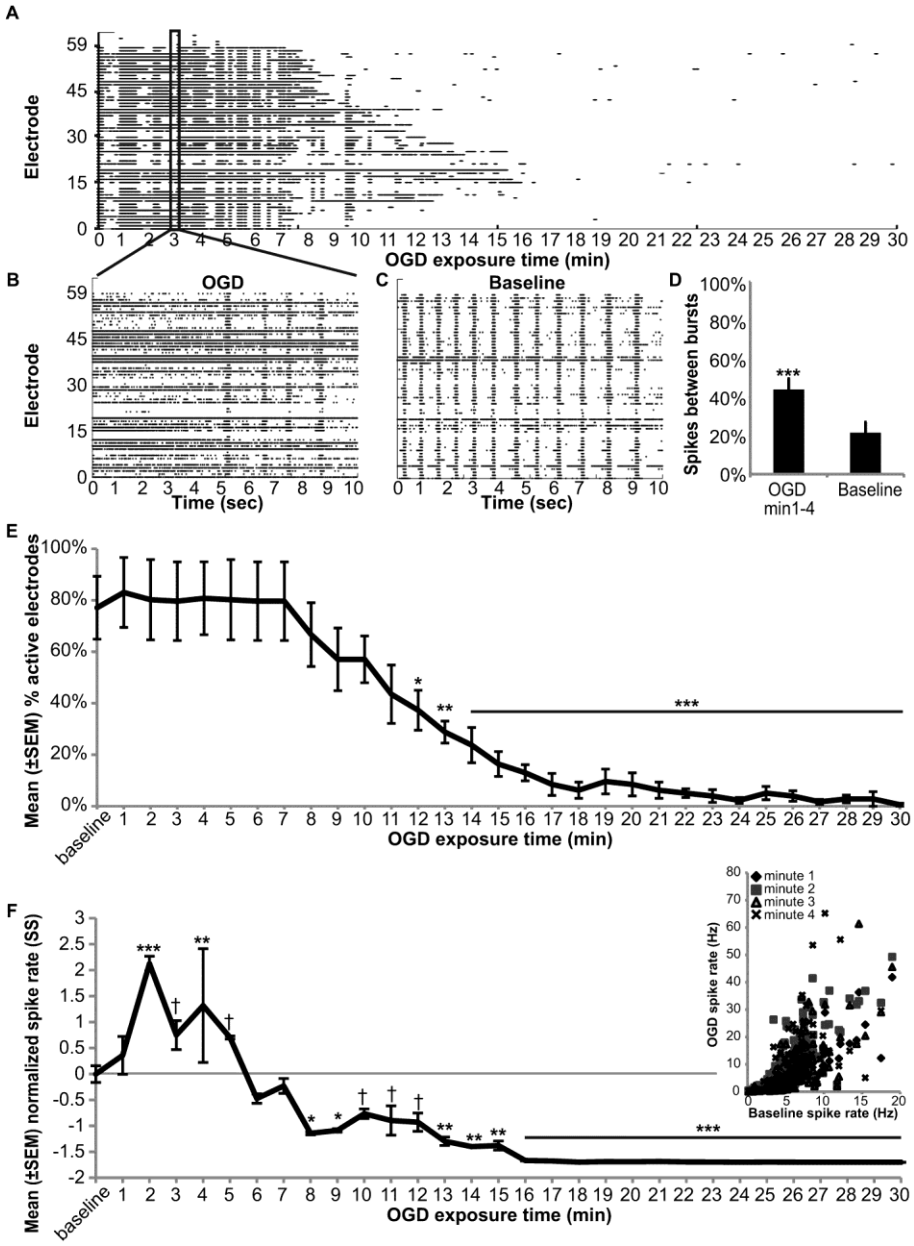

Figure 3-4. MEA recordings during OGD reveal an increase in asynchronous activity before complete silencing. **(A)** A raster plot of action potentials detected during the first 30min of OGD (x-axis) by electrodes 1-59 (y-axis) reveals network bursts were entangled by brief periods of rapid asynchronous firing of individual electrodes that was followed by total silence by ~16min. **(B)** A zoomed-in rasterplot of the boxed 10 sec region during OGD shows more asynchronous firing compared to 10 sec of the same MEA before OGD **(C)**, where the majority of spikes occur during bursts. **(D)** The percent of spikes during interburst intervals increased during minutes 2-4 of OGD, indicating a loss of synchronicity. **(E)** Mean (±S.E.M.) percent active electrodes during OGD exposure significantly decreased by 13min. **(F)** Mean (±S.E.M.)

normalized spike rate of only active electrodes per MEA reveals that OGD initially results in an increase in spike rates per electrode that is silenced by 16 min. Inset reveals a significant correlation between baseline spike rate and increase in spike rate in the first 4 min of OGD (n = 140). $^{\dagger}p < 0.10$*$p < 0.05$, **$p < 0.01$, ***$p < 0.001$

We next examined mean (±S.E.M.) normalized spike rates on active electrodes (Figure 3-4F) during OGD exposure. An ANOVA revealed that spike rates changed significantly with the duration of OGD exposure ($F_{(30,1821)} = 7.2$; $p < 0.001$). During the first 5 min, according to a Fisher LSD post hoc, spike rates either significantly increased (2 and 4 min; *p values* < 0.01) or tended to increase (3 and 5 min *p values* < 0.10) relative to baseline. In fact, baseline spike rate detected on an electrode correlated positively with the spike rate recorded on the same electrode during the first 4 min of OGD exposure when elevated rates were detected (Pearson correlation *r values* = 0.82, 0.77, 0.72 and 0.64, respectively; all *p values* < 0.001; Figure 3-4C Inset), suggesting that spike rate may be related to the number of neurons in contact with each electrode. By 8 min of OGD exposure, spike rates were significantly lower than baseline (8-30 min; *all p values* < 0.05), with little to no activity detected by ~17 min after the onset of OGD exposure.

Neuronal Activity Recovers in an OGD Exposure Duration-Dependent Manner

We first examined the effects of OGD on network activity by quantifying changes in burst rate relative to baseline over the first 16 min of OGD exposure that bursts were detected. An ANOVA revealed that burst rates changed with exposure to OGD ($F_{(15,30)} = 6.15$; $p < 0.001$; Figure 3-5A), tending to decrease at 15 min ($p = 0.06$), and significantly decreasing by 16 min ($p < 0.05$). Although burst duration decreased with time ($F_{(15,30)} = 2.48$; $p < 0.02$; Figure 3-5B), there was no significant change from baseline, suggesting that exposure to OGD produced highly variable burst durations.

Because we observed robust activity for the first 10 min of OGD exposure, we examined the amplitudes of spikes detected on 10 randomly selected active electrodes per MEA during baseline and during the first few minutes of OGD exposure (Figure 3-5C). An ANOVA revealed significant effects of electrode ($F_{(2,54)} = 6.43$; $p < 0.01$), a significant effect of time ($F_{(9,486)} = 4.27$; $p < 0.001$), and the effect of OGD approached significance ($F_{(1,54)} = 13.2$; $p = 0.09$). However, there was a significant interaction effect of OGD and time ($F_{(9,486)} = 3.43$; $p = 0.0004$). The overall mean (±S.E.M.) baseline spike amplitude across MEAs was 40.3 ± 0.6 V, whereas mean amplitude during OGD was 36.7 ± 0.6 V. OGD spike amplitudes during minutes 3, 4, and 6-9 were significantly lower compared to baseline (all $p < 0.05$). The inset is an example of spike amplitude at one electrode, showing all spike forms recorded at the same electrode before OGD at baseline, and during OGD.

MEA-plated cultures that exhibited the synchronous bursting activity indicative of mature neuronal networks (> 40 day-old cultures) were exposed to 20-min, 60-min or 180-min OGD (n = 4). Baseline data were recorded 24h prior to OGD exposure (baseline), and recoveries of neural activity data were recorded 1h and 72h after OGD exposure. The spike rates, as percent of baseline spike rate (Figure 3-5D), and active electrodes, as percent of electrodes active at baseline (Figure 3-5E), were calculated. An ANOVA revealed a significant effects of OGD exposure duration ($F_{(2,27)} = 17.4$; $p < 0.001$) and recovery time ($F_{(2,27)} = 25.5$; $p < 0.001$) and a significant OGD exposure duration by recovery time interaction effect ($F_{(4,35)} = 4.74$; $p < 0.01$) on spike rates. An ANOVA also revealed significant effects of OGD exposure duration ($F_{(2,27)} = 762$; $p < 0.001$) and recovery time ($F_{(2,27)} = 661$; *p values* < 0.001) as well as a significant OGD

exposure duration by recovery time interaction effect ($F_{(4,35)} = 191; p < 0.01$) on the percent of active electrodes.

Following a 20-min exposure to OGD, spike rates had returned to baseline by 1h ($p = n.s.$) and remained at baseline when measured 72h after OGD exposure ($p = n.s.$). Interestingly, the percent of electrodes recording activity did not differ from baseline 1h after (*n.s.*) but slightly and significantly increased 3h after ($p < 0.05$) a 20-min exposure to OGD. Following either a 60-min or 180-min OGD exposure, both spike rates and the percent of active electrodes were significantly lower than baseline when measured either 1 or 72h after exposure (*p values* < 0.001). Note that although neuronal activity appeared to recover within 72h following a 60min OGD exposure, there was a large degree of variability. Taken together these data reveal that neural activity is silenced before significant cell death occurs, and that the degree of recovery in neuronal activity is related to the duration of OGD exposure.

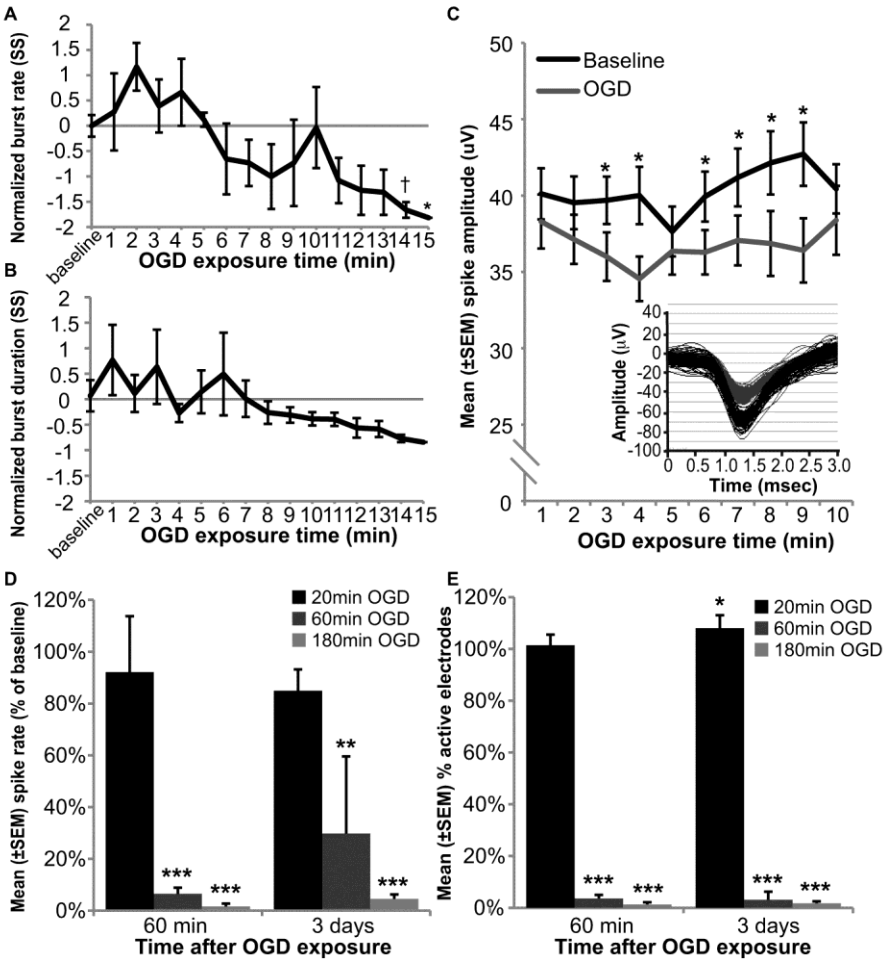

Figure 3-5. OGD causes decreased spike amplitudes, silencing of network activity by ~15 min, but full recovery if reperfused within 20 min. **(A)** Normalized burst rate during the first 15 min of OGD reveals a gradual decline in synchronous activity. **(B)** However, burst duration generally remains unchanged, although OGD initially results in higher variability. **(C)** The amplitude of action potentials was significantly smaller during OGD compared to baseline **(D)** Mean (±S.E.M.) percent change in spike rate approximately 60 min and 3d following 20-min, 60-min or 180-min of OGD-exposure reveals that 20-min of OGD results in recovery of activity, however, 60-180min of OGD results in a significant loss of action potentials. **(E)** Mean (±S.E.M.) percent active electrodes following 20-min, 60-min or 180-min OGD from electrodes active at baseline reveal that 3d after 20-min OGD there was an increase in active electrodes, but 60-180min of OGD exposure resulted in significant loss of active electrodes. $^{\dagger}p < 0.10$*$p < 0.05$, **$p < 0.01$, ***$p < 0.001$

Discussion

In this study, we found that MEA-plated primary neurons exposed to OGD could provide an excellent platform for studying the mechanisms that silence neurons following shorter duration OGD exposures and those that produce cell death, particularly among neurons at longer duration OGD. Specifically, we found little cell death following a 20-60 min exposure to OGD and significant cell death following a 120-180 min exposure to OGD. Acute cell death was particularly detected in the mature neuron population by PI-labeling, as well as cell density, immediately following OGD. There was also a loss of integrity of the morphology of neurons and oligodendrocytes, with notable swollen and fragmented processes. Activity recorded during OGD detected an initial increase in asynchronous spiking, and a decrease in spike amplitude. The extent to which spike rate increased per electrode correlated with the baseline spike rate of the individual electrode, and an increase in interburst activity. There was no initial change to burst rate or duration, but network bursts subsided by approximately 15 minutes. Activity recovered after reperfusion from shorter durations of OGD (20 min), but remained silent after longer durations (60 min).

As expected, cell death among electrophysiologically mature neuronal cultures was dependant upon the duration of exposure to OGD. Consistent with other work showing that 30 min of exposure produced approximately 20% cell death in hippocampal slice cultures (Hirt et al., 2004), we found that 20-60 min of OGD also produced ~20% cell death. This was not significantly elevated relative to the rate of cell death observed in control cultures. Our 120-180 min durations of exposure to OGD killed 35-45% of cell in culture. Interestingly, 120-160 min of OGD, in purely neuronal cultures, produces ~100% death (Meloni et al., 2002). Indeed, mature neurons

appeared to be significantly more vulnerable to cell death that either immature neurons or glial. Therefore, these data suggest that glia protect neurons even in culture systems of dissociated cells.

Prior to OGD exposure, the activity of neurons in primary cultures evolved along an expected timeline (Kamioka et al., 1996; Wagenaar et al., 2006; Stephens et al., 2012). They produced isolated action potentials within a few days after plating, network-wide bursts after about one week, and after evolving through a transient superbursting period, generated a slow, steady 'mature' bursting pattern. The number of active electrodes during OGD exposure significantly decreased by 12 min compared to baseline (37.3 ± 7.8%; $p < 0.03$), and gradually decreased to ~1 electrode by 27 min. Interestingly, normalized spike rate initially increased during the first 5 min of OGD, similar to intracellular recordings on slice preps that reported a rapid initial membrane depolarization at 6 min of OGD (Tanaka et al., 1997; Pisani et al., 1998).

Stroke-induced reductions in blood flow rapidly deplete intracellular ATP, which inactivates ATP-dependent Na^+/K^+ transporters on neuron and astrocyte membranes, and ATP-dependent glutamate transporters on astrocyte membranes (Madl and Burgesser, 1993). Inactivated Na^+/K^+ transporters lead to prolonged elevations in intracellular Na^+ concentrations that produce cell swelling and prolonged depolarizations that contribute to increased extracellular glutamate levels (Calabresi et al., 1999). Inactivated glutamate transporters on astrocytes now not only fail to mop up extracellular glutamate, but spill additional glutamate into the extracellular space (Szatkowski et al., 1990; Zerangue and Kavanaugh, 1996). This could explain the initial spike rate increase and asynchronous activity observed during the first few minutes of

OGD. Failure to maintain the Na^+/K^+ gradient and consequential chronic depolarization may explain the decrease in spike amplitude, and how spike rates declined after 8 minutes of OGD exposure followed by complete silencing by 17 minutes. Previous work reported reduced spike amplitudes after 30-minute OGD in hippocampal slices (Mielke et al., 2007), and an initial increase in beat frequency but reduction in beat amplitude in cardiomyocytes plated on MEAs (Yeung et al., 2009). In the current study, stable normalized burst rates interspersed with asynchronous spikes during the first 4 minutes of OGD also suggest a gradual degradation of synchronous activity. Indeed, burst duration decreased during with time of OGD exposure until no bursts were detected at 16 minutes. Interestingly, there was a significant positive correlation between baseline spike rate per electrode and spike rate during minutes 1-4 of OGD. If an increase in overall activity at individual electrodes is correlated with baseline activity, then elevated spike rates at the onset of OGD likely relates to a higher number of overexcited neurons in contact with that particular electrode.

During severe ischemia, prolonged depolarizations are also associated with the rise of intracellular Na^+, whereas neuronal death is associated with increased intracellular Ca^{2+} (Calabresi et al., 1999). Ultimately, elevated intracellular Ca^{2+} levels render mitochondria dysfunctional. Coupled with generation of reactive oxygen species, including the overexpression of Cu/Zn SOD (Fukui et al., 2002), and the activation of proteases, phospholipases, and endonucleases, neurons ultimately succumb to cell death (Rossi et al., 2000). Cu/Zn SOD blocks cytosolic release of cytochrome C, a critical step in apoptosis, and thus reduces apoptosis after transient focal cerebral ischemia (Fujimura et al., 2000). The percent of Cu/Zn SOD cells was significantly

higher in neurons one day following OGD, but consistently high in astrocytes (~40%) This coincides with reports that free radical production peaks after reperfusion (Perez Velazquez et al., 1997). Although SOD over-expression is a sign of oxidative stress, it can also be neuroprotective (Zaghloul et al., 2012). Therefore, perhaps astrocytes are less vulnerable to OGD because they primarily produce more Cu/Zn SOD.

Previous work has shown that transient focal ischemia in the brain increases $_{v}$glut1 (Kim et al., 2005) until 3d reperfusion, that then decreases after 7d. The proportion of $_{v}$Glut- and $_{v}$GAT-positive, mature neurons increased following OGD, but there was no change in the percent of $_{v}$Glut- or $_{v}$GAT-positive immature neurons. Ischemic conditions lead to cleavage of $_{v}$GAT via calpains inducing a loss of synaptic delivery, leading to a homogeneous distribution along neurites for ~24h following MCA_o. The $_{v}$GAT antibody recognizes both $_{v}$GAT and the cleaved $_{v}$GAT, which may explain the increase (Gomes et al., 2011). However, activation of glutamate transporters results in release of GABA through reversal of glial GABA transporters, which may function as a negative feedback to combat excitation in pathological conditions such as ischemia (Heja et al., 2009). However, there are conflicting reports that $_{v}$GAT may actually decrease after 180min reperfusion (Vemuganti, 2005). 10-minute OGD produced irreversible loss of field potential from striatal slices but AMPA anatagonists (not NMDA antagonists) allowed for recovery (Calabresi et al., 1999). Thus, neuroprotection may be dependent on reducing glutamate release.

Interestingly, oligodendrocyte precursors exhibited increased vulnerability to OGD-induced cell death. Death of oligodendrocytes and their progenitors is mediated by Ca^{2+} influx via nonNMDA receptors by the release of glutamate from autologous reversed

glutamate transport (Fern and Moller, 2000; Tekkok and Goldberg, 2001; Back et al., 2002). $NG2^+$ oligodendrocyte precursors in normal cultures versus 1d post OGD cultures had noticeably condensed and fragmented processes (Figure 3-1K versus 1L), which coincides with previous observations of fragmented and swollen myelinating processes following 60-min MCAo in rats (McIver et al.). $NG2^+$ cells may be susceptible to ischemia because they receive functional glutamatergic synapses from neurons (Mangin and Gallo, 2000) and like neurons, display an inward current and increase in internal $Ca2^+$ during ischemia (Domercq et al.). However, they also actively proliferate in all areas in the brain, which may hide any loss in cell density (Back et al., 2002). Notably, some of the mitotic cells that we detected expressed oligodendrocyte precursor phenotypes.

Reports of recovery following shorter durations of OGD show conflicting results. A 30-min exposure in hippocampal slice cultures led to reduced activity, evident in reduced evoked potential amplitude localized by 6 locations in the CA1, induced by stimulation in the CA3 (Hirt et al., 2004). Using one electrode on the dentate gyrus following OGD, however, there was almost no recovery of evoked population bursts after 10 min OGD (Kass and Lipton, 1982). Previous work using 4-7 electrodes placed in the cortex *in vivo* during transient middle cerebral artery occlusion (MCAo) saw recovery of neuronal activity from 10-180 min OGD (Rosner et al., 1986). With the utility of recording from 59 sites, MEAs provide more data simultaneously, thus less variation in results can be achieved relative to what is found by just a few electrodes. Neural activity recovered following reperfusion after a 20-minute OGD exposure in our experiment, but significantly diminished following a 60-minute OGD exposure. However,

a 60-minute OGD exposure did not lead to significant cell death, indicating that neuron silencing occurs while cells remain viable. In the brain, an area called the penumbra, encircles the necrotic tissue of the stroke core (Astrup et al., 1981). The penumbra is composed functionally silent, yet structurally intact tissue in which blood supply is constrained but energy metabolism is preserved. If shorter durations of OGD cultures are functionally silent but structurally intact, and longer OGD exposed cultures are completely dead, perhaps this model would be most useful by customizing the level of damage to fit the type of injury for the treatment strategy being tested.

The MEA-OGD model provides a global view into the disintegration of neuronal networks, similar to ischemic stroke pathology described *in situ*. Furthermore, the extent of cell death in stroke models may not be the ideal benchmark for establishing OGD models, because activity is silenced long before significant cell death is observed. Future research could benefit by utilizing this model by applying treatments or cells following OGD, and monitoring MEA recordings for functional recovery of individual neurons, as well as network bursts. Perhaps shorter durations of exposure provide a more representative model that could be customized for the type of treatment strategy (treating penumbra or core). OGD-exposed MEA-plated neurons nonetheless, appear to be an effective platform for investigating the effects of hypoxic-ischemic stroke on neuronal networks, and could potentially be utilized as an effective bioassay for cell transplantation or pharmacological treatment on mature neural networks.

CHAPTER 4
ADULT NEURAL PROGENITOR CELLS PARTIALLY PROTECT MICROELECTRODE ARRAY-PLATED NEURAL NETWORKS FROM OXYGEN-GLUCOSE DEPRIVATION-INDUCED DEATH AND SILENCING

Introduction

Neural stem and progenitor cell strategies to repair the central nervous system (CNS) have improved function in some animal models of human disease and injury (Nikkhah et al., 1994a; Dziewczapolski et al., 2003; Ben-Hur et al., 2004; Gao et al., 2006). Understanding whether transplantable cells provide trophic support or integrate functionally into surviving neural circuits would be beneficial for optimizing these strategies and subsequently translating them into the clinical setting. *In vitro* assay systems that collect optical and electrophysiological data simultaneously online may provide insight into how neural stem cell progeny mature over several weeks and affect the activity of these damaged neural circuits, which could be applied to animal models.

Neurons in MEA-plated primary cultures harvested from embryonic day-18 rat neocortices have been well characterized to generate activity that evolves predictably over several weeks to a mature, stable bursting state by 35-40 days (Kamioka et al., 1996; van Pelt et al., 2004; Stephens et al., 2012). In these cultures, asynchronous spike activity emerges coincident with immature neuronal phenotypes (within days) and permanently robust numbers of astrocytes and oligodendrocyte precursors. Superbursting activity emerges coincident with neuronal phenotypes that appear transitional between immature and mature (~2 weeks), and permanent bursting activity emerges coincident with mature neuronal phenotypes (~4 weeks). Previously, we found that NPCs re-evoke developmental superbursting activity in electrophysiologically

mature neural cultures, potentially because some mature neuronal NPC progeny integrate functionally into neural networks (Chapter 2).

MEA-plated cultures are amenable to the development of injury models because their activity can be evoked or monitored for months or years after injury, and/or following the addition of potentially therapeutic factors or cells to their media after injury (Potter and DeMarse, 2001; Scarlatos et al., 2008). Their optical transparency permits the concomitant examination of cell death and the behavior of transplanted cells. The effects of oxygen-glucose deprivation (OGD) on cardiomyocytes behavior has been characterized using MEA technology (Yeung et al., 2009), but the effects of OGD on network activity in stroke models has only been investigated previously using 1-7 electrodes *in vivo* (Kass and Lipton, 1982; Rosner et al., 1986). MEA-plated neural cultures may be particularly valuable as *in vitro* models of stroke because the well-known effects of stroke on both cell death and neuronal network activity can be monitored simultaneously using MEA technology, and culture models of stroke are thought to resemble the *in vivo* post-stroke milieu (Meloni et al., 2001; Harms et al., 2010).

For example, stroke-induced blood hypofusion rapidly depletes ATP stores, which inactivates ATP-dependent Na^+/K^+ pumps on neurons (Madl and Burgesser, 1993), and reverses glutamate transporters primarily expressed on astrocytes (Szatkowski et al., 1990; Zerangue and Kavanaugh, 1996; Calabresi et al., 1999). The combination of prolonged neuronal depolarizations and inefficient clearance of now excess glutamate from the extracellular space by astrocytes leads to excitotoxic cell death and increased oxidative stress among surviving cells primarily because of mitochondrial dysfunction

(Rossi et al., 2000; Fukui et al., 2002). We have previously shown that MEA-plated cultures contain all of the cell players that mediate the effects of stroke *in vivo* (Chapter 3), and that while all cell subtypes express markers of cell death following exposure to long duration OGD, mature neurons and oligodendrocytes may be particularly vulnerable. Here we investigate the effects of NPCs on neural activity and cell death in MEA-plated cultures exposed to OGD.

NPCs transplanted into the cortex, hippocampus, or striatum of rodents following middle cerebral artery occlusion can improve neuronal survival and promote behavioral recovery (Hodges et al., 1996; Sinden et al., 1997; Modo et al., 2002; Harms et al., 2010). Some evidence suggests that neuronal NPC progeny integrate functionally into the post-ischemic hippocampal CA1 region because they eventually express pre- and post-synaptic markers and resemble normal hippocampal neurons found within the infarct (Aoki et al., 1993). Other evidence suggests that NPCs stimulate plasticity or reduce cell death among compromised circuits by secreting trophic factors or by perhaps physically buffering the compromised circuitry from damage (Andres et al., 2010; Modo et al., 2003; Boehler et al., 2007; Lee et al., 2007). Identifying these mechanisms may facilitate their potential capacity for neuroregeneration.

Of course, a hypoxic/ischemic environment may also affect NPC behavior beneficially or detrimentally. The hypothesis that transplantable NPCs are as exquisitely sensitive to systems' regulators as endogenous NPCs (for example, hormones, stress, neuroinflammation, glutamaterigic transmission and life experience (Gould et al., 1992; Cameron et al., 1993; Nilsson et al., 1999; van Praag et al., 1999; Mizumatsu et al., 2003; Monje et al., 2003; Ormerod et al., 2003; Nacher and McEwen, 2006) is highly

conceivable. NPCs express metabolic glutamate receptors that would likely be highly activated in an excitotoxic environment to modulate the proliferative, differentiative and survival-promoting activities they have been implicated in (Melchiorri et al., 2007). Indeed, NPCs resident to the neurogenic hippocampal dentate gyrus proliferate in response to ischemia (Liu et al., 1998; Takagi et al., 1999; Kee et al., 2001; Yagita et al., 2001). Furthermore, neurons are produced in non-neurogenic regions, such as the striatum, following ischemia but their survival is transient (Arvidsson et al., 2002; Zhang et al., 2004; Thored et al., 2006). Therefore, we also investigate the effects of the post-OGD environment on the survival and phenotypes of NPCs and their progeny.

Material and Methods

Primary Culture Preparation

MEA- and LabTek-plated primary cultures were generated from the same pool of dissociated cells for each experiment. Before plating, 100µl of 0.1% (w/v) polyethylene-imine (PEI) in borate buffer (Sigma-Aldrich; St. Louis, MO) was placed on the center of each autoclaved MEA dish or sterile LabTek well. After 1h, the dishes and chambers were rinsed and dried before a 20µl droplet of mouse laminin (Sigma; 1mg/ml in PBS) was placed on the center of each MEA or LabTek well, and incubated at 37°C for 1h.

Embryonic day 18 (E18) Sprague Dawley rat neocortices were purchased from Brain Bits (Springfield, Illinois) and dissociated in papain (20 units/ml; Worthington Biochemical; Lakewood, NJ) and DNase 1 (2000 units/ml, Worthington Biochemical) in GlutaMax-supplemented DMEM (Gibco; Grand Island, NY) at 37°C for 30min before gentle trituration, and pelleted by centrifugation for 3min at 1500rpm. The cells were re-suspended in ‘10% equine serum (Hyclone; Logan, UT), 1% Cellgro Antibiotic-Antimycotic (Mediatech, Inc.; Herndon, VA) in DMEM/GlutaMax and plated by placing a

100µl droplet of cell suspension containing 25K cells directly onto a laminin droplet placed in the center of the MEAs (n = 21) or LabTeks (n = 24; ≥2 wells per staining set) to ensure equal plating densities of ~4,000 cells/mm^2. Once the cells adhered to the substrate (~10min) media was added to 400µl/LabTek well and 1ml/MEA. One half of the media was replaced with fresh media 24h prior to recording sessions, or every 72h to avoid disrupting electrophysiological activity.

Each MEA and LabTek was assigned randomly to one condition group (control, OGD) and treatment group (10K NPCs, 10K HDFs, NPC-conditioned media) after the recording session conducted on day 38 confirmed that the electrophysiological activity among MEA-plated primary cultures had matured and the OGD experiment initiated on Day 40. As expected, neurons in primary cultures generated mean spike rates and burst rates that increased across days after plating (spike rate: $F_{(14,168)} = 28.8$; $p < 0.001$ and burst rate: $F_{(14,168)} = 29.1$; $p < 0.001$) but that did not differ by eventual condition (spike rate: $F_{(1,12)} = 0.68$; *n.s.* and burst rate: $F_{(1,12)} = 0.07$; *n.s.*) or treatment (spike rate: $F_{(2,12)} = 0.01$; *n.s.* and burst rate: $F_{(2,12)} = 1.57$; *n.s.*) groups and no interaction between day and eventual condition or treatment group on either spike rate ($F_{(14,168)} = 1.34$; *n.s.* and $F_{(28,168)} = 0.89$; *n.s.,* respectively) or burst rate ($F_{(14,168)} = 0.71$; *n.s*. and $F_{(28,168)} = 0.61$; *n.s*., respectively) was observed. The mean percent active electrodes within MEA dishes increased across days after plating ($F_{(14,168)} = 198.8$; $p < 0.001$), with increases detected over each recording session (days 15-38 > 12, 9 > 6 > 3; all $p < 0.001$) until stabilizing on day 15. Eventual condition and treatment groups were not different ($F_{(1,12)} = 1.12$; *n.s*. and $F_{(2,12)} = 1.89$; *n.s*., respectively), and the interaction between days after plating and eventual condition or treatment group on percent active electrodes did not

approach significance ($F_{(14,168)}$ = 1.11; *n.s*. and $F_{(28,168)}$ = 1.41; *n.s*., respectively). Burst duration increased across days after plating ($F_{(12,144)}$ = 13.5; $p < 0.001$), peaking when immature bursting was observed (days 12-18 > days 21-38; all $p < 0.05$) and then plateaued by day 24 (days 24-38, *n.s.*) with mean (±S.E.M.) burst duration of 0.41 ± 0.235sec at 5.97 ± 0.75bursts/min. Again, eventual condition and treatment groups were not different ($F_{(1,12)}$ = 0.02; *n.s*. and $F_{(2,12)}$ = 1.28; *n.s*., respectively), and the interaction between days after plating and eventual group did not approach statistical significance ($F_{(12,144)}$ = 1.41; *n.s*.). However, there was an interaction effect between eventual treatment group and day ($F_{(24,144)}$ = 2.0; $p < 0.01$), probably due to high variability in burst duration during immature activity (days 12-18). Because planned comparisons confirmed that mean spike rates, burst rates, percent active electrodes and burst durations recorded before day 40 were consistent between groups, in line with previous reports (Stephens et al., 2012), we felt confident that the random distribution of primary cultures did not confound our interpretation of the effects of cell addition on neuronal activity following OGD exposure.

Neural Progenitor Cells

The adult rat hippocampal NPC line used in the present study was generated from the hippocampus of a male GFP-expressing Wistar-TgN(CAG-GFP)184Ys rat obtained from our breeding colony maintained by University of Florida Animal Care Services and descended from breeding pairs obtained from the Rat Resource and Research Center (University of Missouri, MO). All animals produced in this specific pathogen free facility-housed colony (maintained on a 12:12h light:dark cycle at 23 ± 1^0 C) were pair-housed after weaning in shoebox cages and had free access to water and food (Teklad LM-485;

Harlan Laboratories). Briefly, the rat was anaesthetized with CO_2 and decapitated. The hippocampi were rapidly dissected, minced and digested enzymatically in papain (2.5 units/ml), dispase II (1 unit/ml; Roche Applied Science; Indianapolis, IN) and DNase I (250 units/ml) at 37°C for 45min. The dissociated tissue was fractionated in a 50% and then 20% Percoll solution by centrifugation (20,000xg) for 10min. The fractionated cells were plated onto poly-L-ornithine/laminin-coated dishes in DMEM/F-12 (1:1) medium (Mediatech; Manassas, VA) containing 10% fetal bovine serum (FBS) for 24h and then the medium was replaced with DMEM/F12 (1:1) w/ L-glutamine supplemented with N2 (Invitrogen) and 20ng/ml recombinant human fibroblast growth factor-2 (FGF-2; Peprotech, Inc. Rocky Hill, NJ). NPCs were passaged 10x before use. Before co-culture, NPCs were resuspended in primary growth media to wash out any remnant growth factors that may influence primary cells. Conditioned media was collected fresh from NPCs grown on 10cm tissue culture plates in 8ml of primary cell growth media, and centrifuged to filter any aggregate NPCs that could have been collected.

Human Dermal Fibroblasts

Adult HDFs (Cascade Biologics; Portland, OR) were plated at ~150,000 cells were plated into T-25 culture flasks with 5ml media (Media 106 (Gibco), 2% FBS, 1% antibiotic-antimycotic, hydrocortisone (1µg/ml), heparine (10µg/ml), epithelial growth factor (EGF; 10ng/ml) and FGF-2 (3ng/ml)), grown to confluency (~7d), and passaged via trypsinization. After three passages, $1x10^6$ cells were suspended in 1ml media, 1ml lentitangerine (produced by DD; titer=$1.8x10^7$TU/mL), and 10µl polybrene (Sigma-Aldrich). The cells were incubated in virus for 30min at room temperature and then overnight at 37°C. The following day the media was replaced. At 5d post-infection,

58.03+/-.03% cells expressed $_m$tangerine. HDFs were passaged ~6x after infection before being used in co-culture.

Oxygen-Glucose Deprivation and Co-Culture

Before the MEA experiment, we first examined total cell death in 40d LabTek-plated primary cultures exposed to OGD for 60, 120 or 180 min, or 100% fresh media change (control), in order to find an optimum exposure time to conduct the experiments. Immediately following OGD, the cultures were PI-stained and fixed. An ANOVA on the mean (±S.E.M.) % of $DAPI^+$ nuclei co-labeled with the cell death marker PI revealed significant effects of OGD exposure duration on cell death ($F_{(3,23)} = 31.51$; $p < 0.001$). Significantly more dead cells were found in cultures exposed to OGD for either 120 minutes ($p < 0.001$) or 180 minutes ($p < 0.001$; Figure 1A), relative to control cultures. We further characterized the effects of a 180 min OGD exposure on cell death and oxidative stress because this duration of OGD exposure killed ~50% of the culture, which often serves as a benchmark for exploring the mechanisms of stroke-induced cell death (Meloni et al., 2001; Hirt et al., 2004).

On day 40, media was removed and replaced with DMEM containing no glucose, no sodium pyruvate, low L-glutamine (Gibco) pre-exposed to hypoxia overnight, for MEAs/LabTeKs in OGD groups,. The dishes were immediately placed in the hypoxic incubator (37°C, 0.1% O_2, 5.0% CO_2, 94.1% N_2) for 3h. Media was completely replaced with fresh media in non-OGD groups in order to rule out any effect due to media change. After OGD, the DMEM was replaced with fresh media, and the cultures were returned to an incubator at normal conditions (37°C, 20.95% O_2, 5.0% CO_2). 24h after OGD, the media was removed and 100µl of primary growth media containing 10K

NPCs, 10K HDFs or no cells was added to the center of each LabTek chamber and MEA. Once the NPCs adhered to the primary cultures (5-10min), media was added to fill the dish. Every 24h-48h, ~50% of the media was replaced with fresh media. The conditioned-media control group was given 75% fresh media, 25% NPC-conditioned media, for the remainder of the experiment.

Immunocytochemistry and Microscopy

LabTek-plated cells were exposed to PI (250 μg/ml TBS; Sigma-Aldrich) to visualize dead/dying cells, fixed with 4% paraformaldehyde for 10min and rinsed repeatedly between immunostaining steps with TBS (pH 7.4). The cells were blocked in 3% normal donkey serum (NDS) and then incubated overnight in a cocktail of 3 primary antibodies that included rabbit or mouse anti-β-Tubulin (1:500; Covance), mouse anti-neuronal nuclei (NeuN; 1:500; Chemicon International), guinea pig anti-glial fibrillary acidic protein (GFAP; 1:750; Advanced Immunochemical), rabbit anti-NG2 (1:1000; Chemicon International), and Cu-Zn superoxide dismutase (SOD; 1:500; Millapore) at 4°C. The following day, the sections were incubated in the appropriate FITC-, Cy3-, or Cy5-conjugated secondary antibody (1:500; Jackson ImmunoResearch) for 4hrs. Then cells were DAPI-stained (1:20,000 in TBS for 20min; Calbiochem), and cover slipped under PVA-DABCO.

lmages of LabTek-plated cultures were taken using a Zeiss LSM 710 fully spectral Laser Scanning Confocal Microscope with a 63x oil objective (5 z-stacks) of $DAPI^+$ and $GFP/DAPI^+$ cells in primary cultures and in co-cultures. Visible laser line intensities were maintained below 15%. $DAPI^+$ cells with appropriate neuron, astrocyte and oligodendrocyte morphologies and intense staining with the appropriate antibodies in

primary cultures served as positive controls to which exposure levels and gain were set to exclude nonspecific staining among GFP^+ cells (NPCs). 8-10 non-overlapping images were taken diagonally from each corner of >2 wells (>500 cells/well). We measured the % PI^+ and %SOD^+ DAPI-labeled nuclei, and primary or GFP+ (NPC-generated) cells co-labeled with the mature neuronal marker NeuN, the immature neuronal marker β-tubulin, the astrocyte marker GFAP, and the oligodendrocyte precursor marker NG2. Mitotic and pyknotic nuclei were noted in each image. Fluorescent images of immunostained MEAs were taken using a Zeiss reflected-light fluorescent microscope using a 20x or 40x objective.

Electrophysiology

Electrophysiological data was collected from cells plated on MEAs with a square grid of 60 planar Ti/TiN microelectrodes 30μm in diameter, spaced 200μm apart (Multichannel Systems, Reutlingen, Germany). As described previously (Stephens et al., 2012), changes in extracellular potential were recorded over 10min sessions every 3d from 3-39d after plating to establish a basline, and then every 4d from 21-68d after OGD to record recovery. Briefly, the signal from 59 recording electrodes was sampled at 25 kHz, and amplified and digitized using Multichannel Systems (Reutlingen, Germany) MEA1060 amplifier and A/D hardware. Cultures were allowed to equilibrate for ~2min after being placed into the amplifier before recording was initiated. Action potentials, or spike events, were detected online as upward or downward excursions beyond 5x the median threshold from the quiescent signal that was estimated during a brief “learning phase” before each recording session. Waveforms between 1ms before and 2ms after detected spikes were saved and used to remove duplicate detections of

multiphasic spikes and visually inspect for artifacts. These data was saved for further offline processing using a software package custom written by Dr. Thomas B. DeMarse.

Electrodes exhibiting spike frequencies <0.1Hz were deemed “inactive” based on previous reports of minimum firing rates (Latham et al., 2000; Boehler et al., 2007). Network bursts were defined in previous reports as >3 or >14 electrodes spiking within 0.1- 2sec inter-spike intervals (Gross and Kowalski, 1999; Tabak and Latham, 2003; van Pelt et al., 2004). We categorized a network burst as a cluster of spikes across >10 electrodes within 0.2sec inter-spike intervals. From these data, spike and burst frequency, number of active electrodes and burst duration were quantified offline.

Statistical Analysis

Statistical tests were conducted using Statistica Software (StatSoft, Inc; Tulsa, OK). Viability (% total PI+ and pyknotic cells), oxidative stress (% total SOD-labeled cells), division (% mitotic), densities and proportions of neurons ($NeuN^+$, β-$tubulin^+$, or β-$tubulin/NeuN^+$) or glia ($GFAP^+$ or $NG2^+$) primary ($DAPI^+$) or NPC ($DAPI/GFP^+$) cell origin was compared between OGD- versus fresh media-exposed cultures supplemented with NPC-conditioned media versus cells (NPCs or HDFs) at 0, 1, 7, 14 or 28 days after reperfusion using mixed ANOVAs. Unit activity (% change in spike rate) and network activity (burst rate, percent active electrodes, and burst duration) were compared between OGD- versus fresh media-exposed cultures supplemented with NPC-conditioned media versus cells (NPCs versus HDFs) across days using repeated measures ANOVAs. Newman-Keuls post-hoc tests were employed to explore main and interaction effects and α levels = 0.05.

Results

NPCs Transiently Protect Neural Cultures from Death and Oxidative Stress

Primary cultures were exposed to 3h OGD or a complete media change at 40d *in vitro*, before being PI-stained and fixed 1d, 7d, 14d, or 28d after reperfusion with and without cell addition (Figure 4-1A-G). An ANOVA revealed significant effects of OGD ($F_{(1,30)}$ = 153; $p < 0.001$), cell addition ($F_{(2,30)}$ = 15.4; $p < 0.001$), and survival time after reperfusion ($F_{(3,90)}$ = 83.8; $p < 0.001$) and significant interactions between OGD and survival time after reperfusion ($F_{(3,90)}$ = 74.5; $p < 0.001$), cell addition and survival time after reperfusion ($F_{(6,90)}$ = 7.59; $p < 0.001$) as well as an overall interaction ($F_{(6,90)}$ = 4.86; $p = 0.001$) on dead cells (Fig 4-1A). The mean (±S.E.M.) % of PI^+ (dead) cells was significantly increased by OGD ($p < 0.001$) and more cell death was observed on Days 1 (*p values* < 0.001) and 7 (*p values* < 0.001) versus 14 and 28. Regardless of OGD exposure or survival time after reperfusion, cell death was significantly lower in NPC versus NPC-conditioned media- ($p < 0.05$) or fibroblast- ($p < 0.001$) supplemented cultures. In control cultures, fibroblast addition slightly increased cell death on Day 1 (*p values* < 0.1) relative to NPC-conditioned media or NPCs. Although lower %'s PI^+ cells were detected in OGD-exposed cultures that had been supplemented with NPCs relative to either NPC-conditioned media or fibroblasts on Day 1 (*all p values* < 0.05), the percentage was not decreased to those observed in control cultures (*all p values* < 0.05). In addition, the beneficial effect of NPC- versus NPC-conditioned media- or fibroblast-addition among OGD exposed cultures was not apparent at 7d, 14 or 28d after reperfusion (*p values* = *n.s.*). Our data include several important findings. First, we found similar effects of OGD on cell death among cultures fed every 72h with fresh media (data not shown) or with NPC-conditioned media (Figure 1A), suggesting that

any protective effects of NPCs on OGD-exposed cultures are cell contact dependent. Second, we found that fibroblasts slightly increase cell death. Third, we show that NPCs may partially mitigate the immediate, but perhaps not later, effects of OGD exposure on cell death.

To further determine the effect of OGD with and without cell addition on overall cell death, we calculated the proportion of pyknotic $DAPI^+$ nuclei indicative of dying cells (Figure 4-1B). An ANOVA revealed significant effects of OGD on the percent of pyknotic cells ($F_{(1,78)} = 103.0$; $p < 0.001$) and days after reperfusion ($F_{(3,234)} = 25.0$; $p < 0.001$), but no effect of cell addition ($F_{(2,78)} = 2.05$; *n.s.*). OGD interacted with days after reperfusion ($F_{(3,234)} = 14.4$; $p < 0.001$) to affect the percent of dying cells observed. Overall, relatively few pyknotic cells were detected. However, OGD increased the percent of pyknotic nuclei (***p's*** < 0.001) detected at Days 1 (*p values < 0.001*) and 7 (*p values < 0.001*) relative to Days 14 and 28.

To quantify the effects of OGD on oxidative stress, we quantified the proportion of cells that expressed Cu/Zn SOD in cultures exposed to a full media change or OGD, 1d, 7d, 14d, or 28d after reperfusion with and without cell addition (Figure 4-1C). An ANOVA revealed significant effects of OGD ($F_{(1,42)} = 37.3$; $p < 0.001$), cell addition ($F_{(2,42)} = 22.0$; $p < 0.001$), and survival time after reperfusion ($F_{(3,126)} = 6.69$; $p < 0.001$), and interaction effects between OGD exposure and survival time after reperfusion ($F_{(3,126)} = 4.20$; $p < 0.01$), cell addition and survival time after reperfusion ($F_{(6,126)} = 4.76$; $p < 0.001$), and OGD exposure and cell addition ($F_{(2,42)} = 4.07$; $p < 0.05$), but no overall interaction ($F_{(6,126)} = 1.36$; *n.s.*). The percent of cells expressing Cu/Zn SOD was significantly higher after OGD exposure ($p < 0.001$) and at 1 versus Days 14 and 28

after OGD exposure (*p values* < 0.01). In control cultures, the percent of cells expressing Cu/Zn SOD was similarly low regardless of cell addition but in OGD-exposed cultures, the percent of cells expressing Cu/Zn SOD was significantly higher in the NPC-conditioned media supplemented cultures on Day 1 versus either the fibroblast- ($p < 0.001$) or NPC-supplemented cultures (p values < 0.001) and in NPC-conditioned media supplemented control cultures (p values < 0.001). These data suggest that either fibroblasts or NPCs can minimize oxidative stress in cultures exposed to OGD.

As neurons transition from immature to mature they alter their expression of neuron-specific proteins. For example, young neurons that exhibit immature morphological and electrophysiological phenotypes express proteins such as β-tubulin while those expressing more mature phenotypes express proteins such as NeuN. We also find that there is a transitional neuronal phenotype that expresses both β-tubulin and NeuN (Figure 4-1D; and Chapter 2). To ascertain whether immature, transitioning or mature neurons in our primary cultures may be selectively vulnerable to the effects of OGD, we quantified densities of β-tubulin$^+$ immature neurons, β-tubulin/ NeuN$^+$ transitioning neurons and NeuN$^+$ mature neurons. An ANOVA revealed no significant effect of OGD ($F_{(1,42)} = 0.12$; *n.s.*), but did reveal significant effects of neuron age ($F_{(2,42)} = 28.0$; $p < 0.001$) and survival time after reperfusion ($F_{(3,126)} = 3.38$; $p < 0.05$) on cell densities. Furthermore OGD by neuron age ($F_{(2,42)} = 26.4$; $p < 0.001$), neuron age by survival time after reperfusion ($F_{(6,126)} = 7.27$; $p < 0.001$) and an overall ($F_{(6,126)} = 2.83$; $p < 0.05$) interaction effects were observed. Overall, higher densities of immature neurons were observed than either transitioning ($p < 0.001$) or mature neurons ($p < 0.001$).

Regardless of neuron age, neuron densities were higher at 14 and 28 days after reperfusion relative to Days 7 (*p values* < 0.05). These effects largely appear due to the fact that densities of immature neurons increased at 14 and 28 days after OGD exposure (*p values* < 0.001). These data suggest that young neurons may either be produced or driven to express β-tubulin in the weeks following OGD.

Because the densities of immature neurons increased after OGD exposure, we quantified mitotic-phase nuclei to determine whether OGD potentially stimulated the production of new neurons. Mitotic phase nuclei were detected at extremely low levels (< 1%; data not shown). However, an ANOVA revealed significant effects of OGD ($F_{(1,78)}$ = 10.5; $p < 0.01$) and cell addition ($F_{(2,312)}$ = 8.94; $p = 0.001$), but not survival time after reperfusion ($F_{(3,234)}$ = 0.20; *n.s.*) on the % of mitotic cells. Overall OGD exposure increased the % percent of mitotic nuclei ($p < 0.01$) a higher % of mitotic nuclei were detected in NPC- versus NPC-conditioned media or fibroblast-supplemented cultures regardless of OGD exposure (*p values* < 0.01). While OGD exposure and cell addition *could* have stimulated the proliferation of latent NPCs in our primary cultures, the low density of mitotic figures that we detected after OGD did not warrant further investigation.

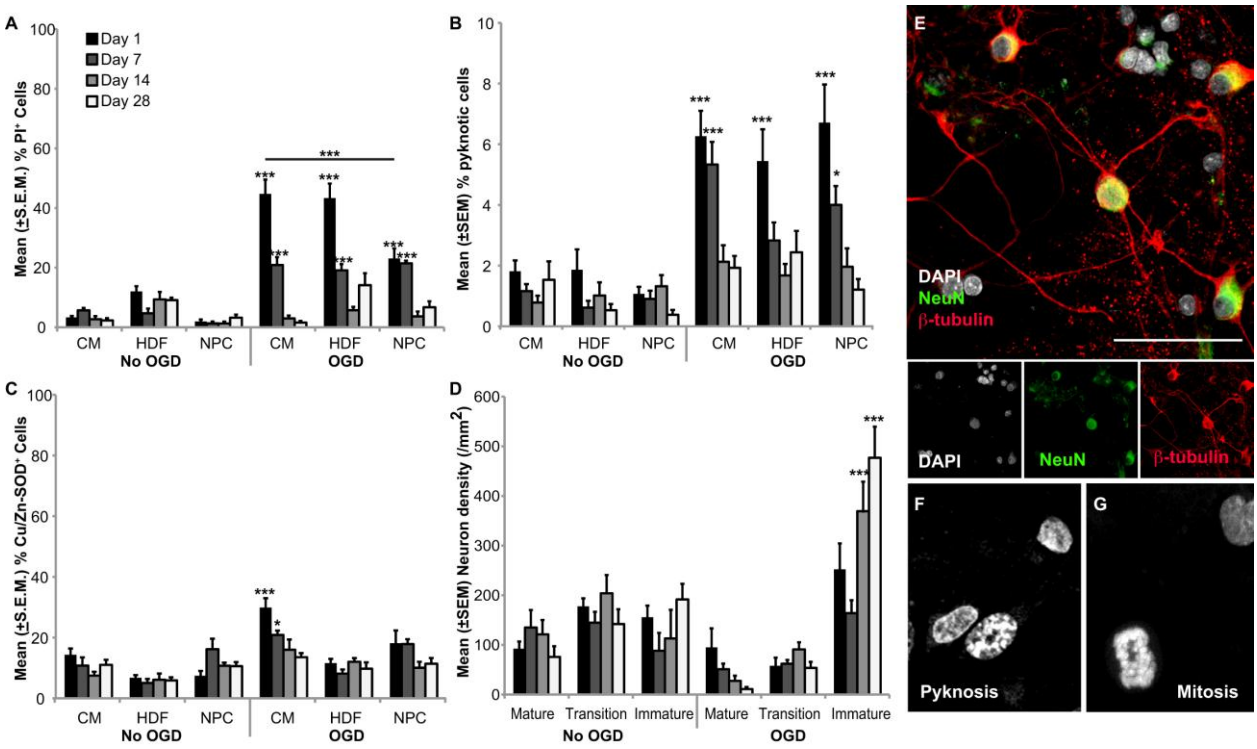

Figure 4-1. NPC addition ameliorates initial cell death, but OGD increases the presence of pyknotic nuclei, Cu/Zn SOD and immature neurons. **(A)** The percent of PI^+ dead/dying cells increased following OGD, but by 14d was no different from controls. When comparing the different treatment groups (n = 4), there was a significant increase in cell death following OGD in all groups; however, fewer dead cells were found in the NPCs-added group 1d post-OGD. **(B)** Pyknotic nuclei were also quantified to measure dying cells (n = 4), and increased in all groups following OGD that declined with time, and did not differ from controls 28d post-OGD. **(C) %** Cu/Zn SOD cells increased latently, increasing 7-14d following OGD. There were fewer Cu/Zn SOD^+ cells in the NPCs-added group and no difference in the HDFs-added group (n = 4). **(D)** The transition of neurons from immature (β-$tubulin^+$), to transition (β-$tubulin^+$ and $NeuN^+$), mature ($NeuN^+$) states overtime was monitored (n = 8). OGD actually increased the number of immature neurons, 14 and 28 days after OGD exposure. Confocal images of **(E)** transition-state neurons, **(F)** middle cell in pyknosis, with a fragmented nucleus, and **(G)** bottom left nucleus in mitotic phase, with condensed, splitting chromatin, compared to normal top right nucleus. Mitotic-phase nuclei, although present at low levels (<1%), did increase after OGD. Scale bar – 50μm. $^{\dagger}p<0.1$, $*p<0.05$, $**p<0.01$, $***p<0.001$

OGD-Exposed Primary Cells Did Not Affect NPC Fate

The obvious goal of stem/progenitor cell strategies is to promote the integrity of compromised circuitry, but testing the effects of variable post-injury milieus on the behavior of neural stem/progenitor cells may also be critical to generating clinically relevant strategies. We first examined the fate of GFP^+ adult hippocampal NPCs 1d, 7d, 14d or 28d after their addition to OGD-exposed or control cultures (Figure 4-2A). An ANOVA revealed similar fates among GFP^+ co-cultured with OGD-exposed versus control cultures ($F_{(1,24)} = 0.01$; *n.s.*), but preferred phenotypes among co-cultured GFP^+ cells ($F_{(3,24)} = 60.9$; $p < 0.001$) that changed significantly with time after co-culture ($F_{(3,72)} = 17.0$; $p < 0.001$), and interacted significantly with time after co-culture ($F_{(9,72)} = 6.03$; $p < 0.001$). A higher percent of NPC-derived (GFP^+) cells expressed β-tubulin versus NG2, GFAP or NeuN (*all p values* < 0.001), more NeuN than GFAP or NG2 (*all p values* < 0.05) and more GFAP than NG2 (p = 0.05). Relative to Day 1, the percent of GFP/β-$tubulin^+$ neurons increased at Day 7 ($p < 0.001$), Day 14 ($p < 0.001$) and Day 28 ($p < 0.001$). More GFP/NeuN+ progeny were detected at Days 28 and 14 versus Days 1 and 7 when none were detected (*p values* < 0.01). The percent of GFP/$GFAP^+$ astrocytes remained consistently low across days in co-culture and few GFAP/$NG2^+$ oligodendrocyte precursors were detected. Interestingly, NPCs grown alone for 28d differentiated into 7.7 ± 1.3% β-$tubulin^+$ immature neurons and 7.9 ± 3.2% $GFAP^+$ astrocytes (data not shown).

The proportion of GFP^+ NPCs to total DAPI-labeled cells in co-culture approached significance among conditions ($F_{(1,120)} = 3.67$; $p = 0.060$) and significantly changed with time ($F_{(3,120)} = 28.0$; $p < 0.001$), but there was no interaction effect ($F_{(3,120)} = 1.06$; *n.s.*).

Overall, there were fewer NPC-derived cells in the OGD group ($p = 0.058$). There were ~3-5% GFP^+ NPCs of all cells in co-culture 1d after plating that increased over time (all $p < 0.001$), suggesting that NPCs continued to divide (Figure 4-2B). By 28d, there was a significantly smaller percent of GFP^+ cells in the OGD-exposed co-cultures than the controls ($p < 0.05$), which could be contributed to faster differentiation into mature cells and/or an increase in primary cell division.

The proportion of $_m$tangerine$^+$ HDFs (Figure 4-2G) to total DAPI-labeled cells in co-culture did not differ with condition ($F_{(1,120)} = 0.07$; *n.s.*), but changed over time ($F_{(3,120)} = 11.2$; $p < 0.001$) After one day in co-culture, HDFs composed ~3-5% of total DAPI-labeled cells and decreased slowly over time (14d and 28d versus 1d, all $p < 0.05$), suggesting that either the HDFs may not survive long-term in co-culture.

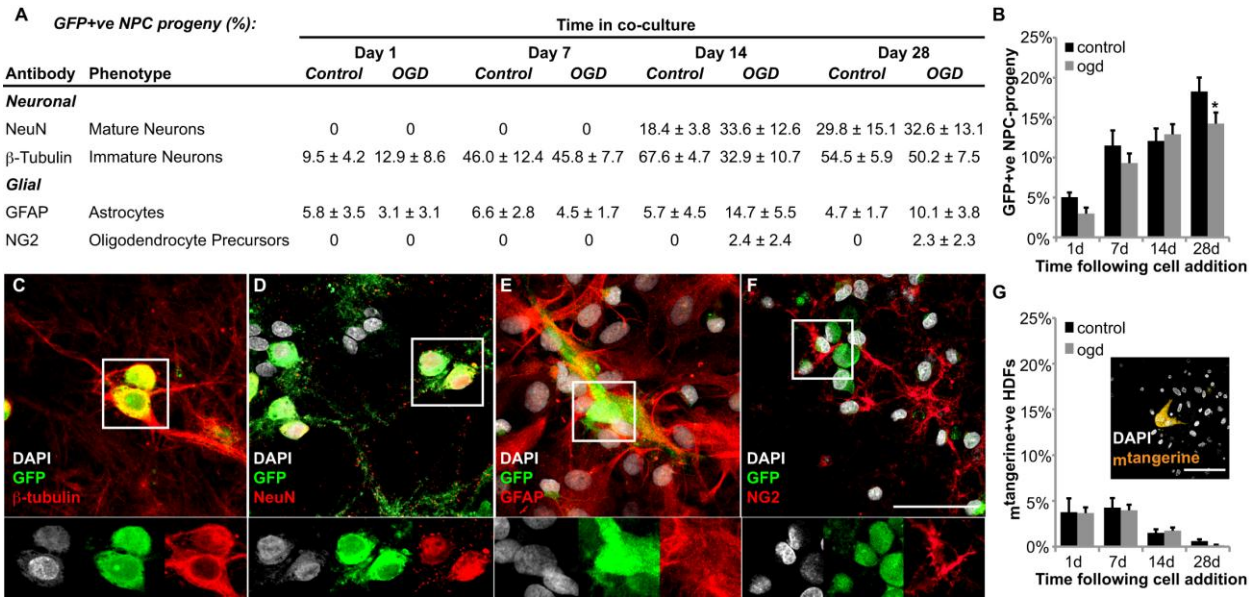

Figure 4-2. Co-culture with OGD-exposed cells does not affect NPC fate. The proportion of adult hippocampal NPC-derived (GFP^+) cells expressing immature neuronal (β-tubulin), mature neuronal (NeuN), astroglial (GFAP) or oligodendroctye precursor (NG2) at 1d, 7d, 14d and 28d after addition to OGD-exposed or non-OGD cultures was quantified on confocal laser scanning microscope digital images (n = 4). **(A)** NPC progeny began to express immature neuronal and glial markers 1-7d in co-culture. $NeuN^+$ mature neurons derived from NPCs were observed 14d in co-culture, and few (~2%) $NG2^+$ oligodendrocyte precursors derived from NPCs were observed in co-culture with OGD-exposed primary cells. **(B)** The proportion of GFP^+ NPCs to total DAPI-labeled cells in co-culture was ~3-5% at plating and increased over time, suggesting that NPCs continued to divide (n = 16). By 28d, there was a siginificantly smaller percent GFP^+ cells in the OGD-exposed co-cultures than the controls (*$p < 0.05$), which could be contributed to faster differentiation into mature cells (evident in greater % phenotypes at 14d) and/or and increase in primary cell division. **(C-F)** Confocal images of GFP^+ NPC progeny (green) expressing β-tubulin (**C**; red), NeuN (**D**; red GFAP (**E**; red) and NG2 (**F**; red). Note that all cell nuclei are DAPI-labeled (grey). **(G)** The proportion of $mtangerine^+$ HDFs to total DAPI-labeled cells in co-culture was ~3-5% at plating and decreased slowly over time (n = 16). Inset is a confocal image showing $mtangerine^+$ HDFs (orange) and DAPI-labeled nuclei (grey). Scale bar – 50μm.

Neuronal Death Following OGD is Less Severe Following NPC Addition

The percent of PI^+ cells co-labeled with NeuN, β-tubulin, GFAP and NG2 was quantified in order to detect a cell type that may be more susceptible to OGD (Figure 4-3A). There was, in fact, an effect of phenotype ($F_{(3,72)} = 12.5$; $p < 0.001$), an interaction of OGD and phenotype ($F_{(3,72)} = 5.49$; $p < 0.01$), treatment group and phenotype ($F_{(6,72)} = 3.31$; $p < 0.01$), and day and phenotype ($F_{(9,216)} = 6.39$; $p < 0.001$), as well as an overall interaction effect ($F_{(18,216)} = 2.44$; $p < 0.01$). The mean (±S.E.M.) percent of PI^+ cells significantly increased following exposure to OGD ($p < 0.001$) and on Days 0-14 after reperfusion (*all p values* < 0.001). The percent of PI^+ NeuN-labeled mature neurons was higher (~19%) than the percent PI^+ β-tubulin-labeled immature neurons (~13%; $p < 0.01$), $GFAP^+$ astrocytes (~6%; $p < 0.01$) and $NG2^+$ oligodendrocyte precursors (~11%; $p < 0.01$). In fact, astrocytes had the lowest proportion of dead/dying cells (all $p < 0.05$). The conditioned media and HDFs-added treatment groups had significantly higher PI^+ mature neurons one day after OGD (all $p < 0.001$), however, the percent of PI^+ mature neurons in the NPCs-added group was not statistically higher than the conditioned media non-OGD control group. However, by one week, the conditioned media OGD group was not different from non-OGD controls, the HDFs-added OGD group had more dead/dying mature neurons, and the percent PI^+ NeuN-labeled cells approached significance in the NPCs-added group ($p = 0.072$). One day following OGD, the conditioned media OGD group and HDFs-added had significantly higher proportions of PI^+ immature neurons and astrocytes (*p's* < 0.001), but by 7d was not significantly different from controls. On the other hand, the percent PI^+ immature neurons in the NPCs-added OGD did not differ from the conditioned media control at 1d 14d and 28d,

but approached significance at 7d following OGD ($p = 0.072$). In addition, the percent of PI^+ astrocytes in the NPCs-added group did not differ from conditioned media controls. The conditioned media OGD group and HDFs-added OGD group had significantly higher proportions of PI^+ oligodendrocyte precursors (all $p < 0.001$), but by 14d were not significantly different from controls. The percent PI^+ NG2-labeled cells in NPCs-added OGD group did not differ from controls at 1, 14 and 28, but was significantly different at 7d ($p < 0.001$). These data suggest NPC addition ameliorated some cell death, at least temporarily.

A *%PI+ve cells:*

			Time after cell or media addition							
			Day 1		Day 7		Day 14		Day 28	
Antibody	**Phenotype**	**Post-OGD treatment**	***Control***	***OGD***	***Control***	***OGD***	***Control***	***OGD***	***Control***	***OGD***
Neuronal										
NeuN	Mature Neurons	Conditioned media	**2.9 ± 2.9**	94.6 ± 13.2***	5.1 ± 3.5	22.1 ± 2.8	1.3 ± 0.8	8.3 ± 8.3	1.4 ± 1.4	7.1 ± 4.7
		HDFs	**37.0 ± 6.2**$^{\tau}$	94.2 ± 5.3***	11.0 ± 8.6	42.2 ± 17.0*	6.3 ± 4.0	19.8 ± 15.9	8.3 ± 8.3	0.0 ± 0.0
		NPCs	**0.0 ± 0.0**	**32.8 ± 16.5**	1.8 ± 1.8	37.5 ± 23.9$^{\tau}$	1.4 ± 1.4	9.8 ± 6.1	0.0 ± 0.0	2.8 ± 2.8
β-Tubulin	Immature Neurons	Conditioned media	**3.1 ± 3.1**	51.8 ± 8.5***	6.1 ± 3.8	35.0 ± 7.7	0.9 ± 0.9	1.7 ± 1.2	1.6 ± 1.6	2.8 ± 2.1
		HDFs	**9.4 ± 2.6**	**19.5 ± 6.8**	4.2 ± 2.5	**65.6 ± 7.2*****	8.5 ± 3.6	3.9 ± 2.2	8.3 ± 3.3	12.5 ± 4.7
		NPCs	**0.0 ± 0.0**	25.5 ± 2.4	1.5 ± 1.5	38.7 ± 9.2$^{\tau}$	0.0 ± 0.0	11.4 ± 5.1	0.0 ± 0.0	5.2 ± 3.4
Glial										
GFAP	Astrocytes	Conditioned media	**4.3 ± 2.1**	47.5 ± 3.2***	4.6 ± 1.6	16.4 ± 5.2	0.0 ± 0.0	1.5 ± 0.9	0.9 ± 0.6	0.3 ± 0.3
		HDFs	**6.2 ± 3.6**	21.2 ± 2.8	0.0 ± 0.0	9.2 ± 2.0	0.0 ± 0.0	0.0 ± 0.0	6.3 ± 4.9	0.0 ± 0.0
		NPCs	**0.0 ± 0.0**	**8.0 ± 2.3**	0.0 ± 0.0	20.8 ± 5.4	0.0 ± 0.0	0.0 ± 0.0	1.3 ± 1.3	1.2 ± 1.2
NG2	Oligodendrocyte Precursors	Conditioned media	**0.0 ± 0.0**	73.1 ± 8.1***	**0.0 ± 0.0**	58.3 ± 4.8*	0.0 ± 0.0	0.0 ± 0.0	2.5 ± 2.5	0.0 ± 0.0
		HDFs	**0.0 ± 0.0**	54.2 ± 20.8***	**0.0 ± 0.0**	**0.0 ± 0.0**	3.6 ± 3.6	4.2 ± 4.2	5.0 ± 5.0	0.0 ± 0.0
		NPCs	**0.0 ± 0.0**	**11.8 ± 6.8**	**0.0 ± 0.0**	50.0 ± 28.9***	0.0 ± 0.0	0.0 ± 0.0	0.0 ± 0.0	5.0 ± 5.0

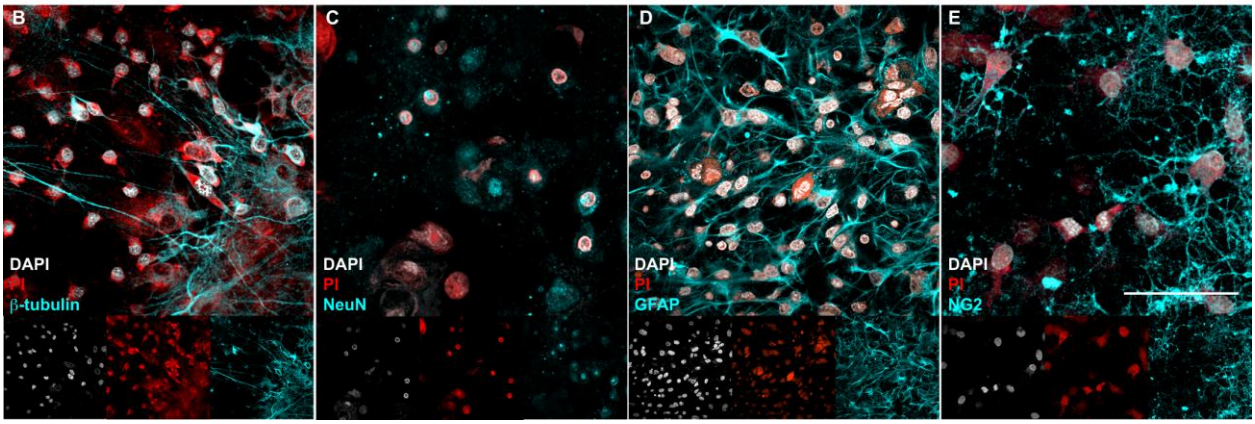

Figure 4-3. Cell death following OGD is less severe with NPC addition. Cells were stained with propidium iodide (PI) and subsequently fixed immediately following 3h of OGD or after total fresh media change (control), or 1d, 7d, 14d, or 28d later. **(A)** The percent PI^+ cells expressing different phenotype markers was quantified (n = 4), and revealed that NPC addition may protect mature neurons, and glia, at least after 1d. **(B-E)** Confocal images display PI^+ nuclei (red) of dead/dying cells 1d following OGD co-expressing β-tubulin (cyan; **B**), NeuN (cyan; **C**), GFAP (cyan; **D**) and NG2 (cyan; **E**). Note that all cell nuclei are DAPI-labeled (grey). Scale bar – 50μm. $^{\tau}p$<0. 1, *p<0.05, and ***p<0.001 versus conditioned media control; **BOLD** p<0.05 versus conditioned media OGD

OGD Increases Cu/Zn SOD in Neurons Immediately, and in Astrocytes After 14 Days

When the percent of Cu/Zn SOD^+ NeuN-, β-tubulin-, GFAP- and NG2-labeled cells was quantified to detect a cell type that may react to OGD with Cu/Zn SOD more than others (Figure 4-4A), there was an effect of phenotype ($F_{(3,72)} = 87.6$; $p < 0.001$), an interaction of condition and phenotype ($F_{(3,72)} = 2.76$; $p < 0.05$), treatment and phenotype ($F_{(6,72)} = 6.15$; $p < 0.001$), and day and phenotype approached significance ($F_{(9,216)} = 1.72$; $p = 0.086$), as well as an overall interaction effect of all four independent variables ($F_{(18,216)} = 1.82$; $p < 0.05$). After 1d, the conditioned media OGD group had a greater number of SOD^+ mature and immature neurons (all $p < 0.001$) that subsided by 7-28d (*n.s.*). On the other hand, there was a greater percent of SOD^+ astrocytes at 7d and 14d (all $p < 0.01$). The percent SOD^+ cells in the HDFs-added and NPCs-added OGD groups generally did not differ from the conditioned media control group, except for more Cu/Zn SOD^+ astrocytes at 7d (all $p < 0.001$).

A

%Cu/Zn-SOD+ve cells:

			Time after cell or media addition							
			Day 1		Day 7		Day 14		Day 28	
Antibody	Phenotype	Post-OGD treatment	*Control*	*OGD*	*Control*	*OGD*	*Control*	*OGD*	*Control*	*OGD*
Neuronal										
NeuN	Mature Neurons	Conditioned media	**3.1 ± 1.8**	36.9 ± 15.1***	7.9 ± 3.8	21.3 ± 5.7	0.0 ± 0.0	18.8 ± 6.0	2.4 ± 2.4	0.0 ± 0.0
		HDFs	**1.1 ± 1.1**	**13.1 ± 7.6**	0.0 ± 0.0	0.0 ± 0.0	0.0 ± 0.0	0.0 ± 0.0	0.0 ± 0.0	12.5 ± 8.0
		NPCs	**0.0 ± 0.0**	**0.0 ± 0.0**	0.0 ± 0.0	4.0 ± 2.6	4.2 ± 4.2	3.1 ± 3.1	3.2 ± 2.1	0.0 ± 0.0
β-Tubulin	Immature Neurons	Conditioned media	**8.1 ± 1.2**	40.4 ± 10.5***	3.4 ± 2.0	17.3 ± 3.6	0.0 ± 0.0	5.3 ± 5.3	4.7 ± 1.0	2.0 ± 1.6
		HDFs	**0.0 ± 0.0**	**0.0 ± 0.0**	0.0 ± 0.0	2.3 ± 2.3	0.0 ± 0.0	3.4 ± 3.4	0.0 ± 0.0	2.5 ± 1.5
		NPCs	**6.2 ± 3.7**	29.1 ± 11.2	0.0 ± 0.0	0.0 ± 0.0	6.9 ± 4.7	5.5 ± 3.4	0.0 ± 0.0	2.1 ± 2.1
Glial										
GFAP	Astrocytes	Conditioned media	24.7 ± 8.1	40.6 ± 3.4	**8.2 ± 3.2**	34.8 ± 4.6**	**8.7 ± 3.3**	36.7 ± 6.8**	17.7 ± 4.1	27.1 ± 6.3
		HDFs	**6.9 ± 3.5**	**24.2 ± 3.0**	**6.3 ± 6.3**	11.0 ± 6.4$^{\tau}$	21.9 ± 10.3	26.6 ± 9.5	6.3 ± 2.9	**2.9 ± 2.9**
		NPCs	25.3 ± 8.1	41.8 ± 8.3	46.1 ± 15.4***	46.6 ± 9.0***	24.6 ± 2.7	**7.7 ± 4.4**	20.9 ± 4.3	22.4 ± 6.3
NG2	Oligodendrocyte Precursors	Conditioned media	0.0 ± 0.0	12.5 ± 12.5	0.0 ± 0.0	47.6 ± 9.0	0.0 ± 0.0	0.0 ± 0.0	0.0 ± 0.0	0.0 ± 0.0
		HDFs	0.0 ± 0.0	0.0 ± 0.0	0.0 ± 0.0	0.0 ± 0.0	0.0 ± 0.0	0.0 ± 0.0	0.0 ± 0.0	0.0 ± 0.0
		NPCs	3.6 ± 3.6	0.0 ± 0.0	0.0 ± 0.0	0.0 ± 0.0	0.0 ± 0.0	4.2 ± 4.2	0.0 ± 0.0	0.0 ± 0.0

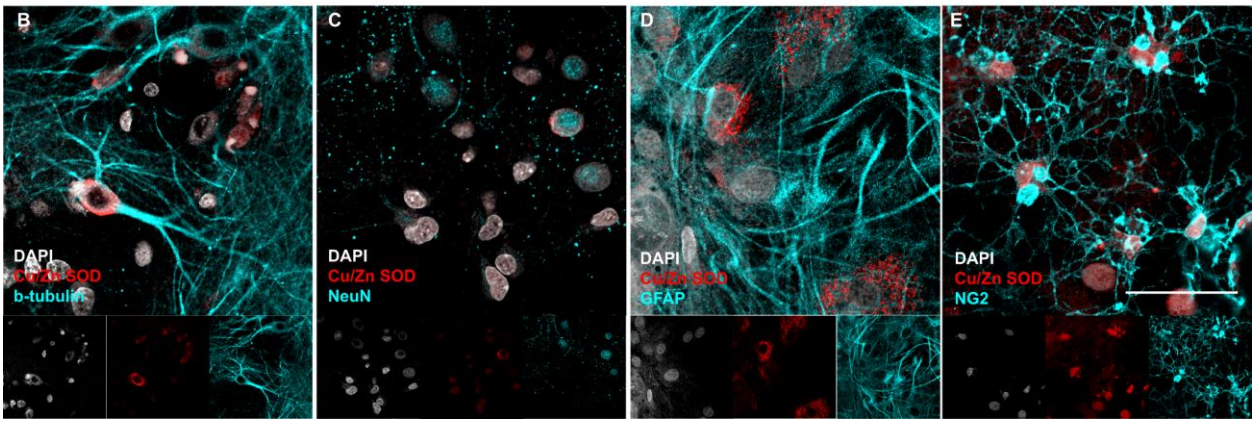

Figure 4-4. Oxidative stress increases in neurons following OGD, but is not changed by NPC addition. **(A)** Cells were fixed and stained for Cu/Zn SOD, which is expressed in cells as a response to oxidative stress, immediately following (0d) 3h of OGD or after total fresh media change (control), or 1d, 7d, 14d, or 28d later (n = 4). The %Cu/Zn SOD^{+} cells expressing different phenotype did not change in response to NPC addition. **(B-E)** Confocal images display Cu/Zn SOD^{+} (red) cells 1d following OGD co-expressing immature neuronal marker β-tubulin (cyan; **B**), mature neuronal marker NeuN (cyan; **C**), astrocyte marker GFAP (cyan; **D**) and oligodendrocyte precursor marker NG2 (cyan; **E**). Note that all cell nuclei are DAPI-labeled (grey). Scale bar – 50μm. $^{\tau}p$<0. 1, **p<0.01, and ***p<0.001 versus conditioned media control; **BOLD** p<0.05 versus conditioned media OGD

NPC Addition After OGD Protects Neural Activity and May Lead to New Activity

In order to characterize recovered activity following OGD, the type of activity detected in groups following OGD was quantified as Recovered (active electrodes at baseline that remained active after OGD), Transiently New (inactive electrodes at baseline that became active for 1 day after OGD), and Lasting New (inactive electrodes at baseline that became active for >1 day after OGD; Figure 4-5A-B). The proportions of the different types of recovery changed with treatment group ($F_{(2,18)} = 4.25$; $p < 0.05$), and there was a preferred type of recovery ($F_{(2,18)} = 258$; $p < 0.001$), but there was no significant interaction effect ($F_{(4,26)} = 1.19$; *n.s.*). All groups had similar numbers of transiently new electrodes (*n.s.*), which was the preferred type of recovery compared to Recovered and Lasting New (*all* $p < 0.001$). Although Lasting New activity appeared in the NPCs-added group, it appeared on only a few electrodes (n.s.). Interestingly, the NPCs-added group had significantly more recovered activity (all $p < 0.05$).

NPC Addition Leads to Partial Recovery of Network Activity Following OGD

The electrophysiological activity of primary cultures plated on MEAs was recorded for 10 min every 3-4d following OGD and subsequent cell addition, to record any recovery of activity following OGD (Figure 4-6). Mean (±S.E.M.) spike rates (Hz) changed with condition ($F_{(1,11)} = 18.8$; $p < 0.01$), and there was an overall interaction effect of condition, treatment and day ($F_{(14,84)} = 1.85$; $p < 0.05$). Spike rates in the OGD groups were significantly lower than the control groups ($p < 0.01$). Compared to the conditioned media control group, spike rates recovered in the NPCs-added OGD group (days 1; $p = 0.062$; days7-14, *n.s.*), but recovery did not last (day 28; $p < 0.05$).

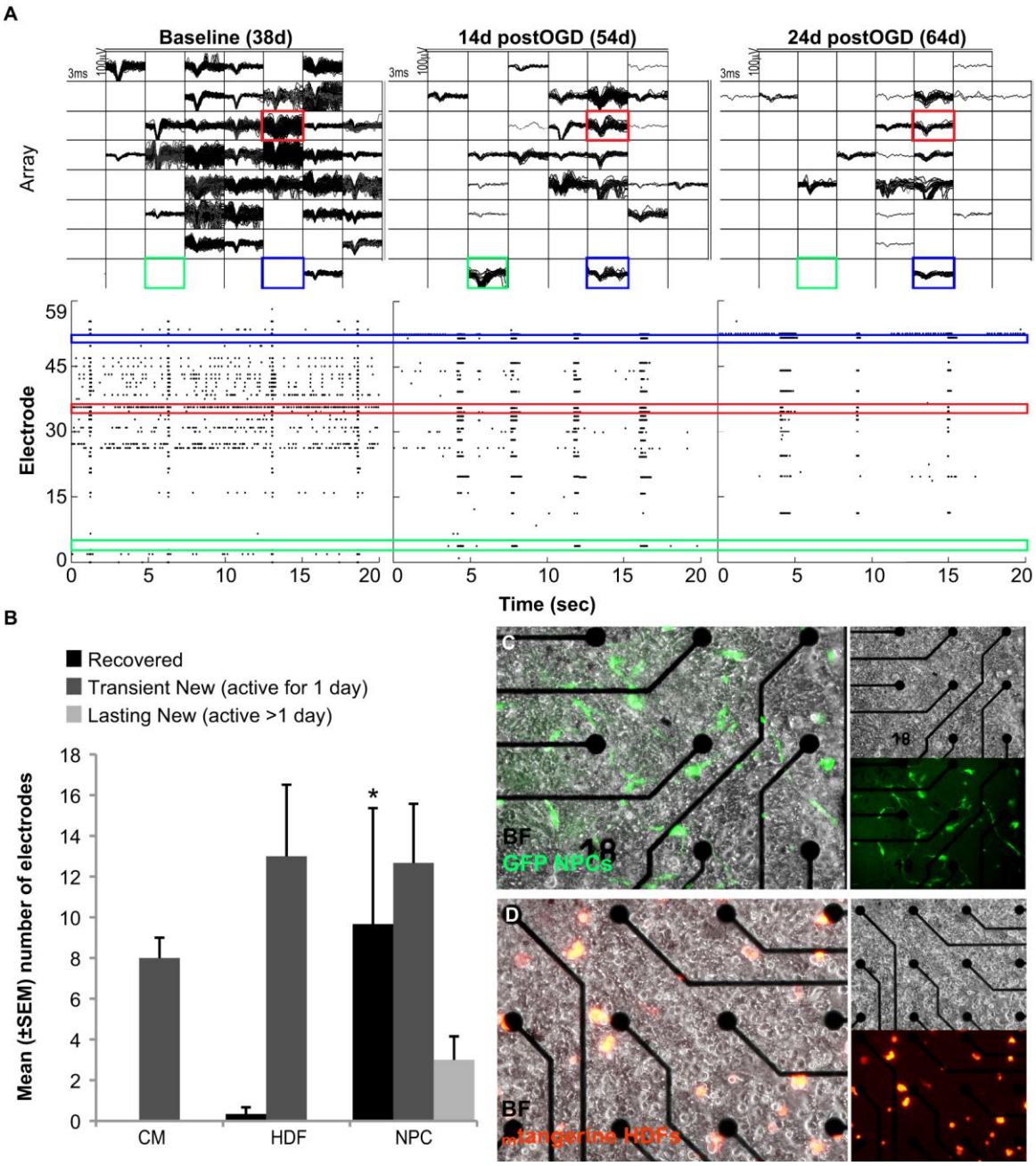

Figure 4-5. NPC addition may lead to new activity. **(A)** MEA context plots show the added spikeforms of detected spikes on the electrodes respective to the arrangement on the array. The example shown is 20s from an NPCs-added OGD MEA before OGD at baseline day 38, 14d post OGD/NPC-addition and 24d post OGD/NPC-addition. Below are the respective raster plots of the spikes detected at all 59 electrodes (y-axis) across time (x-axis). The colored boxes highlight examples of electrodes and corresponding spikes on the rasterplots that was categorized as Recovered (red; active electrodes at baseline that remained active after OGD), Transient New (green; inactive electrodes at baseline that became active for 1 day after OGD), and Lasting

New (blue; inactive electrodes at baseline that became active for >1 day after OGD). **(B)** All groups had similar numbers of transiently new electrodes, but few electrodes recovered exclusively in the NPCs-added group (n = 3). However, the NPCs-added group had significantly more lasting new activity. Reflected-light fluorescent images merge with bright field images show **(C)** GFP-expressing NPCs, and **(D)** $_{m}$tangerine-expressing HDFs after 1d in co-culture with primary neural cells plated on MEAs.

The conditioned media or HDFs-added OGD groups did not show recovery (all $p < 0.05$; Figure 4-6A). The mean (±S.E.M.) percent active electrodes had a significant effect of condition ($F_{(1,11)} = 83.1$; $p < 0.001$), and day ($F_{(7,84)} = 4.14$; $p = 0.001$), but not with treatment ($F_{(2,11)} = 0.508$; *n.s.*). However, there was an overall interaction effect ($F_{(14,84)} = 2.21$; $p < 0.05$). There were significantly fewer active electrodes in the OGD groups (all $p < 0.001$). However, the NPCs-added OGD group had significantly more active electrodes compared to the conditioned media OGD group (days 1-14, all $p < 0.05$; day 28, $p = 0.099$; Figure 4-6B). Network bursts, on the other hand, had a significant effect of OGD ($F_{(1,11)} = 88.1$; $p < 0.001$) but did not have an overall interaction effect of condition, treatment and day ($F_{(14,84)} = 0.49$; *n.s.*). Although bursts were observed in the NPCs-added group after OGD, the rates were small and variable and did not differ from the conditioned media or HDFs-added groups (Figure 4-6C). Mean (±S.E.M.) burst duration significantly changed with condition ($F_{(1,11)} = 6.92$; $p < 0.05$), but not with day ($F_{(7,84)} = 0.81$; *n.s.*), or with treatment ($F_{(2,11)} = 2.13$; *n.s.*). However, there was an overall interaction effect ($F_{(14,84)} = 2.29$; $p < 0.01$). Burst duration peaked in the NPC-added OGD group after 4-8d (all $p < 0.10$) in co-culture and then plateaued by day 16 (Figure 4-6D).

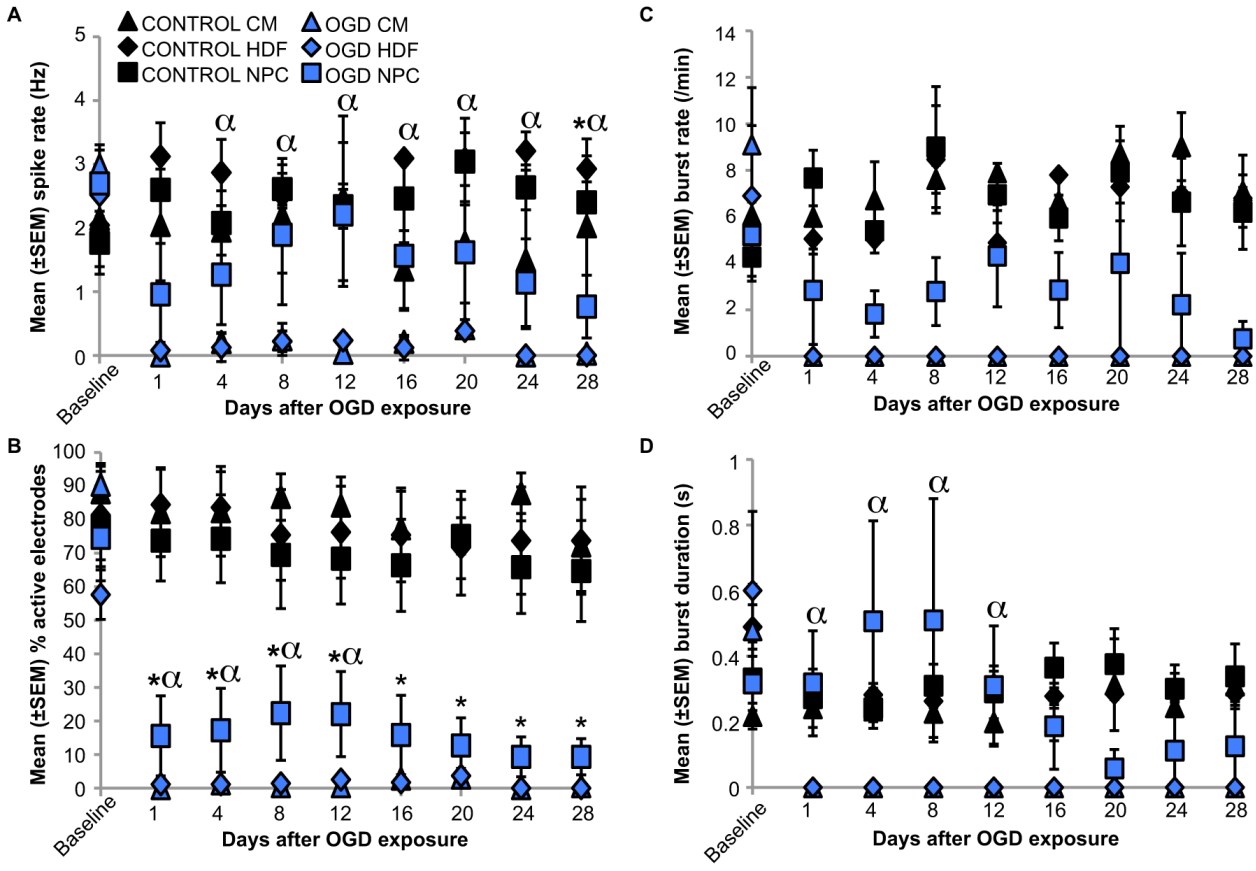

Figure 4-6. NPC addition after OGD leads to partial recovery of neural activity. The electrophysiological activity of primary cultures plated on MEAs was recorded for 10min every 4d following OGD and subsequent cell addition 1d later, to record any recovery of activity following OGD (n = 3). **(A)** Mean (±S.E.M.) spike rates (Hz) recovered in the NPCs-added OGD group, but not in the conditioned media or HDFs-added OGD groups after 8d in co-culture. **(B)** The mean (±S.E.M.) percent active electrodes show that activity recovered in the NPCs-added OGD group, but not in the conditioned media or HDFs-added groups. The number of active electrodes was not different in the NPCs-added OGD group compared to the conditioned media OGD group after 24d. **(C)** Network bursts also recovered in the NPCs-added group, however, the rates were small and variable and did not differ from the conditioned media or HDFs-added groups. **(D)** Mean (±S.E.M.) burst duration peaked in the NPC-added OGD group after 4-8d in co-culture and then plateaued by day 16. **p*<0.05 NPC OGD versus CM control; $^{\alpha}$*p*<0.05 NPC OGD versus CM OGD

Discussion

In this study, we demonstrated that MEA-plated primary neurons exposed to OGD could be an effective platform for investigating the effects of OGD and potentially protective/regenerative effects of adult NPCs on mature neural networks. As expected, OGD produced significant cell death and oxidative stress that persisted for a week after OGD exposure. Surprisingly, we noted a latent (2-4 weeks post-injury) increase in the proportion of primary cells that expressed the immature neuronal marker β-tubulin, which could reflect injury-induced neurogenesis or perhaps even de-differentiation. Primary cells in OGD-exposed cultures that were supplemented with NPCs exhibited low-level proliferation as well as decreased death among mature neurons and oxidative stress among all cells, at least in the first week after injury. Importantly, the post-OGD milieu of these primary cultures did not overtly affect the fate of NPCs or their progeny. Network activity in electrophysiologically mature primary cultures was silenced immediately by exposure to OGD. In fresh media control cultures, NPCs but not NPC-conditioned media or HDFs stimulated a developmental pattern of superbursting activity (Chapter 2). In OGD-exposed cultures NPCs, but not NPC-conditioned media or HDFs partially protected single unit and network activity for ~2 weeks, which may be significant in a clinical setting where combined approaches are employed. Our observations that NPC-conditioned media neither affects the activity of control or OGD-exposed cultures and that novel activity emerges in both control and OGD-exposed primary cultures after NPC supplementation suggests that NPC progeny are capable of integrating functionally into established neural circuits potentially after injury.

In vivo and *in vitro* ischemic stroke can kill cells in a number of ways. Signs of necrotic cell death include aberrant Ca^{2+} and Na^{+} homeostasis, mitochondrial and

organelle swelling, ruptured plasma membranes and randomly degraded DNA (Walker et al., 1988). Signs of apoptotic cell death include condensed cytoplasm, fusing of the endoplasmic reticulum with the plasma membrane and nuclear material that becomes fragmented into “clumps” before cellular fragmentation become obvious (Wyllie et al., 1981). Because PI and other cell death markers cannot differentiate between necrotic and apoptotic cell death (Banasiak et al., 2000) we quantified pyknotic (condensed and/or fragmented) nuclei as a secondary measure of apoptosis following OGD. Overall, OGD exposure increased the percent of PI^+ dead cells and pyknotic dying cells in the 2 weeks after exposure. NPC addition decreased the percent PI^+ cells but did not impact the percent of pyknotic cells. While these data tempt speculation that NPCs may protect neurons from the primary necrotic cell death typically observed immediately after stroke but not the secondary apoptotic cell death typically observed later, more experiments are required to reveal the mechanisms by which NPCs promote neuronal survival after stroke. Our result do concur, however, with the work of others showing that NPCs increase cell survival following ischemia *in vivo* (Harms et al., 2010).

Among cells that survived OGD exposure, a large proportion expressed Cu/Zn SOD, which is a marker of cell stress that blocks the cytosolic release of cytochrome C, ultimately reducing apoptosis after ischemia (Fujimura et al., 2000). The percent of Cu/Zn SOD cells was significantly higher 1-14d following OGD, peaking 1d after treatment. This coincides with reports that free radical production peaks after reperfusion (Perez Velazquez et al., 1997). Interestingly, the percent of neurons in OGD-exposed cultures supplemented with either NPCs or fibroblasts (but not NPC-conditioned media) remained at control levels. Although SOD up-regulation is a sign of

oxidative stress, it is also neuroprotective (Fujimura et al., 2000) and interestingly remains upregulated in astrocytes following OGD exposure regardless of cell supplementation. For example, transgenic mice that overexpression Cu/Zn SOD had smaller infarcts following ischemic stroke (Kinouchi et al., 1991). Therefore, perhaps astrocytes are less vulnerable to OGD because they primarily produce Cu/Zn SOD. Although an increase in Cu/Zn SOD after OGD further demonstrates that OGD in cultured cells reflects what is seen *in situ,* NPCs do not appear to be protective by affecting Cu/Zn SOD directly. Lower Cu/Zn SOD in NPC-added groups may indicate that primary cells are facing less oxidative stress, perhaps either by NPC progeny blocking excitoxicity, or offering trophic support.

Mitotic-phase nuclei among primary cells were also quantified in order to estimate proliferation. Although we detected mitosis in less than 1% of all cells, OGD exposure increased the percent of mitotic nuclei particularly after NPCs (but not NPC-conditioned media or fibroblasts) were added to the cultures. Interestingly the impact of transplantable cells on the behavior of endogenous NPCs may be more robust than what we've observed *in vitro*. NPCs are resident to the neurogenic hippocampal dentate gyrus and SVZ (Liu et al., 1998; Takagi et al., 1999; Kee et al., 2001; Yagita et al., 2001). New neurons are even generated in non-neurogenic regions following ischemic injury but their survival is transient (Arvidsson et al., 2002; Thored et al., 2006). Transplanted NPCs may in fact stimulate the local production of factors that promote the proliferation, differentiation and survival of endogenous NPCs, such as EGF, FGF, GDNF and PSA-NCAM (Craig et al., 1996; Kuhn et al., 1997; Kitagawa et al., 1998; Iwai et al., 2001).

Understanding whether the post-injury or disease milieu that cells will be transplanted into affects their behavior may be critical for the success of stem/progenitor cell strategies for human CNS syndromes. In both OGD- and fresh media-exposed cultures we found that ~3-5% of all cells were GFP^+ (and therefore of NPC origin) 1d after plating. The proportion of NPCs increased similarly over time, regardless of condition, suggesting that NPCs proliferated. We did however, detect a slight but significant decrease in the percent of GFP^+ cells in OGD- versus fresh media control-exposed co-cultures at 28d, which could represent a post-stroke milieu effect on the speed with which NPC progeny divided and/or differentiated, or even an increase in primary cell division. Although the surrounding environment can influence NPC survival and fate (Ormerod et al., 2008), the percent of NPC-derived (GFP^+) cells acquiring neuronal or glial phenotypes quantified at 28 was unaffected by OGD, suggesting that there was no significant effect on their fates. In fact, the proportions of 4 week-old NPC progeny detected in OGD- and fresh media-exposed co-cultures in the current study were remarkably similar to the proportions of phenotypes of 4 week-old co-cultured NPC progeny (derived from a different cell line) in our previous work (Chapter 2). Together these data suggest that transplantable adult NPCs may be fairly resilient to the effects of post-injury milieus.

Both single unit and network activity was rapidly silenced by exposure to OGD. In addition to protecting primary cells and particularly neurons from OGD-induced cell death and oxidative stress, we found that NPCs also partially but transiently protected neurons from the effects of OGD-induced silencing. In control cultures, we found that NPCs, but not fibroblasts or NPC-conditioned media, stimulated a developmental

pattern of superbursting activity consistent with our previous work (Chapter 2). In NPC-supplemented cultures, we also detected novel activity over time suggesting that new NPC-generated neurons are capable of integrating functionally into existing neuronal circuitry. This evidence is further supported by our finding that NPC-conditioned media neither stimulates superbursting activity nor the emergence of novel activity in electrophysiologically mature cultures. The most exciting data showed that although activity never returned to control levels in OGD-exposed cultures following NPC supplementation they did exhibit activity for several weeks after the insult.

Spike rates on active electrodes almost retained control levels in OGD-exposed cultures supplemented with NPCs but not with fibroblasts or NPC-conditioned media until the 4th week after OGD, and we did detect more active electrodes among OGD-exposed cultures supplemented with NPCs versus NPC-conditioned media. The ability of NPCs to protect network activity was less pronounced than their ability to protect single unit activity. For example, more network bursts were observed in OGD-exposed cultures supplemented with NPCs- versus either fibroblasts or NPC-conditioned media but the rates were small and variable and did not recover to those observed in control cultures. Although OGD-exposed cultures supplemented with NPCs (but not fibroblasts or NPC-conditioned media) exhibited burst durations that peaked 4-8d and plateaued ~16d after OGD (resembling the evolution of burst durations in developing primary cultures) they did not maintain bursting activity much longer than 2-3 weeks after the injury. Discovering how to prolong this effect may be critical for increasing the efficacy of transplant, or delaying cell death until other treatments can be applied.

All groups had similar numbers of transiently new electrodes, but few electrodes had lasting new activity and were not significantly different from zero. However, the NPCs-added group had significantly more recovered activity. Neural stem cell grafts into ischemic CA1 lesions in the rat hippocampus exhibit pre- and post-synaptic markers and have been shown to develop properties of mature, normal hippocampal neurons within the infarct (Aoki et al., 1993). Indeed, some functional improvement has been reported in animal models of stroke following NPC transplantation despite variable rates of survival among the transplanted cells and their progeny (Nikkhah et al., 1994a; Hodges et al., 1996; Sinden et al., 1997; Modo et al., 2002; Dziewczapolski et al., 2003; Ben-Hur et al., 2004; Gao et al., 2006). Hypotheses regarding the mechanisms of functional improvement in these studies have included that transplanted cells and/or their progeny provide trophic support that thwarts further cell death, stimulate an endogenous repair process or the production/secretion of neurotransmitter, or perhaps integrate into existing circuitry to amplify compromised signaling (Ben-Hur et al., 2004; Ormerod et al., 2008). Neural stem cells could also induce plasticity by secreting factors such as VEGF and Apolipoprotein E (Andres et al.; Modo et al., 2003; Lee et al., 2007).

These results demonstrate that the MEA-OGD co-culture model provides an effective benchmark for investigating the efficacy of potential therapies on the damage caused by ischemic stroke, because electrophysiological and immunocytochemical analyses resemble ischemic stroke pathology described *in situ*. Future research could benefit by utilizing this model by applying treatments and cells following OGD, and monitoring MEA recordings for functional recovery of individual neurons, as well as network bursts.

CHAPTER 5
GENERAL DISCUSSION

Summary

Treatments or even cures for CNS injury or neurodegenerative disease could be based on NPC transplantation to replace dead or damaged tissue. Recent breakthroughs in stem cell research suggest that NPC-derived cells can produce CNS cell subtypes, including mature neurons, which may synapse with target areas to affect their function (Aoki et al., 1993; Stephens et al., 2012). Experiments have shown that ESC-derived NPC progeny readily form *de novo* neural networks, and functionally integrate into existing host circuitry (Copi et al., 2005; Lepski et al., 2011; Tonnesen et al., 2011). More recent data, including the data contained in this dissertation, suggest that adult-tissue derived NPC progeny may not form networks independently, but may also integrate functionally into existing neural networks (Chapters 2 and 4), demonstrated by stimulating plasticity among intact neural circuits (Chapter 2), and protecting cells and preserving activity among networks compromised by injury (Chapter 4). Although endogenous NPCs are exquisitely sensitive to systems' regulators, Chapter 4 shows that transplanted NPCs are surprisingly unaffected by the post-stroke milieu. Nevertheless, any effects that the addition of NPCs may have on existing neural activity, and in turn, any effects existing tissue may have on progenitor cell fate, are questions that must be addressed before effective treatments can be developed.

The work in this dissertation began by asking whether adult NPCs form *de novo* neural networks. Based on current knowledge of neural stem cell biology, adult NPCs in the right conditions will hypothetically form glia and mature neurons with functional synapses that are capable of integrating into the surrounding network as they do in the

daily turnover of new neurons in the adult hippocampus and olfactory bulb (Zhao et al., 2008). Although the exact function of these new cells remains unknown, endogenous NPC-derived hippocampal neurons exhibit both GABAergic and glutamatergic synapses within approximately four weeks (Esposito et al., 2005), and show some evidence of spontaneous activity (van Praag et al., 2002). Before investigating how adult-derived NPCs affect existing activity of mature primary neurons, it was important to first examine whether adult NPC-derived neurons were capable of integrating functionally with one another by testing their ability to develop spontaneous activity and network bursting independently. The capability of NPC-derived neurons to autonomously form networks would be highly desirable for prospective treatments seeking to replace dead circuitry. However, extraneous novel circuits or heavily modified existing circuits may even compromise residual function. For example, cognitive deficits are often reported in animal models of epilepsy that are associated with drastically elevated rates of ectopic neurogenesis (Parent et al., 1997). If adult-derived NPCs possess a unique ability to augment existing neural networks without being able to form new networks of their own, adult NPCs may be perfectly adept for reparative therapies seeking to amplify, strengthen or reinforce damaged neural circuitry.

MEAs were previously used to test spontaneous networking ability in ESC-derived cultures (Illes et al., 2007); however, the networking capability of purely NPC-derived cells was put into question and tested on MEAs for the first time in Chapter 2 of this dissertation. Similar to ESC-derived neural cultures, NPC development was hypothesized to be slightly delayed, and develop on a much smaller scale compared to primary neural populations. As expected, NPCs plated alone on MEAs in normal culture

conditions displayed delayed development of spontaneous action potentials, as well as delayed expression of mature neural and glial markers. Interestingly, NPC progeny grown alone in culture did not produce synchronous network-wide bursts, even after eight weeks in normal culture conditions. This lack of network capability of adult NPCs may or may not be useful in treatment strategies, depending on its purpose and target. Adult NPCs could be utilized when the goal of transplant is to augment existing neural activity, rather than replace the entire circuit. However, electrical stimulation and/or manipulation of the microenvironment with external factors may be necessary to promote network formation (Piatti et al., 2011). For example, NPC progeny matured faster in co-culture than when grown alone (Chapter 2). Perhaps optimizing culture conditions and techniques to direct differentiation could change the future of NPC applications.

Although several groups have linked the contribution of new neurons in the hippocampus to learning and memory (Gould et al., 1999; Kempermann and Gage, 2002; Ormerod et al., 2004; Winocur et al., 2006), a direct connection between functional integration of new neurons and its affect on existing circuitry remains unclear. Chapter 2 of this dissertation took advantage of well-characterized, stable activity in primary rat cortical cultures, and used it as a benchmark to directly observe how NPCs influence established activity. After two weeks in co-culture, as NPCs began to express mature neural and glial markers, network burst patterns reverted to superbursts, to reflect those observed during network development *in vitro* and in various areas in the developing cortex. The appearance of superbursts, indicative of induced plasticity, occurred approximately two weeks after addition at Day 40, and again after an addition

at Day 64. Superbursting was also observed in NPC-supplemented, non-OGD control cultures during the experiments described in Chapter 4 using a completely different NPC line. Highly excitable, naïve young neurons in primary cultures hypothetically drive transient superbursts when networks are developing at 4-5 weeks in primary neural cultures, and again by added NPC-generated young neurons 1-2 weeks after NPC addition. This is an exciting discovery that demonstrates NPC addition does influence neural activity that may be favorable in some therapeutic strategies where the existing neural network is damaged and needs remodeling or enhancement, but may not be favorable in other strategies where disrupting existing circuitry could impede normal brain functions. The stroke penumbra, consisting of surviving but silenced neural circuits, is an excellent example of post-injury environment where improvement to function could be made by stimulating plasticity, perhaps without generating novel networks.

Next, the co-culture MEA model of NPC transplant was taken a step further, and applied for the first time to a compromised neural network, by modeling hypoxic-ischemic stroke with oxygen-glucose deprivation (Chapter 3). Recording primary neural cultures during OGD is a novel application of MEA technology, and gives an unprecedented view of the massive depolarization and network degradation of spontaneous activity that has only previously been recorded from a handful of electrodes placed *in vivo* (Kass and Lipton, 1982; Rosner et al., 1986). The behavior of network activity in primary cultures closely mirrors what is seen *in situ,* but data is collected from 59 sites simultaneously. This model adds a new, comprehensive view of activity during ischemia that encompasses neuron behavior on a network scale, adding

to the picture of stroke dynamics in culture and *in vivo.* Spike rates initially increased during the first five minutes of OGD due to the emergence of asynchronous activity between bursts. Action potentials decreased in amplitude, and all activity ultimately ceased by approximately sixteen minutes. Neural activity recovered following reperfusion after 20-minute OGD, but little recovery was observed after longer durations. Shorter duration OGD may effectively model the silenced circuits found in the penumbra of a stroke, while longer OGD might effectively model the dying circuits found with the stroke core. By defining the parameters needed to silence neuronal activity but maintain viability, this work has pioneered a culture model of a stroke penumbra versus stroke core. Each substrate can be utilized in the future to develop approaches to treat both areas.

Overall, OGD exposure increased the percent of PI^+ dead cells and pyknotic dying cells two weeks after exposure. NPC addition decreased the percent PI^+ cells but did not impact the percent of pyknotic cells. These results may point to NPCs as protecting neurons from the primary necrotic cell death typically observed immediately after stroke, but not the secondary apoptotic cell death typically observed later. However, more experiments are required to reveal the mechanisms by which NPCs promote neuronal survival after stroke. Although we detected mitosis in less than 1% of all cells, OGD exposure increased the percent of mitotic nuclei, particularly after NPCs were added to the cultures. Interestingly, the impact of transplantable cells on the behavior of endogenous NPCs may be more robust than what we've observed *in vitro*. In addition, co-culture in OGD-compromised primary cultures did not affect the rate of NPC differentiation or phenotype relative to those in co-culture with intact primary cells. We

also detected novel activity over time in NPC-supplemented cultures, suggesting that new NPC-generated neurons are capable of becoming functional in existing neuronal circuitry. This evidence is further supported by our finding that NPC-conditioned media neither stimulates superbursting activity nor the emergence of novel activity in electrophysiologically mature cultures.

The most exciting data showed that although activity never returned to control levels in OGD-exposed cultures following NPC supplementation, they did exhibit activity for several weeks after the insult. These results demonstrated that this MEA co-culture model could be an effective bioassay for potential neuroregenerative therapies on existing network activity. An *in vitro* assay system may help the translation of NPC transplant strategies to clinic by investigating these effects in a highly sensitive, biologically relevant neuronal network.

Future Work

Additional studies that build on the MEA-based co-culture system may reveal that NPCs have the capability to form *de novo* networks on their own, given the correct conditions. In Chapter 2, NPC-derived cultures did not produce many glia, however, a certain number of glial cells are necessary for synapse formation and network development (Johnson et al., 2007; Kucukdereli et al., 2011). Future experiments to optimize different media conditions that promote heterogenous cell fate, through chemical and/or electrical stimulation may potentiate the regenerative capabilities of adult-derived NPCs. Results in Chapter 2 and 4 suggest that NPCs functionally integrate, because they altered existing neural activity in primary cultures. Unfortunately, MEA technology lacks the ability to isolate single unit activity and conclusively identify which neuron is the source of the particular activity in question.

Future experiments should look directly at if and how NPC-derived neurons become functional, and by what mechanism(s) do they influence existing activity.

Researchers have and are currently finding many factors that influence NPC fate and functionality in the brain. When added to primary neural cultures, NPCs differentiate into mature neurons and glia at a faster rate; exhibiting neural and glial markers within two weeks, versus six weeks when cultured alone (Chapter 2). NPC-derived mature cells also display more mature morphology, in terms of more extensive branching, than when grown alone. Although NPCs did not exhibit *de novo* networking ability, perhaps the co-cultured NPC-derived neurons were able to form synapses with primary cells and other NPC-progeny, and participate in network bursting. Co-culture with other stem or progenitor cells, such as oligodendrocyte progenitor cell lines, could yield the right number of astrocytes and/or oligodentrocytes for spontaneous network bursting activity to develop. Moreover, changing the culture conditions by growth factor-supplemented media and/or chronic electrical stimulation, which is known to affect NPCs and the development of neurons, may also direct NPC-derived neurons to form network bursts (Tateno et al., 2005; Wagenaar et al., 2005). MEAs have the capability to stimulate, as well as record, activity. An experiment that applies chronic stimulation of NPC-derived cultures for days or weeks after plating may induce network formation.

Whole-cell patch clamp is often paired with MEAs (Pancrazio et al., 2001; O'Shaughnessy et al., 2003; Meyer et al., 2008; Chiappalone et al., 2009), because it is low throughput, but gives refined, cell-specific information, while MEAs give more global data of the impact on neuronal networks. I would have liked to pair whole-cell patch clamp methods with my MEA co-culture experiment in order to determine if and when

NPC-derived neurons became functional, and if participated in network bursts. Whole-cell patch clamp under current clamp mode can record spontaneous activity of an NPC-derived neuron and would determine if NPC-derived neurons become spontaneously active and participate in network bursts. Furthermore, voltage clamp recordings could reveal the fundamental mechanisms underlying NPC functional integration. This analysis should be performed to investigate whether the changes observed in network activity occurred directly because of functional integration of NPC progeny, or indirectly, by secreted factors to induce neurogenesis and/or plasticity within the primary neural cultures. The latter seems unlikely because the conditioned-media groups yielded no change in activity. However, patch clamp techniques paired with MEA analysis could provide direct evidence of NPC-derived neuron and primary cell functional interactions.

Live cell imaging is another method of providing evidence of the functional integration of NPC-derived neurons that could be paired with MEA recordings. Synaptic stimuli produce Ca^{2+} elevations that are largely restricted to dendritic spines, where activated synapses terminate. The intracellular Ca^{2+} increase is due to, for the most part, NMDA receptor activation by glutamate. Live cell imaging can report transient changes in neuronal cytosolic Ca^{2+} signaling to show the release of glutamate from individual synaptic terminals. In the MEA-plated cultures, live Ca^{2+} imaging could show network bursting, and the participation of individual neurons in network bursts. Specifically, a red-shifted Ca^{2+} indicator, such as rhod-3 (Molecular Probes; Eugene, OR), would be ideal for imaging in GFP^{+} NPC-derived neurons. A non-fluorescent Rhod-3 is passively loaded into cells in a wash, where intracellular esterases cleave the dye to a cell impermeant, active form that fluoresces upon Ca^{2+} binding (Ieda et al.,

2010). MEAs can be imaged on a reflected-light fluorescent microscope, and bursts can be video recorded with the Rhod-3. The intensity of Rhod-3 in specific cells can be plotted as spikes for comparison to the MEA recordings.

Improvements to the translational potential of the variable-duration OGD model of stroke could also be made with future experiments. For example, a time series experiment of OGD exposure with 5-10 minute intervals could refine the 20-60 minute, silenced penumbra model versus the 2-3 hour, stroke core model. In addition, a time series on NPC supplementation could investigate immediate versus delayed neuroprotective effects of adding NPCs after hours or days or reperfusion.

In addition, pairing patch clamp experiments with future applications of the ischemic stroke model could also provide valuable information about whether NPCs become active, are the cause of some or all of the activity recovered after OGD, and whether the activity is due to rescued primary neurons, or even new neurons generated by primary cells. Endogenous NPCs in the primary cultures could be activated by factors secreted by the added NPCs. The mere presence of endogenous NPCs could be ruled out by the application of an anti-mitotic, or irradiation after plating. I would also like to delve further into how NPCs rescue mature neurons from OGD-induced death and silencing. Future experiments pairing patch-clamp with the MEA and/or stimulation of the cultures, may detect the mechanisms behind the survival of primary neurons, and define possible treatment strategies for silencing and regeneration.

Lastly, combining the MEA co-culture transplantation model with *in vivo* studies designed to measure effects of NPC transplant on intact brain circuitry is essential to moving any effective treatments to clinic. The work for my dissertation developed a

simplified *in vitro* model of NPC transplantation that is easily accessible, relatively inexpensive, does not require the use of animals, is highly sensitive to manipulation, and can be paired with extensive immunocytochemical analysis to monitor changes in a biologically relevant neural network. However, it is merely an assay for testing the efficacy of NPC-transplant or other strategies for neural repair without confounding factors found *in vivo*. Future researchers should consider combining the MEA-based co-culture model when developing a translational approach for scaling up therapies found to be beneficial through this assay.

Conclusions

Although some NPC transplantation experiments have yielded successful graft survival, and even limited behavioral recovery (Jgamadze et al., 2012), researchers are not yet capable of manipulating NPC-derived neurons and glia to control functional integration and effectively treat the injured or diseased CNS. Some may stand to argue that studying treatment strategies *in vitro* is impractical, because any solution that is found by this assay would probably not work when translated *in vivo*. Of course, many variables are excluded in the *in vitro* model that could drastically alter the fate and functionality of NPCs and their progeny *in vivo* (i.e. hormones, inflammation, vasculature; Duan et al., 2008; Mu et al., 2012). However, such a highly controllable environment is crucial to the scientific method, and it would be a disadvantage to stem cell research to underestimate or disregard its utility. As quickly as investigative technology is advancing, researchers are persistently discovering new ways to regulate NPC behavior (Kim et al., 2012). As strategies are conceived *in vitro*, additional variables can be introduced to gradually engineer an *in vivo* strategy that preserves the treatment's effect.

In conclusion, the MEA co-culture model of NPC transplantation established through this dissertation research can help understand part of the basic mechanisms that accompany the functional integration of transplanted neural cells. My work has contributed to the need for further knowledge of how to engineer connections to target neural networks, or induce plasticity in existing neural networks, to prevent unintentional consequences, such as upsetting normal brain function or causing epilepsy. Therefore my findings, together with future extensions of this work will hopefully help build a foundation for establishing transplant strategies for neural repair. This work developed an *in vitro* model of NPC transplantation that is easily accessible in terms of monitoring cells optically and electrophysiologically on a network-wide scale across thousands of cells that can be paired with extensive immunocytochemical analysis to provide an assay for testing the efficacy of NPC-transplant or other strategies for neural repair without confounding factors found *in vivo*. This model gives insight into the networking ability of cells by plating NPCs alone, and the impact of cell engraftment on existing neural circuitry by way of co-culture. Furthermore, this model demonstrated its utility by the adding the application of hypoxic-ischemic conditions to simulate a post-stroke environment. This work, along with future extensions of this research, will establish a foundation for testing customized strategies for neural repair before introducing them into much more complex *in-vivo* environments, and ultimately to the clinic.

APPENDIX:
CHAPTER 2 SUPPLEMENTARY DATA

NPC media optimization for co-culture

First, we confirmed that NPC cultures would survive long-term in media formulations typical of MEA experiments with primary cultures that predictably develop mature bursting activity. A 100µl droplet of each of eight media formulations containing 5,000 NPCs was placed in the center of PEI/laminin coated wells in a 12-well culture dish (to model the surface area of an MEA dish), and the cells were grown for 21 days (n = 3 wells per media formulation). The eight media formulations chosen were: (1) NPC differentiation media prepared with GlutaMax-supplemented DMEM, (2) NPC differentiation media prepared with high glucose DMEM/F12, (3) N2-supplemented NPC differentiation media prepared with GlutaMax-supplemented DMEM, (4) N2-supplemented NPC differentiation media prepared with high glucose DMEM/F12, (5) primary culture growth media (10% ES) prepared in GlutaMax-DMEM, and (6) primary culture growth media (10%) prepared in high glucose DMEM/F12, (7) 10% fetal bovine serum in Glutamax-supplemented DMEM and (8) 10% fetal bovine serum in high glucose DMEM/F12. On Day 21, propidium iodide (250µg/ml) was added to each well for 15min to label the DNA of non-viable cells before the cells were paraformaldehyde-fixed and DAPI-stained. Densities of live (GFP^+) and dead (PI/GFP^+) cells were counted on images taken using a Zeiss AxioObserver microscope (20x objective). We found that media formulation ($F_{(3,16)} = 10.10$, $p = 0.0005$) and GlutaMax supplementation ($F_{(1,16)} = 8.96$, $p = 0.008$) significantly impacted cell death. Cell death was significantly lower among NPC cultures grown in primary culture growth media (10% equine serum; 17.33±3.26%), relative to 10% fetal bovine serum in DMEM (29.17±5.16%; $p = 0.022$),

N2-supplemented NPC differentiation media (32.50±3.63%; $p = 0.013$) or NPC differentiation media (42.67±3.60%; p = 0.0004). Cell death was highest in media without N2-supplementation relative to all other formulations (p's < 0.044). Overall GlutaMax-supplemented DMEM slightly, but significantly increased cell death relative to glutamine supplementation (25.5±3.87% versus 35.33±3.15%; $p < 0.010$). However, we chose to use GlutaMax-supplemented primary culture growth media for our initial co-culture experiments because it only slightly increased cell death (23.00±3.78%) and promotes the reliable development of electrophysiological activity among neurons in primary cultures.

NPC plating density optimization

Next we tested plating densities that would permit the long-term culture of proliferative adult NPCs at cell densities that produced consistent monolayer cultures. A 100µl droplet of 'NPC differentiation media' containing 1K, 5K, 10K or 15K NPCs was placed into the center of a PEI/laminin-coated well in a 12-well tissue culture plate (n = 3 wells per condition) and the cells grown for 21 days. Every three days, ~50% of the media was replaced to model the feeding regime used in MEA experiments. Cell densities were quantified at Days 2, 7, 14 and 21 after plating, using digital phase contrast images (20x objective) taken in random well locations (n = 7 locations in 3 wells per plating density). As expected, cell density was directly proportional to plating density two days after plating ($F_{(3,24)} = 16.35$, $p < 0.0001$; Newman-Keuls p's < 0.010; Mean±S.E.M cells/mm^2: 1K = 37.3±7.4; 5K = 313.4±29.3; 10K = 644.1±85.6; 15K = 706.7±124.2). Note that although some death occurs after plating, cells rapidly migrate out of the droplet zone reducing the cell densities observed at plating. At later time

points, cell densities were not affected by plating densities ($F_{(3,24)}$ = 2.14, p = 0.12) but did change across day after plating ($F_{(2,48)}$ = 31.55, p < 0.0001; interaction effect : $F_{(6,48)}$ = 0.456, p = 0.837). Specifically, cell fold-increases diminished from their mean peak of ~9.7-fold at Day 7 (1K = 12-fold; 5K = 12-fold; 10K = 8-fold and 15K = 8-fold) to ~ 1.3-fold on Day 14 (p's < 0.0001) and ~0.6-fold on Day 21 (p's < 0.0001). We chose to employ the 10K NPCs/droplet concentration for further experiments because this concentration sufficiently covered the well surface without overwhelming the culture dish, produced cells with a healthy appearance, and would comprise ~5% of the co-culture. Because we hypothesized that NPC-derived cells co-cultured with established neural networks may undergo less extensive proliferation, we also included a 50K NPC/droplet condition in our co-culture experiment.

LIST OF REFERENCES

Aimone JB, Wiles J, Gage FH (2006) Potential role for adult neurogenesis in the encoding of time in new memories. Nat Neurosci 9:723-727.

Altman J, Das GD (1965) Post-natal origin of microneurones in the rat brain. Nature 207:953-956.

Andres RH, Horie N, Slikker W, Keren-Gill H, Zhan K, Sun G, Manley NC, Pereira MP, Sheikh LA, McMillan EL, Schaar BT, Svendsen CN, Bliss TM, Steinberg GK Human neural stem cells enhance structural plasticity and axonal transport in the ischaemic brain. Brain 134:1777-1789.

Aoki H, Onodera H, Yae T, Jian Z, Kogure K (1993) Neural grafting to ischemic CA1 lesions in the rat hippocampus: an autoradiographic study. Neuroscience 56:345-354.

Arsenijevic Y, Villemure JG, Brunet JF, Bloch JJ, Deglon N, Kostic C, Zurn A, Aebischer P (2001) Isolation of multipotent neural precursors residing in the cortex of the adult human brain. Exp Neurol 170:48-62.

Arvidsson A, Collin T, Kirik D, Kokaia Z, Lindvall O (2002) Neuronal replacement from endogenous precursors in the adult brain after stroke. Nat Med 8:963-970.

Astrup J, Siesjo BK, Symon L (1981) Thresholds in cerebral ischemia - the ischemic penumbra. Stroke 12:723-725.

Babu H, Ramirez-Rodriguez G, Fabel K, Bischofberger J, Kempermann G (2009) Synaptic Network Activity Induces Neuronal Differentiation of Adult Hippocampal Precursor Cells through BDNF Signaling. Front Neurosci 3:49.

Back SA, Han BH, Luo NL, Chricton CA, Xanthoudakis S, Tam J, Arvin KL, Holtzman DM (2002) Selective vulnerability of late oligodendrocyte progenitors to hypoxia-ischemia. J Neurosci 22:455-463.

Bain G, Kitchens D, Yao M, Huettner JE, Gottlieb DI (1995) Embryonic stem cells express neuronal properties in vitro. Dev Biol 168:342-357.

Bambrick LL, Kostov Y, Rao G In vitro cell culture pO(2) is significantly different from incubator pO(2). Biotechnol Prog.

Ban J, Bonifazi P, Pinato G, Broccard FD, Studer L, Torre V, Ruaro ME (2007) Embryonic stem cell-derived neurons form functional networks in vitro. Stem Cells 25:738-749.

Banasiak KJ, Xia Y, Haddad GG (2000) Mechanisms underlying hypoxia-induced neuronal apoptosis. Prog Neurobiol 62:215-249.

Banker GA (1980) Trophic interactions between astroglial cells and hippocampal neurons in culture. Science 209:809-810.

Ben-Ari Y (2001) Developing networks play a similar melody. Trends Neurosci 24:353-360.

Ben-Ari Y, Cherubini E, Corradetti R, Gaiarsa JL (1989) Giant synaptic potentials in immature rat CA3 hippocampal neurones. J Physiol 416:303-325.

Ben-Hur T, Idelson M, Khaner H, Pera M, Reinhartz E, Itzik A, Reubinoff BE (2004) Transplantation of human embryonic stem cell-derived neural progenitors improves behavioral deficit in Parkinsonian rats. Stem Cells 22:1246-1255.

Benninger F, Beck H, Wernig M, Tucker KL, Brustle O, Scheffler B (2003) Functional integration of embryonic stem cell-derived neurons in hippocampal slice cultures. J Neurosci 23:7075-7083.

Berridge MJ (1998) Neuronal calcium signaling. Neuron 21:13-26.

Boehler MD, Wheeler BC, Brewer GJ (2007) Added astroglia promote greater synapse density and higher activity in neuronal networks. Neuron Glia Biol 3:127-140.

Brederlau A, Correia AS, Anisimov SV, Elmi M, Paul G, Roybon L, Morizane A, Bergquist F, Riebe I, Nannmark U, Carta M, Hanse E, Takahashi J, Sasai Y, Funa K, Brundin P, Eriksson PS, Li JY (2006) Transplantation of human embryonic stem cell-derived cells to a rat model of Parkinson's disease: effect of in vitro differentiation on graft survival and teratoma formation. Stem Cells 24:1433-1440.

Buffo A, Rite I, Tripathi P, Lepier A, Colak D, Horn AP, Mori T, Gotz M (2008) Origin and progeny of reactive gliosis: A source of multipotent cells in the injured brain. Proc Natl Acad Sci U S A 105:3581-3586.

Buzsáki G (2010) Neural syntax: cell assemblies, synapsembles, and readers. Neuron 68:362-385.

Buzsáki G, Masliah E, Chen LS, Horváth Z, Terry R, Gage FH (1991) Hippocampal grafts into the intact brain induce epileptic patterns. Brain Res 554:30-37.

Calabresi P, Marfia GA, Centonze D, Pisani A, Bernardi G (1999) Sodium influx plays a major role in the membrane depolarization induced by oxygen and glucose deprivation in rat striatal spiny neurons. Stroke 30:171-179.

Cameron HA, Woolley CS, McEwen BS, Gould E (1993) Differentiation of newly born neurons and glia in the dentate gyrus of the adult rat. Neuroscience 56:337-344.

Chiappalone M, Casagrande S, Tedesco M, Valtorta F, Baldelli P, Martinoia S, Benfenati F (2009) Opposite changes in glutamatergic and GABAergic transmission underlie the diffuse hyperexcitability of synapsin I-deficient cortical networks. Cereb Cortex 19:1422-1439.

Clarkson ED (2001) Fetal tissue transplantation for patients with Parkinson's disease: a database of published clinical results. Drugs Aging 18:773-785.

Colucci-D'Amato L, Bonavita V, di Porzio U (2006) The end of the central dogma of neurobiology: stem cells and neurogenesis in adult CNS. Neurol Sci 27:266-270.

Copi A, Jungling K, Gottmann K (2005) Activity- and BDNF-induced plasticity of miniature synaptic currents in ES cell-derived neurons integrated in a neocortical network. J Neurophysiol 94:4538-4543.

Craig CG, Tropepe V, Morshead CM, Reynolds BA, Weiss S, van der Kooy D (1996) In vivo growth factor expansion of endogenous subependymal neural precursor cell populations in the adult mouse brain. J Neurosci 16:2649-2658.

Curtis MA, Kam M, Nannmark U, Anderson MF, Axell MZ, Wikkelso C, Holtas S, van Roon-Mom WM, Bjork-Eriksson T, Nordborg C, Frisen J, Dragunow M, Faull RL, Eriksson PS (2007) Human neuroblasts migrate to the olfactory bulb via a lateral ventricular extension. Science 315:1243-1249.

de Lima AD, Voigt T (1997) Identification of two distinct populations of gamma-aminobutyric acidergic neurons in cultures of the rat cerebral cortex. J Comp Neurol 388:526-540.

Dhamoon MS, Moon YP, Paik MC, Boden-Albala B, Rundek T, Sacco RL, Elkind MS (2010) Quality of life declines after first ischemic stroke. The Northern Manhattan Study. Neurology 75:328-334.

Doetsch F, Garcia-Verdugo JM, Alvarez-Buylla A (1997) Cellular composition and three-dimensional organization of the subventricular germinal zone in the adult mammalian brain. J Neurosci 17:5046-5061.

Domercq M, Perez-Samartin A, Aparicio D, Alberdi E, Pampliega O, Matute C P2X7 receptors mediate ischemic damage to oligodendrocytes. Glia 58:730-740.

Duan X, Kang E, Liu CY, Ming GL, Song H (2008) Development of neural stem cell in the adult brain. Curr Opin Neurobiol 18:108-115.

Dupont E, Hanganu IL, Kilb W, Hirsch S, Luhmann HJ (2006) Rapid developmental switch in the mechanisms driving early cortical columnar networks. Nature 439:79-83.

Dziewczapolski G, Lie DC, Ray J, Gage FH, Shults CW (2003) Survival and differentiation of adult rat-derived neural progenitor cells transplanted to the striatum of hemiparkinsonian rats. Exp Neurol 183:653-664.

Ehninger D, Kempermann G (2003) Regional effects of wheel running and environmental enrichment on cell genesis and microglia proliferation in the adult murine neocortex. Cereb Cortex 13:845-851.

Ekdahl CT, Kokaia Z, Lindvall O (2009) Brain inflammation and adult neurogenesis: the dual role of microglia. Neuroscience 158:1021-1029.

Eroglu C, Barres BA (2011) Regulation of synaptic connectivity by glia. Nature 468:223-231.

Esposito MS, Piatti VC, Laplagne DA, Morgenstern NA, Ferrari CC, Pitossi FJ, Schinder AF (2005) Neuronal differentiation in the adult hippocampus recapitulates embryonic development. J Neurosci 25:10074-10086.

Fabel K, Toda H, Palmer T (2003) Copernican stem cells: regulatory constellations in adult hippocampal neurogenesis. J Cell Biochem 88:41-50.

Fern R, Moller T (2000) Rapid ischemic cell death in immature oligodendrocytes: a fatal glutamate release feedback loop. J Neurosci 20:34-42.

Fisher M (1997) Characterizing the target of acute stroke therapy. Stroke 28:866-872.

Freed CR, Greene PE, Breeze RE, Tsai WY, DuMouchel W, Kao R, Dillon S, Winfield H, Culver S, Trojanowski JQ, Eidelberg D, Fahn S (2001) Transplantation of embryonic dopamine neurons for severe Parkinson's disease. N Engl J Med 344:710-719.

Fujimura M, Morita-Fujimura Y, Noshita N, Sugawara T, Kawase M, Chan PH (2000) The cytosolic antioxidant copper/zinc-superoxide dismutase prevents the early release of mitochondrial cytochrome c in ischemic brain after transient focal cerebral ischemia in mice. J Neurosci 20:2817-2824.

Fukui S, Ookawara T, Nawashiro H, Suzuki K, Shima K (2002) Post-ischemic transcriptional and translational responses of EC-SOD in mouse brain and serum. Free Radic Biol Med 32:289-298.

Gage FH (2000) Mammalian neural stem cells. Science 287:1433-1438.

Gage FH, Kempermann G, Palmer TD, Peterson DA, Ray J (1998) Multipotent progenitor cells in the adult dentate gyrus. J Neurobiol 36:249-266.

Galli L, Maffei L (1988) Spontaneous impulse activity of rat retinal ganglion cells in prenatal life. Science 242:90-91.

Gao J, Prough DS, McAdoo DJ, Grady JJ, Parsley MO, Ma L, Tarensenko YI, Wu P (2006) Transplantation of primed human fetal neural stem cells improves cognitive function in rats after traumatic brain injury. Exp Neurol 201:281-292.

Goldman S (2003) Glia as neural progenitor cells. Trends Neurosci 26:590-596.

Gomes JR, Lobo AC, Melo CV, Inacio AR, Takano J, Iwata N, Saido TC, de Almeida LP, Wieloch T, Duarte CB (2011) Cleavage of the vesicular GABA transporter under excitotoxic conditions is followed by accumulation of the truncated transporter in nonsynaptic sites. J Neurosci 31:4622-4635.

Gould E, Cameron HA, Daniels DC, Woolley CS, McEwen BS (1992) Adrenal hormones suppress cell division in the adult rat dentate gyrus. J Neurosci 12:3642-3650.

Gould E, Beylin A, Tanapat P, Reeves A, Shors TJ (1999) Learning enhances adult neurogenesis in the hippocampal formation. Nat Neurosci 2:260-265.

Gross GW, Kowalski JM (1999) Origins of Activity Patterns in Self-Organizing Neuronal Networks in Vitro. Journal of Intelligent Material Systems and Structures 10:558-564.

Harms C, Lautenschlager M, Bergk A, Katchanov J, Freyer D, Kapinya K, Herwig U, Megow D, Dirnagl U, Weber JR, Hortnagl H (2001) Differential mechanisms of neuroprotection by 17 beta-estradiol in apoptotic versus necrotic neurodegeneration. J Neurosci 21:2600-2609.

Harms KM, Li L, Cunningham LA (2010) Murine neural stem/progenitor cells protect neurons against ischemia by HIF-1alpha-regulated VEGF signaling. PLoS One 5:e9767.

Heikkila TJ, Yla-Outinen L, Tanskanen JM, Lappalainen RS, Skottman H, Suuronen R, Mikkonen JE, Hyttinen JA, Narkilahti S (2009) Human embryonic stem cell-derived neuronal cells form spontaneously active neuronal networks in vitro. Exp Neurol 218:109-116.

Heja L, Barabas P, Nyitrai G, Kekesi KA, Lasztoczi B, Toke O, Tarkanyi G, Madsen K, Schousboe A, Dobolyi A, Palkovits M, Kardos J (2009) Glutamate uptake triggers transporter-mediated GABA release from astrocytes. PLoS One 4:e7153.

Hicks AU, Lappalainen RS, Narkilahti S, Suuronen R, Corbett D, Sivenius J, Hovatta O, Jolkkonen J (2009) Transplantation of human embryonic stem cell-derived neural precursor cells and enriched environment after cortical stroke in rats: cell survival and functional recovery. Eur J Neurosci 29:562-574.

Hirt L, Badaut J, Thevenet J, Granziera C, Regli L, Maurer F, Bonny C, Bogousslavsky J (2004) D-JNKI1, a cell-penetrating c-Jun-N-terminal kinase inhibitor, protects against cell death in severe cerebral ischemia. Stroke 35:1738-1743.

Hodges H, Sowinski P, Fleming P, Kershaw TR, Sinden JD, Meldrum BS, Gray JA (1996) Contrasting effects of fetal CA1 and CA3 hippocampal grafts on deficits in spatial learning and working memory induced by global cerebral ischaemia in rats. Neuroscience 72:959-988.

Hoehn BD, Palmer TD, Steinberg GK (2005) Neurogenesis in rats after focal cerebral ischemia is enhanced by indomethacin. Stroke 36:2718-2724.

Hoglinger GU, Rizk P, Muriel MP, Duyckaerts C, Oertel WH, Caille I, Hirsch EC (2004) Dopamine depletion impairs precursor cell proliferation in Parkinson disease. Nat Neurosci 7:726-735.

Ieda M, Fu JD, Delgado-Olguin P, Vedantham V, Hayashi Y, Bruneau BG, Srivastava D (2010) Direct reprogramming of fibroblasts into functional cardiomyocytes by defined factors. Cell 142:375-386.

Illes S, Fleischer W, Siebler M, Hartung HP, Dihne M (2007) Development and pharmacological modulation of embryonic stem cell-derived neuronal network activity. Exp Neurol 207:171-176.

Illes S, Theiss S, Hartung HP, Siebler M, Dihne M (2009) Niche-dependent development of functional neuronal networks from embryonic stem cell-derived neural populations. BMC Neurosci 10:93.

Iwai M, Hayashi T, Zhang WR, Sato K, Manabe Y, Abe K (2001) Induction of highly polysialylated neural cell adhesion molecule (PSA-NCAM) in postischemic gerbil hippocampus mainly dissociated with neural stem cell proliferation. Brain Res 902:288-293.

Jaako-Movits K, Zharkovsky A (2005) Impaired fear memory and decreased hippocampal neurogenesis following olfactory bulbectomy in rats. Eur J Neurosci 22:2871-2878.

Jefferys JG, Haas HL (1982) Synchronized bursting of CA1 hippocampal pyramidal cells in the absence of synaptic transmission. Nature 300:448-450.

Jgamadze D, Bergen J, Stone D, Jang JH, Schaffer DV, Isacoff EY, Pautot S (2012) Colloids as mobile substrates for the implantation and integration of differentiated neurons into the mammalian brain. PLoS One 7:e30293.

Johnson MA, Weick JP, Pearce RA, Zhang SC (2007) Functional neural development from human embryonic stem cells: accelerated synaptic activity via astrocyte coculture. J Neurosci 27:3069-3077.

Kamioka H, Maeda E, Jimbo Y, Robinson HP, Kawana A (1996) Spontaneous periodic synchronized bursting during formation of mature patterns of connections in cortical cultures. Neurosci Lett 206:109-112.

Kandel ER, Schwartz JH, Jessell TM (2000) Principles of neural science, 4th Edition. New York: McGraw-Hill, Health Professions Division.

Kass IS, Lipton P (1982) Mechanisms involved in irreversible anoxic damage to the in vitro rat hippocampal slice. J Physiol 332:459-472.

Kee NJ, Preston E, Wojtowicz JM (2001) Enhanced neurogenesis after transient global ischemia in the dentate gyrus of the rat. Exp Brain Res 136:313-320.

Kempermann G, Gage FH (2002) Genetic determinants of adult hippocampal neurogenesis correlate with acquisition, but not probe trial performance, in the water maze task. Eur J Neurosci 16:129-136.

Khazipov R, Esclapez M, Caillard O, Bernard C, Khalilov I, Tyzio R, Hirsch J, Dzhala V, Berger B, Ben-Ari Y (2001) Early development of neuronal activity in the primate hippocampus in utero. J Neurosci 21:9770-9781.

Kim DS, Kwak SE, Kim JE, Won MH, Choi HC, Song HK, Kwon OS, Kim YI, Choi SY, Kang TC (2005) Bilateral enhancement of excitation via up-regulation of vesicular glutamate transporter subtype 1, not subtype 2, immunoreactivity in the unilateral hypoxic epilepsy model. Brain Res 1055:122-130.

Kim H, Cooke MJ, Shoichet MS (2012) Creating permissive microenvironments for stem cell transplantation into the central nervous system. Trends Biotechnol 30:55-63.

Kinouchi H, Epstein CJ, Mizui T, Carlson E, Chen SF, Chan PH (1991) Attenuation of focal cerebral ischemic injury in transgenic mice overexpressing CuZn superoxide dismutase. Proc Natl Acad Sci U S A 88:11158-11162.

Kitagawa H, Abe K, Hayashi T, Mitsumoto Y, Koga N, Itoyama Y (1998) Ameliorative effect of glial cell line-derived neurotrophic factor on brain edema formation after permanent middle cerebral artery occlusion in rats. Neurol Res 20:333-336.

Krinke D, Jahnke HG, Panke O, Robitzki AA (2009) A microelectrode-based sensor for label-free in vitro detection of ischemic effects on cardiomyocytes. Biosens Bioelectron 24:2798-2803.

Kucukdereli H, Allen NJ, Lee AT, Feng A, Ozlu MI, Conatser LM, Chakraborty C, Workman G, Weaver M, Sage EH, Barres BA, Eroglu C (2011) Control of excitatory CNS synaptogenesis by astrocyte-secreted proteins Hevin and SPARC. Proc Natl Acad Sci U S A 108:E440-449.

Kuhn HG, Winkler J, Kempermann G, Thal LJ, Gage FH (1997) Epidermal growth factor and fibroblast growth factor-2 have different effects on neural progenitors in the adult rat brain. J Neurosci 17:5820-5829.

Latham PE, Richmond BJ, Nirenberg S, Nelson PG (2000) Intrinsic dynamics in neuronal networks. II. experiment. J Neurophysiol 83:828-835.

Le Belle JE, Svendsen CN (2002) Stem cells for neurodegenerative disorders: where can we go from here? BioDrugs 16:389-401.

Lee HJ, Kim KS, Park IH, Kim SU (2007) Human neural stem cells over-expressing VEGF provide neuroprotection, angiogenesis and functional recovery in mouse stroke model. PLoS One 2:e156.

Lepski G, Maciaczyk J, Jannes CE, Maciaczyk D, Bischofberger J, Nikkhah G (2011) Delayed functional maturation of human neuronal progenitor cells in vitro. Mol Cell Neurosci 47:36-44.

Leuner B, Gould E, Shors TJ (2006) Is there a link between adult neurogenesis and learning? Hippocampus 16:216-224.

Levy YS, Stroomza M, Melamed E, Offen D (2004) Embryonic and adult stem cells as a source for cell therapy in Parkinson's disease. J Mol Neurosci 24:353-386.

Liu J, Solway K, Messing RO, Sharp FR (1998) Increased neurogenesis in the dentate gyrus after transient global ischemia in gerbils. J Neurosci 18:7768-7778.

Lledo PM, Hjelmstad GO, Mukherji S, Soderling TR, Malenka RC, Nicoll RA (1995) Calcium/calmodulin-dependent kinase II and long-term potentiation enhance synaptic transmission by the same mechanism. Proc Natl Acad Sci U S A 92:11175-11179.

Lois C, Alvarez-Buylla A (1993) Proliferating subventricular zone cells in the adult mammalian forebrain can differentiate into neurons and glia. Proc Natl Acad Sci U S A 90:2074-2077.

Luskin MB (1993) Restricted proliferation and migration of postnatally generated neurons derived from the forebrain subventricular zone. Neuron 11:173-189.

Maccione A, Gandolfo M, Tedesco M, Nieus T, Imfeld K, Martinoia S, Berdondini L (2010) Experimental Investigation on Spontaneously Active Hippocampal Cultures Recorded by Means of High-Density MEAs: Analysis of the Spatial Resolution Effects. Front Neuroengineering 3:4.

Madl JE, Burgesser K (1993) Adenosine triphosphate depletion reverses sodium-dependent, neuronal uptake of glutamate in rat hippocampal slices. J Neurosci 13:4429-4444.

Maeda E, Robinson HP, Kawana A (1995) The mechanisms of generation and propagation of synchronized bursting in developing networks of cortical neurons. J Neurosci 15:6834-6845.

Mangin JM, Gallo V (2000) The curious case of NG2 cells: transient trend or game changer? ASN Neuro 3:e00052.

Marrone DF, Ramirez-Amaya V, Barnes CA (2012) Neurons generated in senescence maintain capacity for functional integration. Hippocampus.

McIver SR, Muccigrosso M, Gonzales ER, Lee JM, Roberts MS, Sands MS, Goldberg MP Oligodendrocyte degeneration and recovery after focal cerebral ischemia. Neuroscience 169:1364-1375.

Melchiorri D, Cappuccio I, Ciceroni C, Spinsanti P, Mosillo P, Sarichelou I, Sale P, Nicoletti F (2007) Metabotropic glutamate receptors in stem/progenitor cells. Neuropharmacology 53:473-480.

Meloni BP, Majda BT, Knuckey NW (2001) Establishment of neuronal in vitro models of ischemia in 96-well microtiter strip-plates that result in acute, progressive and delayed neuronal death. Neuroscience 108:17-26.

Meloni BP, Majda BT, Knuckey NW (2002) Evaluation of preconditioning treatments to protect near-pure cortical neuronal cultures from in vitro ischemia induced acute and delayed neuronal death. Brain Res 928:69-75.

Mercier F, Kitasako JT, Hatton GI (2002) Anatomy of the brain neurogenic zones revisited: fractones and the fibroblast/macrophage network. J Comp Neurol 451:170-188.

Merkle FT, Tramontin AD, Garcia-Verdugo JM, Alvarez-Buylla A (2004) Radial glia give rise to adult neural stem cells in the subventricular zone. Proc Natl Acad Sci U S A 101:17528-17532.

Meyer DA, Carter JM, Johnstone AF, Shafer TJ (2008) Pyrethroid modulation of spontaneous neuronal excitability and neurotransmission in hippocampal neurons in culture. Neurotoxicology 29:213-225.

Mi R, Luo Y, Cai J, Limke TL, Rao MS, Hoke A (2005) Immortalized neural stem cells differ from nonimmortalized cortical neurospheres and cerebellar granule cell progenitors. Exp Neurol 194:301-319.

Mielke JG, Comas T, Ahuja T, Preston E, Mealing GA (2007) Synaptic activity and triphenyltetrazolium chloride metabolism are correlated after oxygen-glucose deprivation in acute, but not cultured, hippocampal slices. Brain Res 1176:113-123.

Mirzadeh Z, Merkle FT, Soriano-Navarro M, Garcia-Verdugo JM, Alvarez-Buylla A (2008) Neural stem cells confer unique pinwheel architecture to the ventricular surface in neurogenic regions of the adult brain. Cell Stem Cell 3:265-278.

Mistry SK, Keefer EW, Cunningham BA, Edelman GM, Crossin KL (2002) Cultured rat hippocampal neural progenitors generate spontaneously active neural networks. Proc Natl Acad Sci U S A 99:1621-1626.

Mizumatsu S, Monje ML, Morhardt DR, Rola R, Palmer TD, Fike JR (2003) Extreme sensitivity of adult neurogenesis to low doses of X-irradiation. Cancer Res 63:4021-4027.

Modo M, Hopkins K, Virley D, Hodges H (2003) Transplantation of neural stem cells modulates apolipoprotein E expression in a rat model of stroke. Exp Neurol 183:320-329.

Modo M, Stroemer RP, Tang E, Patel S, Hodges H (2002) Effects of implantation site of stem cell grafts on behavioral recovery from stroke damage. Stroke 33:2270-2278.

Monje ML, Toda H, Palmer TD (2003) Inflammatory blockade restores adult hippocampal neurogenesis. Science 302:1760-1765.

Mu Y, Lee SW, Gage FH (2012) Signaling in adult neurogenesis. Curr Opin Neurobiol 20:416-423.

Nacher J, McEwen BS (2006) The role of N-methyl-D-asparate receptors in neurogenesis. Hippocampus 16:267-270.

Nikkhah G, Bentlage C, Cunningham MG, Bjorklund A (1994a) Intranigral fetal dopamine grafts induce behavioral compensation in the rat Parkinson model. J Neurosci 14:3449-3461.

Nikkhah G, Cunningham MG, Jödicke A, Knappe U, Björklund A (1994b) Improved graft survival and striatal reinnervation by microtransplantation of fetal nigral cell suspensions in the rat Parkinson model. Brain Res 633:133-143.

Nilsson M, Perfilieva E, Johansson U, Orwar O, Eriksson PS (1999) Enriched environment increases neurogenesis in the adult rat dentate gyrus and improves spatial memory. J Neurobiol 39:569-578.

Nissant A, Pallotto M (2011) Integration and maturation of newborn neurons in the adult olfactory bulb--from synapses to function. Eur J Neurosci 33:1069-1077.

O'Donovan MJ (1989) Motor activity in the isolated spinal cord of the chick embryo: synaptic drive and firing pattern of single motoneurons. J Neurosci 9:943-958.

O'Shaughnessy TJ, Liu JL, Ma W (2009) Passaged neural stem cell-derived neuronal networks for a portable biosensor. Biosens Bioelectron 24:2365-2370.

O'Shaughnessy TJ, Zim B, Ma W, Shaffer KM, Stenger DA, Zamani K, Gross GW, Pancrazio JJ (2003) Acute neuropharmacologic action of chloroquine on cortical neurons in vitro. Brain Res 959:280-286.

Olanow CW, Goetz CG, Kordower JH, Stoessl AJ, Sossi V, Brin MF, Shannon KM, Nauert GM, Perl DP, Godbold J, Freeman TB (2003) A double-blind controlled trial of bilateral fetal nigral transplantation in Parkinson's disease. Ann Neurol 54:403-414.

Opitz T, De Lima AD, Voigt T (2002) Spontaneous development of synchronous oscillatory activity during maturation of cortical networks in vitro. J Neurophysiol 88:2196-2206.

Ormerod BK, Galea LA (2001) Reproductive status influences cell proliferation and cell survival in the dentate gyrus of adult female meadow voles: a possible regulatory role for estradiol. Neuroscience 102:369-379.

Ormerod BK, Galea LA (2003) Reproductive status influences the survival of new cells in the dentate gyrus of adult male meadow voles. Neurosci Lett 346:25-28.

Ormerod BK, Falconer EM, Galea LA (2003) N-methyl-D-aspartate receptor activity and estradiol: separate regulation of cell proliferation in the dentate gyrus of adult female meadow vole. J Endocrinol 179:155-163.

Ormerod BK, Lee TT, Galea LA (2004) Estradiol enhances neurogenesis in the dentate gyri of adult male meadow voles by increasing the survival of young granule neurons. Neuroscience 128:645-654.

Ormerod BK, Palmer TD, Caldwell MA (2008) Neurodegeneration and cell replacement. Philos Trans R Soc Lond B Biol Sci 363:153-170.

Ostenfeld T, Tai YT, Martin P, Deglon N, Aebischer P, Svendsen CN (2002) Neurospheres modified to produce glial cell line-derived neurotrophic factor increase the survival of transplanted dopamine neurons. J Neurosci Res 69:955-965.

Palmer TD, Ray J, Gage FH (1995) FGF-2-responsive neuronal progenitors reside in proliferative and quiescent regions of the adult rodent brain. Mol Cell Neurosci 6:474-486.

Palmer TD, Takahashi J, Gage FH (1997) The adult rat hippocampus contains primordial neural stem cells. Mol Cell Neurosci 8:389-404.

Palmer TD, Schwartz PH, Taupin P, Kaspar B, Stein SA, Gage FH (2001) Cell culture. Progenitor cells from human brain after death. Nature 411:42-43.

Pancrazio JJ, Keefer EW, Ma W, Stenger DA, Gross GW (2001) Neurophysiologic effects of chemical agent hydrolysis products on cortical neurons in vitro. Neurotoxicology 22:393-400.

Parent JM, Yu TW, Leibowitz RT, Geschwind DH, Sloviter RS, Lowenstein DH (1997) Dentate granule cell neurogenesis is increased by seizures and contributes to aberrant network reorganization in the adult rat hippocampus. J Neurosci 17:3727-3738.

Pasquale V, Massobrio P, Bologna LL, Chiappalone M, Martinoia S (2008) Self-organization and neuronal avalanches in networks of dissociated cortical neurons. Neuroscience 153:1354-1369.

Peinado A (2000) Traveling slow waves of neural activity: a novel form of network activity in developing neocortex. J Neurosci 20:RC54.

Peljto M, Wichterle H Programming embryonic stem cells to neuronal subtypes. Curr Opin Neurobiol 21:43-51.

Perez Velazquez JL, Frantseva MV, Carlen PL (1997) In vitro ischemia promotes glutamate-mediated free radical generation and intracellular calcium accumulation in hippocampal pyramidal neurons. J Neurosci 17:9085-9094.

Pessoa L (2008) On the relationship between emotion and cognition. Nat Rev Neurosci 9:148-158.

Piatti VC, Davies-Sala MG, Esposito MS, Mongiat LA, Trinchero MF, Schinder AF (2011) The timing for neuronal maturation in the adult hippocampus is modulated by local network activity. J Neurosci 31:7715-7728.

Pine J (1980) Recording action potentials from cultured neurons with extracellular microcircuit electrodes. J Neurosci Methods 2:19-31.

Pisani A, Calabresi P, Tozzi A, D'Angelo V, Bernardi G (1998) L-type Ca2+ channel blockers attenuate electrical changes and Ca2+ rise induced by oxygen/glucose deprivation in cortical neurons. Stroke 29:196-201; discussion 202.

Potter SM, DeMarse TB (2001) A new approach to neural cell culture for long-term studies. J Neurosci Methods 110:17-24.

Raber J, Rola R, LeFevour A, Morhardt D, Curley J, Mizumatsu S, VandenBerg SR, Fike JR (2004) Radiation-induced cognitive impairments are associated with changes in indicators of hippocampal neurogenesis. Radiat Res 162:39-47.

Reynolds BA, Weiss S (1992) Generation of neurons and astrocytes from isolated cells of the adult mammalian central nervous system. Science 255:1707-1710.

Rola R, Raber J, Rizk A, Otsuka S, VandenBerg SR, Morhardt DR, Fike JR (2004) Radiation-induced impairment of hippocampal neurogenesis is associated with cognitive deficits in young mice. Exp Neurol 188:316-330.

Rosner G, Graf R, Kataoka K, Heiss WD (1986) Selective functional vulnerability of cortical neurons following transient MCA-occlusion in the cat. Stroke 17:76-82.

Rossi DJ, Oshima T, Attwell D (2000) Glutamate release in severe brain ischaemia is mainly by reversed uptake. Nature 403:316-321.

Roybon L, Christophersen NS, Brundin P, Li JY (2004) Stem cell therapy for Parkinson's disease: where do we stand? Cell Tissue Res 318:261-273.

Sanai N, Tramontin AD, Quinones-Hinojosa A, Barbaro NM, Gupta N, Kunwar S, Lawton MT, McDermott MW, Parsa AT, Manuel-Garcia Verdugo J, Berger MS, Alvarez-Buylla A (2004) Unique astrocyte ribbon in adult human brain contains neural stem cells but lacks chain migration. Nature 427:740-744.

Scarlatos A, Cadotte AJ, DeMarse TB, Welt BA (2008) Cortical networks grown on microelectrode arrays as a biosensor for botulinum toxin. J Food Sci 73:E129-136.

Scoville WB, Milner B (2000) Loss of recent memory after bilateral hippocampal lesions. 1957. J Neuropsychiatry Clin Neurosci 12:103-113.

Seaberg RM, Smukler SR, van der Kooy D (2005) Intrinsic differences distinguish transiently neurogenic progenitors from neural stem cells in the early postnatal brain. Dev Biol 278:71-85.

Shimada IS, Spees JL (2011) Stem and progenitor cells for neurological repair: minor issues, major hurdles, and exciting opportunities for paracrine-based therapeutics. J Cell Biochem 112:374-380.

Sinden JD, Rashid-Doubell F, Kershaw TR, Nelson A, Chadwick A, Jat PS, Noble MD, Hodges H, Gray JA (1997) Recovery of spatial learning by grafts of a conditionally immortalized hippocampal neuroepithelial cell line into the ischaemia-lesioned hippocampus. Neuroscience 81:599-608.

Smith AG (2001) Embryo-derived stem cells: of mice and men. Annu Rev Cell Dev Biol 17:435-462.

Snyder EY, Deitcher DL, Walsh C, Arnold-Aldea S, Hartwieg EA, Cepko CL (1992) Multipotent neural cell lines can engraft and participate in development of mouse cerebellum. Cell 68:33-51.

Snyder JS, Hong NS, McDonald RJ, Wojtowicz JM (2005) A role for adult neurogenesis in spatial long-term memory. Neuroscience 130:843-852.

Song H, Stevens CF, Gage FH (2002a) Astroglia induce neurogenesis from adult neural stem cells. Nature 417:39-44.

Song HJ, Stevens CF, Gage FH (2002b) Neural stem cells from adult hippocampus develop essential properties of functional CNS neurons. Nat Neurosci 5:438-445.

Song J, Christian K, Ming GL, Song H (2012) Modification of hippocampal circuitry by adult neurogenesis. Dev Neurobiol.

Steiner B, Kronenberg G, Jessberger S, Brandt MD, Reuter K, Kempermann G (2004) Differential regulation of gliogenesis in the context of adult hippocampal neurogenesis in mice. Glia 46:41-52.

Stephens CL, Toda H, Palmer TD, Demarse TB, Ormerod BK (2012) Adult neural progenitor cells reactivate superbursting in mature neural networks. Exp Neurol 234:20-30.

Strubing C, Ahnert-Hilger G, Shan J, Wiedenmann B, Hescheler J, Wobus AM (1995) Differentiation of pluripotent embryonic stem cells into the neuronal lineage in vitro gives rise to mature inhibitory and excitatory neurons. Mech Dev 53:275-287.

Suhonen JO, Peterson DA, Ray J, Gage FH (1996) Differentiation of adult hippocampus-derived progenitors into olfactory neurons in vivo. Nature 383:624-627.

Svendsen CN, Caldwell MA, Ostenfeld T (1999) Human neural stem cells: isolation, expansion and transplantation. Brain Pathol 9:499-513.

Svendsen CN, ter Borg MG, Armstrong RJ, Rosser AE, Chandran S, Ostenfeld T, Caldwell MA (1998) A new method for the rapid and long term growth of human neural precursor cells. J Neurosci Methods 85:141-152.

Szatkowski M, Barbour B, Attwell D (1990) Non-vesicular release of glutamate from glial cells by reversed electrogenic glutamate uptake. Nature 348:443-446.

Tabak J, Latham PE (2003) Analysis of spontaneous bursting activity in random neural networks. Neuroreport 14:1445-1449.

Takagi Y, Nozaki K, Takahashi J, Yodoi J, Ishikawa M, Hashimoto N (1999) Proliferation of neuronal precursor cells in the dentate gyrus is accelerated after transient forebrain ischemia in mice. Brain Res 831:283-287.

Takahashi J, Palmer TD, Gage FH (1999) Retinoic acid and neurotrophins collaborate to regulate neurogenesis in adult-derived neural stem cell cultures. J Neurobiol 38:65-81.

Takahashi K, Yamanaka S (2006) Induction of pluripotent stem cells from mouse embryonic and adult fibroblast cultures by defined factors. Cell 126:663-676.

Takahashi K, Tanabe K, Ohnuki M, Narita M, Ichisaka T, Tomoda K, Yamanaka S (2007) Induction of pluripotent stem cells from adult human fibroblasts by defined factors. Cell 131:861-872.

Tanaka E, Yamamoto S, Kudo Y, Mihara S, Higashi H (1997) Mechanisms underlying the rapid depolarization produced by deprivation of oxygen and glucose in rat hippocampal CA1 neurons in vitro. J Neurophysiol 78:891-902.

Tanapat P, Hastings NB, Reeves AJ, Gould E (1999) Estrogen stimulates a transient increase in the number of new neurons in the dentate gyrus of the adult female rat. J Neurosci 19:5792-5801.

Tashiro A, Makino H, Gage FH (2007) Experience-specific functional modification of the dentate gyrus through adult neurogenesis: a critical period during an immature stage. J Neurosci 27:3252-3259.

Tateno T, Jimbo Y, Robinson HP (2005) Spatio-temporal cholinergic modulation in cultured networks of rat cortical neurons: evoked activity. Neuroscience 134:439-448.

Tavazoie M, Van der Veken L, Silva-Vargas V, Louissaint M, Colonna L, Zaidi B, Garcia-Verdugo JM, Doetsch F (2008) A specialized vascular niche for adult neural stem cells. Cell Stem Cell 3:279-288.

Tekkok SB, Goldberg MP (2001) Ampa/kainate receptor activation mediates hypoxic oligodendrocyte death and axonal injury in cerebral white matter. J Neurosci 21:4237-4248.

Thomson JA, Itskovitz-Eldor J, Shapiro SS, Waknitz MA, Swiergiel JJ, Marshall VS, Jones JM (1998) Embryonic stem cell lines derived from human blastocysts. Science 282:1145-1147.

Thored P, Arvidsson A, Cacci E, Ahlenius H, Kallur T, Darsalia V, Ekdahl CT, Kokaia Z, Lindvall O (2006) Persistent production of neurons from adult brain stem cells during recovery after stroke. Stem Cells 24:739-747.

Toda H, Tsuji M, Nakano I, Kobuke K, Hayashi T, Kasahara H, Takahashi J, Mizoguchi A, Houtani T, Sugimoto T, Hashimoto N, Palmer TD, Honjo T, Tashiro K (2003) Stem cell-derived neural stem/progenitor cell supporting factor is an autocrine/paracrine survival factor for adult neural stem/progenitor cells. J Biol Chem 278:35491-35500.

Tonnesen J, Parish CL, Sorensen AT, Andersson A, Lundberg C, Deisseroth K, Arenas E, Lindvall O, Kokaia M (2011) Functional integration of grafted neural stem cell-derived dopaminergic neurons monitored by optogenetics in an in vitro Parkinson model. PLoS One 6:e17560.

van Pelt J, Wolters PS, Corner MA, Rutten WL, Ramakers GJ (2004) Long-term characterization of firing dynamics of spontaneous bursts in cultured neural networks. IEEE Trans Biomed Eng 51:2051-2062.

van Praag H, Christie BR, Sejnowski TJ, Gage FH (1999) Running enhances neurogenesis, learning, and long-term potentiation in mice. Proc Natl Acad Sci U S A 96:13427-13431.

van Praag H, Schinder AF, Christie BR, Toni N, Palmer TD, Gage FH (2002) Functional neurogenesis in the adult hippocampus. Nature 415:1030-1034.

Vemuganti R (2005) Decreased expression of vesicular GABA transporter, but not vesicular glutamate, acetylcholine and monoamine transporters in rat brain following focal ischemia. Neurochem Int 47:136-142.

Voigt T, Opitz T, de Lima AD (2001) Synchronous oscillatory activity in immature cortical network is driven by GABAergic preplate neurons. J Neurosci 21:8895-8905.

Wagenaar DA, Pine J, Potter SM (2006) An extremely rich repertoire of bursting patterns during the development of cortical cultures. BMC Neurosci 7:11.

Wagenaar DA, Madhavan R, Pine J, Potter SM (2005) Controlling bursting in cortical cultures with closed-loop multi-electrode stimulation. J Neurosci 25:680-688.

Walker NI, Harmon BV, Gobe GC, Kerr JF (1988) Patterns of cell death. Methods Achiev Exp Pathol 13:18-54.

Weick JP, Liu Y, Zhang SC (2011) Human embryonic stem cell-derived neurons adopt and regulate the activity of an established neural network. Proc Natl Acad Sci U S A 108:20189-20194.

Wernig M, Benninger F, Schmandt T, Rade M, Tucker KL, Bussow H, Beck H, Brustle O (2004) Functional integration of embryonic stem cell-derived neurons in vivo. J Neurosci 24:5258-5268.

Winkler C, Kirik D, Bjorklund A (2005) Cell transplantation in Parkinson's disease: how can we make it work? Trends Neurosci 28:86-92.

Winocur G, Wojtowicz JM, Sekeres M, Snyder JS, Wang S (2006) Inhibition of neurogenesis interferes with hippocampus-dependent memory function. Hippocampus 16:296-304.

Wyllie AH, Beattie GJ, Hargreaves AD (1981) Chromatin changes in apoptosis. Histochem J 13:681-692.

Yagita Y, Kitagawa K, Ohtsuki T, Takasawa K, Miyata T, Okano H, Hori M, Matsumoto M (2001) Neurogenesis by progenitor cells in the ischemic adult rat hippocampus. Stroke 32:1890-1896.

Yeung CK, Sommerhage F, Wrobel G, Law JK, Offenhausser A, Rudd JA, Ingebrandt S, Chan M (2009) To establish a pharmacological experimental platform for the study of cardiac hypoxia using the microelectrode array. J Pharmacol Toxicol Methods 59:146-152.

Yu J, Vodyanik MA, He P, Slukvin, II, Thomson JA (2006) Human embryonic stem cells reprogram myeloid precursors following cell-cell fusion. Stem Cells 24:168-176.

Zaghloul N, Nasim M, Patel H, Codipilly C, Marambaud P, Dewey S, Schiffer WK, Ahmed M (2012) Overexpression of extracellular superoxide dismutase has a protective role against hyperoxia-induced brain injury in neonatal mice. FEBS J 279:871-881.

Zerangue N, Kavanaugh MP (1996) Flux coupling in a neuronal glutamate transporter. Nature 383:634-637.

Zhang R, Zhang Z, Wang L, Wang Y, Gousev A, Zhang L, Ho KL, Morshead C, Chopp M (2004) Activated neural stem cells contribute to stroke-induced neurogenesis and neuroblast migration toward the infarct boundary in adult rats. J Cereb Blood Flow Metab 24:441-448.

Zhao C, Deng W, Gage FH (2008) Mechanisms and functional implications of adult neurogenesis. Cell 132:645-660.

Zhu JM, Zhao YY, Chen SD, Zhang WH, Lou L, Jin X (2011) Functional recovery after transplantation of neural stem cells modified by brain-derived neurotrophic factor in rats with cerebral ischaemia. J Int Med Res 39:488-498.

BIOGRAPHICAL SKETCH

Crystal Lynn Stephens was born in St. Petersburg, Florida in 1984. The oldest of four children, she grew up primarily in Clearwater, Florida, and graduated with honors from Countryside High School in 2002.

Crystal obtained her B.S. in agricultural and biological engineering *cum laude* with a minor in biomechanics (concentrating on an area in biological engineering) from the University of Florida in 2006, supported by a Bright Futures Florida Academic Scholarship.

She continued her postgraduate work at the University of Florida in the J. Crayton Pruitt Family Department of Biomedical Engineering as a recipient of the University Alumni Fellowship.

Upon completion of the Ph.D. program, Crystal plans to pursue a career as a research scientist in the private sector for a pharmaceutical or biotechnological company.